Electrochemical Society

101, No. [illegible] October 1954

UNIV. OF MICHIGAN
NOV 17 1954
EAST ENGINEERING
LIBRARY

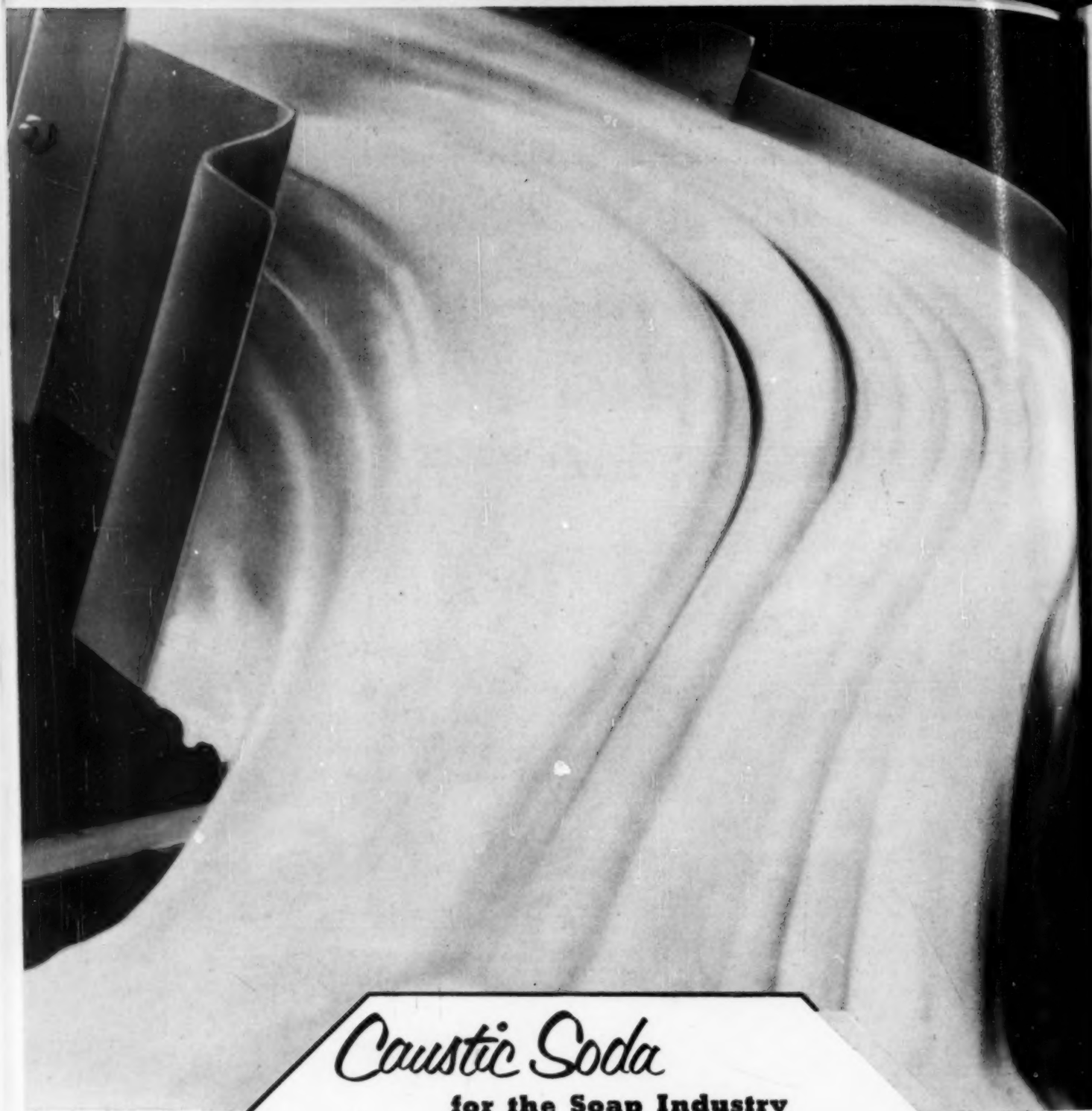

Caustic Soda

for the Soap Industry

Caustic soda is one of the basic chemicals required for the manufacture of modern soaps.

Uniformly high quality GLC GRAPHITE ANODES are basic too—in helping the electrolytic industry meet the growing civilian and defense needs for chlorine and caustic soda.

ELECTRODE DIVISION

Great Lakes Carbon Corporation

Niagara Falls, N.Y. GLC Morganton, N. C.

Graphite Electrodes, Anodes, Molds and Specialties

Sales office: Niagara Falls, N.Y. **Other offices:** New York, N.Y., Oak Park, Ill., Pittsburgh, P

Sales Agents: J. B. Hayes, Birmingham, Ala.; George O'Hara, Long Beach, Cal.; Great Northern Carbon & Chemical Co., Ltd., Montreal, Can

Overseas Carbon & Coke Company, Inc., Geneva, Switzerland; Great Eastern Carbon & Chemical Co., Inc., Chiyoda-Ku, Tokyo

Reaction of Thallium with Oxygen and Moisture[1]

J. T. Waber and G. E. Sturdy

Los Alamos Scientific Laboratory of the University of California, Los Alamos, New Mexico

ABSTRACT

Reactions of thallium with water vapor and air were investigated in the range 25°–75°C to throw light on the mechanism of atmospheric corrosion. It was deduced on the basis of changes in the rate laws, and confirmed by x-ray diffraction, that the principal reaction product changes from Tl_2O to TlOH as the relative humidity of air increases. Parabolic and cubic laws, as well as a new growth law, were observed. Effects of carbon dioxide and of preformed sulfide films were also studied. The tentative x-ray structure of TlOH is presented.

Introduction

Atmospheric attack on thallium is relatively slow (1), the observed initial penetration rate being 2–10μ/day depending on the aggressiveness of the environment.

Several investigations have been made of the dissolution of thallium in mineral acids (2–8), but only two of them (4, 5) contain information which may be applied to atmospheric corrosion. Plank and Urmanczy (4) concluded that the reaction between thallium and water is determined by hydrogen overvoltage, and that dissolved oxygen has a strong effect on the reaction at 25°C. For example, corrosion of thallium occurs 1.4 times as fast in air-saturated water as in hydrogen-saturated water; with oxygen-saturated water the reaction takes place 12.2 times as rapidly. In a later paper (5) they present evidence that thallium does not react with water at 25°C in the absence of oxygen. From these data the rate is probably less than 3 mg/cm²/hr at 25°C.

The data of this paper are divided into five groups; (*a*) oxidation of thallium in dry oxygen and dry air; (*b*) effect of humidity and temperature on the change of mechanism; (*c*) x-ray study of products formed under different conditions; (*d*) effect of a preformed sulfide film; and (*e*) a brief evaluation of the effect of carbon dioxide. Surprisingly, the cubic growth law was observed in addition to the more usual parabolic one. A hitherto unreported time dependence (growth law) was observed, and it plays an important role in the over-all picture of corrosion of this metal.

Experimental Details and Results

High purity thallium metal was rolled to form 2-mil and 20-mil foils, then stored in mineral oil. Before use, the metal foil was degreased with petroleum ether and immersed in a warm perchloric acid solution (11% by volume) to remove surface oxide. The metal remained bright when stored in the cold acid.

At the beginning of each run, samples were cut to the desired size, immersed in acid, then washed with alcohol, acetone, and finally with ethyl ether. They were put in numbered porcelain crucibles which were placed in desiccators containing different saturated salt solutions. The salt solutions were selected to maintain certain constant humidities throughout the run. The desiccators and their contents were then placed in constant temperature ovens. For runs in which a gas other than air was used, the desiccator was purged for 10 min before it was returned to the oven. Periodically, the samples were removed for weighing. The crucible and specimen were weighed together on an Ainsworth Type FDJ microbalance. After weighing, the specimen and crucible were returned to the desiccator, and the desiccator was again purged.

In a few additional runs, samples were weighed by measuring the extension of silica helixes from which samples were suspended within the corrosive medium. Thus, samples were not exposed to air during weighing. This technique did not yield results significantly different from those obtained by the microbalance technique; however, due to certain inherent features of the silica helix method, the data showed more scatter than did those obtained with the microbalance. Since the value of the silica helix data lies only in showing that significantly different products were not formed when air was excluded during the weighings, these data are not included here.

Test periods during which weighings were carried out lasted from 210 to 240 hr. Specimens for x-ray work were repeatedly examined for periods up to 750 hr without detectable change in identity of the products. Although these are not long-term experiments when compared with conventional weathering tests, it was felt that observations were continued

[1] Manuscript received August 20, 1953.

TABLE I. *Reaction parameters for dry oxygen*

Run No.	Temp, °C	Gas present	Time slope, n	Rate constant, k_n
13	38	oxygen	0.56	2.82
14	38	oxygen	0.58	2.97
21	57	oxygen	0.53	1.77
23	57	oxygen	0.53	1.77
19	75	oxygen	0.66	2.81
20	75	oxygen	0.76	0.93
17	38	air	0.59	2.06
18	38	air	0.59	1.65

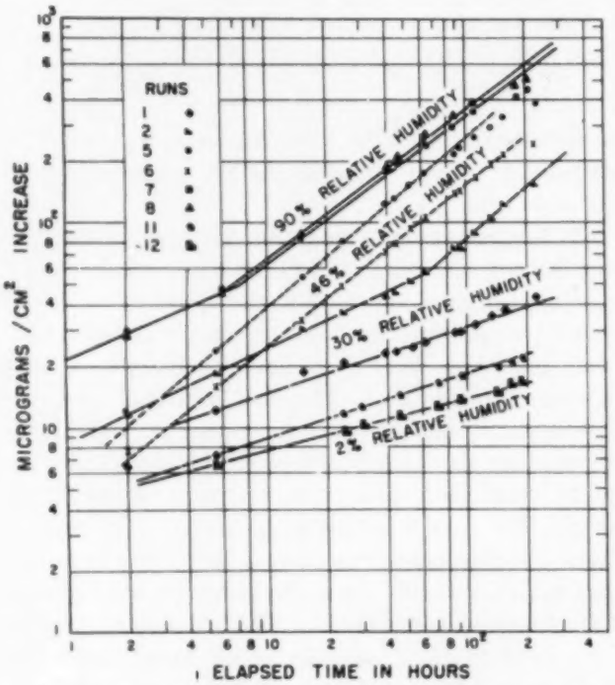

FIG. 1. Graphical summary illustrating the effect of the moisture content of air on the corrosion rates and the rate laws.

TABLE II. *Effect of relative humidity on rate constants and time dependences at 38°C*

Run No.	Relative humitity	Gas present	Time slope, n	Rate constant, k_n
11	2	air	0.31	4.38
12	2	air	0.25	4.34
1	30	air	0.33	6.25
2*	30	air	0.46 0.84	8.40 1.70
15	30	helium	0.36	5.24
16	30	helium	0.36	5.24
5	46	air	0.76	7.2
6	46	air	0.78	4.1
7	90	air	0.70	13.2
8	90	air	0.70	13.2

* Two values of n and k occur successively during this run as shown in Fig. 2.

long enough to give a reasonable idea of corrosion behavior.

X-ray diffractometer patterns of the fresh metal surface were taken with a General Electric XRD-3 instrument. After exposure the samples were again examined. X-ray spectra of pure compounds were obtained wherever possible.

Treatment of Data

Experimental weight gains, w, were plotted on log-log coordinate paper as $\mu g/cm^2$ vs. elapsed time, t, in hours. When a straight line results, one may conclude that the corrosion reaction follows a rate law such as

$$W = k_n t^n \qquad (I)$$

On such a log-log plot the slope of the line is equal to n, and the rate constant, k_n, is equal to the weight gain at the end of 1 hr. Values of n and k_n are tabulated and discussed for each run. Exponents are, respectively, one-half and one-third for the parabolic and cubic laws (9).

Reaction with Dry Oxygen and Dry Air

Rate parameters of metal specimens exposed to oxygen in contact with dry P_2O_5 are listed in Table I. The time dependence is quite different from average values observed for tests with water present, especially at lower temperatures.

In addition, several runs were made in air dried with $MgClO_4$ for x-ray work. Reliable weight gain data could not be obtained in these cases because oxide was lost occasionally during the frequent manipulation necessary to align the specimen in the x-ray diffractometer.

Reaction with Moist Air

In contrast to the parabolic time dependence observed with dry oxygen, the cubic law is followed at low relative humidities and temperatures. However, a new rate law was obtained under more aggressive conditions. This observation led to the conclusion that a change in mechanism was involved. Much of this report is devoted to clarifying what reactions are involved.

The bulk of the data relating to the effect of humidity was obtained at 38°C. This temperature is a practical upper limit for atmospheric corrosion tests. Some of the data are presented graphically in log-log form in Fig. 1. Values of n and k_n for each run were calculated from the lines shown in Fig. 1 and are listed in Table II.

Curves in Fig. 1 show that two different average slopes are needed to describe the whole set of data. Table II shows that the slopes, n (time dependences) are generally greater at higher humidities. At lower humidities (runs 1, 2, 11, 12, 15, 16) the average value[2] of n is 0.34, whereas n increases to an average value of 0.74 for higher humidities. This observation suggests that the mechanism changes significantly in the vicinity of 30% relative humidity. The amount of metal consumed after 200-hr ex-

[2] Excluding the second higher n value for run 2.

posure to low humidities is significantly less than if the 4/3 law had been followed for the same period. Clearly, then, moisture increases the rate of attack.

At higher temperatures the time dependence increases at 30% relative humidity. Corresponding rates and time dependences for temperatures between 38° and 75°C are listed in Table III.

These data suggest that nucleation and growth of the hydroxide are more rapid as the temperature increases, despite a lower degree of supersaturation. The equilibrium pressure, as shown in Appendix A, corresponds to 8 and 11% relative humidity at 57° and 75°C.

Significantly the time dependences in runs 3 and 4 changed from 0.814 and 0.805 to 0.3 and 0.35, respectively, at about 40 hr. This phenomenon is illustrated in Fig. 2. Cubic rate constants are 35 and 28, respectively. At 39 hr, corroded specimens had changed color from rust to chocolate brown. The rust color was commonly observed in tests made at low humidities.

On the basis of x-ray studies, it is probable that the high values of n for 75°C are due to formation of Tl_2O_3 from TlOH.

Rate of Hydration

To substantiate the deduction that the 4/3-law, which is dominant at higher humidities, corresponds to the reaction of the oxide (already formed) with water vapor, the rate of hydration of thallous oxide was studied directly. A specimen of metal was converted to oxide by exposing it to dry oxygen at 75°C. The oxide sample was exposed to air containing 30% relative humidity at 35°C, and weight changes were determined by the microbalance technique.

The resulting time dependence was 0.75 and the rate constant was 1.2, based on the area of the metal specimen. These rate parameters are in reasonably good agreement with results shown in Table III, and in particular with the values $n = 0.84$ and $k_n = 1.7$ found in run 2 (for 38°C).

Dissolution in Boiling Water

Two tests were run in vigorously boiling water. The flask containing the specimens was equipped with a reflux condenser which was loosely stoppered. Reasonably large quantities of thallium dissolved despite the reduced oxygen content of the boiling water. In the first case, 0.57 mg/cm² dissolved in 4.5 hr. In the second, 6.3 mg/cm² dissolved in 2 hr. However, in the second run, the rather adherent hydroxide was removed from the specimen before weighing. Assuming that a linear rate law was followed, these data compute to 130 and 3100 μg/cm²/hr for 92°C. These rates are very large in comparison with those shown in Table II. Certainly the dissolution of thallium proceeds rapidly in the presence of very little air.

TABLE III. *Effect of temperature on rate constants and time dependences at 30% relative humidity*

Run No.	Relative humidity	Gas present	Time slope, n	Rate constant, k_n
1	38	air	0.33	6.25
2	38	air	0.46 0.84	8.40 1.70
15	38	helium	0.36	5.24
16	38	helium	0.36	5.24
3	57	air	0.81	5.87
4	57	air	0.80	4.80
9	75	air	0.95	7.98
10	75	air	0.95	7.98

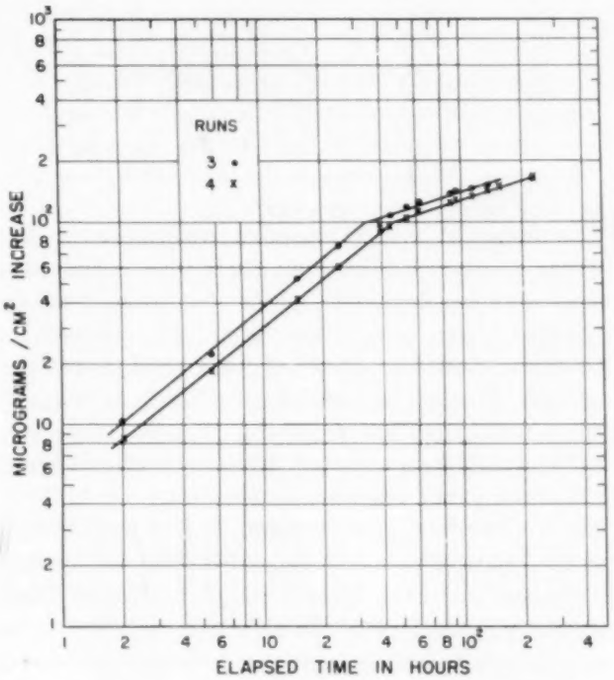

FIG. 2. Unexplained decrease in time dependence with increasing time. Possibly it indicates a change to oxide formation.

X-Ray Studies

Positive identification of products was hampered by a lack of published x-ray diffraction data for the hydroxide. Some preparative chemistry was necessary to connect observed patterns with this product. The crystal structure of TlOH was determined during this investigation.

Two pieces of thallium metal were exposed to dry air at 35° to 70°C in desiccators containing $MgClO_4$. Periodically x-ray diffractograms were taken. The resulting patterns agree quite well with regard to the line positions reported by Halla, Tompa, and Zimmerman (10) for thallous oxide. However, significant differences in line intensities

TABLE IV. *Effectiveness of sulfide films in reducing corrosion*

Run No.	Temp, °C	Gas present	Relative humidity	Time slope, n	Rate constant, k_n
29	38	oxygen	P_2O_5	0.35	15.4
30	38	oxygen	P_2O_5	0.35	12.2
31	38	helium	30	0.81	3.2
32	38	helium	30	0.78	4.55

TABLE V. *Rate parameters for attack by moist and dry carbon dioxide*

Run No.	Relative humidity	Temp, °C	Time slope, n	Rate constant, k_n
23	P_2O_5	38	0.41	5.40
24	P_2O_5	38	0.41	5.40
25	30	38	0.18	27.0
26	30	38	0.18	27.0
27	30	38	0.02	53.0
28	30	38	0.03	36.8

were noticed.[3] A very plausible explanation is that the oxide pattern formed on the heavily rolled (and thus strongly oriented) metal was itself strongly oriented. Such orientation alters the relative intensities from those observed for a random powder sample. Further investigation of the orientation relationship has been deferred.

Because the equilibrium pressure of the thallous hydroxide-oxide reaction varies from 10 to 30% relative humidity over a range of temperatures, as shown in Appendix A, x-ray diffraction patterns of corrosion products formed at two temperatures were studied using humidities above and below this equilibrium value. In agreement with conclusions drawn from reaction rates, Tl_2O is formed in dry air and TlOH is formed in high-humidity air.

Several diffractometer traces were made of a specimen exposed to 50% relative humidity at 70°C. The changes in pattern strongly suggested that TlOH was being oxidized to Tl_2O_3 as time increased. After 233 hr exposure, when the product was mainly Tl_2O_3, the specimen was placed in dry air at 70°C. Diffractograms indicate that TlOH was converted to Tl_2O and that Tl_2O_3 was unaffected.

To confirm this deduction, the specimen, which had been exposed only to dry air at 70°C and which exhibited at Tl_2O pattern, was placed in a desiccator containing air of approximately 20% relative humidity at 70°C. After 10 hr exposure, the x-ray diffractogram indicated formation of TlOH plus some Tl_2O_3. Further exposure indicated the growth of Tl_2O_3.

[3] In addition, there was some evidence to indicate that line positions changed slightly with time in such a way as to suggest a decrease in cell size.

Sulfide Films

Gibney (11) suggested that since thallium is somewhat similar to lead in its behavior and both readily form sulfides, a thin coating of thallous sulfide might be protective. In order to investigate this possibility, samples were dipped into a strong ammonium polysulfide solution for several minutes until a uniform thin coating of the sulfide had formed. The specimens were then washed, dried, and treated as described previously. It was found that the corrosion rate apparently increases in the presence of the sulfide film. Ultimately, in dry oxygen it would appear to be advantageous to use sulfide films since the cubic growth law corresponds to a protective film more than does the parabolic law ($n = \frac{1}{2}$). Table I shows that the parabolic law is characteristic of the reaction with dry oxygen. However, the benefits of using such sulfide films are slight at best (Table IV).

Reaction with Carbon Dioxide

Thallium carbonate was found in corrosion products which had been allowed to stand in the laboratory for years. To ascertain whether carbon dioxide was contributing to atmospheric attack, tests were run in dry and in moist carbon dioxide (Table V). Aside from water and unintentional impurities, the gas was 100% carbon dioxide.

Samples used in four runs with moist carbon dioxide showed very little increase in weight after the large initial increase which had occurred by the end of 1 hr. Inasmuch as the metal samples were not consumed during exposure, it appears that attack is virtually stopped by a protective film formed after the initial rapid attack.

The time dependence observed in runs 25–28 appear sufficiently different from 0.34 and 0.74 to justify the conclusion that carbon dioxide is not contributing significantly to the corrosion mechanism in laboratory atmospheres.

However, 0.41 lies between the values of 0.33 and 0.50 which are characteristic of low humidities and dry air. The rate constant 5.40 for carbon dioxide in contact with phosphorus pentoxide, is larger than those shown in Table IV for phosphorus pentoxide-dried oxygen. Thus, it is possible that carbon dioxide might contribute to weight gain in the low-humidity region. The rate constant for approximately 100% carbon dioxide is only 35% greater than that for runs in air ($n \simeq \frac{1}{3}$) extrapolated to zero humidity. Considering that the carbon dioxide content of air is seldom greater than a few percent, it is reasonable to conclude that direct reaction of the metal with carbon dioxide from laboratory atmospheres is probably unimportant. One cannot conclude that its reaction with the oxide is of neg-

ligible influence on the over-all reaction kinetics. In fact, it is very difficult to prepare carbonate-free thallous oxide by wet chemical methods. However, x-ray patterns of the two specimens exposed to laboratory air contained no lines which could be attributed definitely to thallium carbonate.

When one of these specimens was subsequently exposed to 50% relative humidity at 35°C it exhibited several unidentified lines and gave off gas when immersed in 10% by volume perchloric acid. These observations suggest thallous bicarbonate may form from the hydroxide.[4]

Discussion

The principal conclusions of this paper were deduced from rate data confirmed by x-ray diffraction. The corrosion product is mainly thallous oxide or hydroxide depending on humidity.

On the basis of rate parameter data, the effects of humidity can be explained if one of the two reactions:

$$2Tl + H_2O(g) \rightarrow Tl_2O + H_2(g) \qquad (II)$$

$$4Tl + O_2(g) \rightarrow 2Tl_2O \qquad (III)$$

occurs in the low-humidity range and if either

$$2Tl_2O + H_2O(g) \rightarrow 2TlOH \qquad (IV)$$

$$2Tl + 2H_2O(g) \rightarrow 2TlOH + H_2(g) \qquad (V)$$

occurs in the high-humidity range. Although Plank and Urmanczy (6) state that reaction (II) will not occur in the absence of oxygen, data to the contrary have been presented here.

Runs 15 and 16, made in moist helium, show that direct reaction with water to form thallous oxide occurs at 38°C in the absence of oxygen. Similarly, oxidation of thallium by boiling water occurs in the virtual absence of dissolved oxygen. The rate of reaction with water is small in comparison to the rates Plank and Urmanczy initially observed in aerated solutions (4) and the limit (ca. 3 $\mu g/cm^2/hr$ at 25°C) set later by how much thallium they could detect by titration does not seriously disagree with rates from Tables II and III.

The effect of dissolved oxygen is probably one of depolarization rather than direct reaction. Hence, their statement that rate is strongly dependent upon oxygen content is correct, but the statement that reaction will not occur in the absence of oxygen is in contradiction to the present data, and a slow reaction cannot be excluded by their experiment. In experiments using silica springs, reaction occurred, although oxygen was carefully excluded.

One may estimate the depolarizing effect of aeration by comparing the average value of k_n for runs 1 and 2 and for runs 15 and 16. The ratio is 1.4 in agreement with the figure cited by Plank and Urmanczy (4).

It is interesting to note that at lower humidities (runs 1, 2, 11, 12, 15, and 16) the average value[5] of n is 0.34, whereas n increased to an average value[6] of 0.74 for higher humidities. This observation suggests that the mechanism changes significantly around 30% relative humidity. The rate constant, k_n, is roughly proportional to the relative humidity. A line drawn through k_n values for $n = 0.74$ passes close to the origin. In contrast, the few values available for the cubic law ($n \simeq 1/3$) extrapolate to $k_n \simeq 4$ at 0% relative humidity.

It was not clear from data in Tables II and III whether the reaction to form hydroxide proceeded by steps, such as reaction (II) followed by reaction (IV), or by the over-all reaction (V). Thus the hydration reaction (IV) was studied by using a specimen of thallous oxide. The resulting time dependence and rate constant were almost equal to the average values found for high-humidity runs. One might note that the weight change accompanying formation of hydroxide from a given amount of metal is 2.13 times as great as that for oxide formation. Thus, the hydration reaction would appear to be dominant and rate-controlling in the over-all reaction, even if the rates for reaction (II) and (IV) were approximately equal.

Since the time dependence of reaction (III), $n \simeq 1/2$, is different from that observed at low humidity, $n \simeq 1/3$, it is concluded that reaction (II) is dominant. The hydration reaction (IV) has a time dependence of $n = 3/4$, which is in agreement with that found in the high-humidity range. Therefore, it was concluded that the sequence of reactions, (III) plus (IV), accounts for the over-all behavior represented by equation (V).

The equilibrium water pressure of a thallous-oxide-hydroxide mixture amounts to a relative humidity of 5% or more at 38°C, as shown in Appendix A. Thus, the change from reaction (III) to reactions (III) plus (IV), as relative humidity is increased, is consistent with the change in thermodynamic stability. As humidity is decreased from 30%, it becomes less likely that the hydroxide product is formed by reaction (III) plus (IV), and in dry air this over-all reaction would nearly cease as evidenced by k_n approaching zero. At low humidi-

[4] The x-ray pattern for $TlHCO_3$ is apparently not known.

[5] Excluding the second higher n value for run 2.

[6] In 8 of 26 runs, n was found to be in the range 0.70 to 0.84 and to have a mean value of 0.74. To the best of the authors' knowledge, such a time dependence has not been previously reported. Although no theoretical justification for this time dependence or slope is readily evident, its use appears to be empirically justified.

ties, however, a different reaction is responsible. Even at 30% relative humidity the product is apparently mainly the compound Tl_2O.

It appears that since 30% relative humidity is substantially greater than 5.5% (the equilibrium water pressure estimated from Appendix A at 38°C) one might expect the change in mechanism to occur at somewhat lower humidities. Undoubtedly the formation of TlOH does occur occasionally at humidities near 15 or 20%. The limiting factor is nucleation of the hydroxide.

As Langmuir (12) pointed out, heterogeneous chemical reactions can occur only at the interface between two reacting phases. Numerous examples of hydration and decomposition reactions have supported this hypothesis. Thus nuclei of the hydroxide must either be present or be formed before reaction (IV) can continue.

It is well known that large supersaturations are required to nucleate heterogeneous reactions. One such reaction, a phase change, is formation of drops of moisture from water vapor. The ΔH of formation of the hydroxide from the oxide is balanced by the energy required to form the oxide-hydroxide interface. With the heat of formation (13.6 kcal) having the same magnitude as the latent heat of condensation of water (10.6 kcal/mole), it might be expected that a large degree of supersaturation would be required to nucleate the hydroxide. Of course, for this argument it is assumed that the magnitude of surface energy at the solid interface is comparable to that of the steam-water interface. Experience indicates that solid interfacial energies are large. Thus, a reasonable explanation appears to be that the hydroxide does not form below 30% relative humidity because it cannot be nucleated easily in this humidity range. The rate of formation of hydroxide in comparison with that of the oxide would probably be slow until supersaturation became relatively large.

During run 2, made at 30% relative humidity, the time dependence changed abruptly from 0.46 to 0.84. A reasonable explanation is that the hydroxide was locally nucleated and spread rapidly across the specimen surface.

Conclusion

In the corrosion of thallium the observed change in growth law from the cubic to the $\frac{4}{3}$-power time dependence as the relative humidity is increased is associated with a change from formation of thallous oxide to formation of the hydroxide as the principal product. The reaction of thallium with water vapor in the low humidity range, and the hydration of thallous oxide in the higher humidity range are concluded to be the dominant reactions.

Acknowledgments

The assistance in this investigation of many members of the staff is greatly appreciated. Especially helpful were E. Staritzky's chemical microscopy studies, C. F. Stambaugh's and D. D. Whyte's preliminary x-ray diffraction studies and R. N. R. Mulford's work in preparing and analyzing several compounds. The author is indebted to J. Singer for making available his unpublished results on the crystal structure of thallous hydroxide.

Any discussion of this paper will appear in a Discussion Section to be published in the June 1955 Journal.

References

1. H. E. Howe and A. A. Smith, Jr., *This Journal*, **97**, 167C (1950).
2. J. Plank and A. Urmanczy, *Z. anorg. Chem.*, **238**, 51 (1938).
3. M. Centnerszser, *Atti congr. intern. chim. 10th Congr. Rome*, **3**, 555 (1939).
4. J. Plank and A. Urmanczy, *Z. anorg. Chem.*, **241**, 158 (1939).
5. J. Plank and A. Urmanczy, *ibid.*, **241**, 416 (1939).
6. J. Plank and A. Urmanczy, *Korrosion u. Metallschutz*, **16**, 33 (1940).
7. J. Plank and A. Urmanczy, *Magyar Kém. Folyóirat*, **46**, 113 (1940).
8. J. Plank and A. Urmanczy, *Korrosion u. Metallschutz*, **17**, 141 (1941).
9. J. T. Waber, *Metal Prog.*, **62**, 76 (1952).
10. F. Halla, H. Tompa and L. Zimmerman, *Z. Krist.*, **86**, 303 (1933).
11. R. B. Gibney, Private communication.
12. I. Langmuir, *J. Am. Chem. Soc.*, **38**, 2263 (1916).
13. F. Bahr, *Z. anorg. Chem.*, **71**, 93 (1911).
14. R De Forcrand, *Compt. rend.*, **176**, 873 (1923).
15. J. Singer, Unpublished work (1951).

APPENDIX A

Equilibrium Decomposition Pressure of Thallous Hydroxide

The equilibrium pressure of water vapor over a mixture of thallous oxide and hydroxide has been studied by Bahr (13). His data are plotted both as the pressure in millimeters of mercury and as relative humidity vs. the reciprocal absolute temperature. From such a slope, since the equilibrium constant is proportional to pressure for such a heterogeneous reaction, one calculates ΔH for the reaction

$$2TlOH \rightarrow Tl_2O + H_2O(g) \qquad (VI)$$

to be 13.64 kcal. Heats of solution have been determined by De Forcrand (14) to be 28.327 kcal and 25.210 kcal for 2TlOH. The difference, 3.117 kcal, is the heat of reaction using liquid water. Employing the latent heat of vaporization of water at 10°C as 10.627 kcal/mole, the difference, 3.02 kcal, is the heat of reaction using liquid water. That is, the heat change for the reaction

$$2TlOH \rightarrow Tl_2O + H_2O(l) \qquad (VII)$$

is 3.02 determined from vapor pressures and 3.117 determined calorimetrically. The two values agree well enough to justify the conclusion that the line representing the data in Fig 3 is correct. The ΔH from this graph is the average

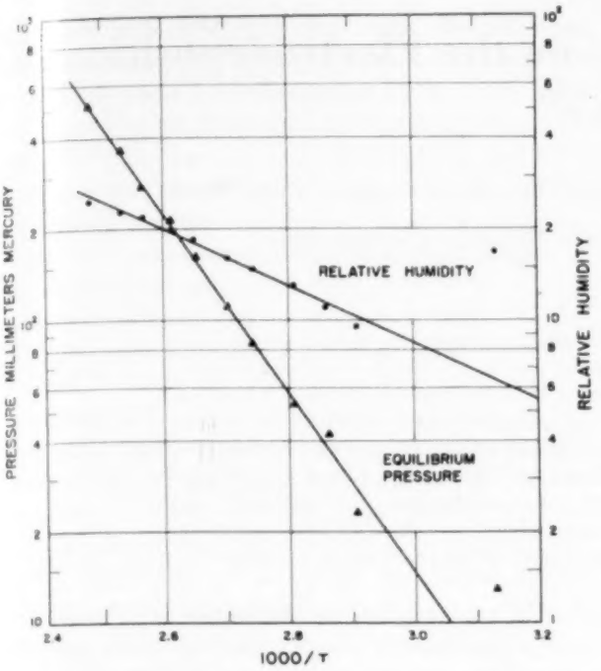

FIG. 3. Variation in equilibrium decomposition pressure of thallous hydroxide with temperature. These pressures correspond to the indicated equivalent relative humidities.

determined for the range 60°–130°C and has not been corrected to 10°C. The effect of ΔC_p, as can be seen from the slight downward concavity of the data, would be to increase the difference slightly and to bring it into better agreement.

APPENDIX B

Crystal lattice parameters and the space group of thallous hydroxide have been determined by Singer (15) from Weissenberg patterns.

The cell is hexagonal with the parameters

$$c = 3.90\ kx$$
$$a = 9.72\ kx$$
$$c/a = 0.402$$

and contains 6 molecules per unit cell with the Laue symmetry $6/m$. The space group is $C6_3/m$. The six thallium ions are at:

$x, y, \frac{1}{4}$	$\bar{x}, \bar{y}, \frac{3}{4}$
$\bar{y}, x-y, \frac{1}{4}$	$y, y-x, \frac{3}{4}$
$y-x, \bar{x}, \frac{1}{4}$	$x-y, x, \frac{3}{4}$

with $x = 0.312 \pm 0.001$ and $y = 0.350 \pm 0.001$.

The oxygen ions are in the same sixfold set, namely $6h$. Here the parameters are $x = 0.165 \pm 0.004$ and $y = 0.530 \pm 0.004$. The Tl-OH distance is $2.65 \pm 0.05\ kx$.

Some refinement in parameters may occur in the course of further detailed Fourier analysis.

The Effect of Ultrasonic Waves on the Electrodeposition of Copper[1,2]

W. R. Wolfe,[3] Hyman Chessin,[4] Ernest Yeager, and Frank Hovorka

Department of Chemistry, Western Reserve University, Cleveland, Ohio

ABSTRACT

Effects of ultrasonic waves on the electrodeposition of copper have been determined at frequencies of 200 and 1000 kc/sec with acid-sulfate plating baths of various concentrations. Polarization measurements indicate that ultrasonic waves produce a marked decrease in polarization, while x-ray diffraction studies indicate that ultrasonic waves increase the tendency for preferred orientation. These effects are correlated with disruption of concentration gradients at the electrode surface by ultrasonic waves. Schlieren photographs of the gradients support these conclusions. Microagitation associated with moderately intense ultrasonic waves seems considerably more effective than ordinary mechanical stirring in breaking up concentration gradients at an electrode.

Introduction

Various workers (1–9) have reported[5] the effects of ultrasonic waves on electrodeposition of metals. These effects extend from the improvement of the metal structure (3–5) to formation of colloidal suspensions of the metal instead of coherent deposits (7, 8). Relatively little specific information is available, however, with the exception of the work of Roll (5, 6) as to the effects of ultrasonic waves on polarization and structure of electrodeposits, particularly under controlled acoustical and electrochemical conditions.

As part of the present investigation, effects of ultrasonic waves on electrodeposition of copper have been ascertained in terms of polarization measurements and x-ray diffraction data. Copper has been chosen for this study because the activation polarization is small, simultaneous deposition of hydrogen is minor, and concentration polarization is significant in determining properties of the deposit. Microagitation associated with moderately intense ultrasonic waves (1 watt/cm^2) should be effective in disrupting concentration gradients normally present adjacent to the cathode surface.

Experimental Techniques

Measurements have been made with ultrasonic waves at frequencies of 200 and 1000 kc/sec, with most of the research at the latter. The acoustical system used for the work at 1000 kc/sec is shown in Fig. 1. A circular, X-cut, quartz plate of 3 in. diameter was used to convert electrical energy from a 1000-watt, radio-frequency generator to acoustical energy. The quartz transducer was mounted in an underwater housing which permitted propagation of ultrasonic waves horizontally into the 80-gal, glass, thermostatic tank (Fig. 1). A similar arrangement was used for the measurements at 200 kc/sec. Acoustical intensities of as much as 20 watts/cm^2 were available directly in front of the quartz transducer, provided the water in the tank was relatively air-free and the unidirectional flow of the water associated with acoustical streaming was not impeded. Otherwise, gas-type cavitation bubbles would accumulate in the sound field and limit the intensity of ultrasonic waves which could be propagated a few centimeters to a few watts/cm^2 or less. Water in the glass tank was partially degassed by boiling under reduced pressure in a separate steel tank then pumping into the tank under a layer of oil to retard resaturation by air.

For part of the work, a reflector was placed at an oblique angle in the tank at the end opposite the transducer. This prevented formation of standing waves and greatly reduced complications associated with reflections from the back of the tank.

Electrochemical measurements were made in the glass cell shown in Fig. 2. This cell was located in the tank so that the cathode-containing section was in the ultrasonic field at a distance of 10 cm or less from the surface of the quartz transducer. Glass walls of the bulb containing the cathode were of the order of 10^{-3} in. in thickness, and hence did not scatter or reflect ultrasonic waves to any appreciable extent. A fritted glass plug was sealed into the bottom of the cell in order that the solutions might be

[1] Manuscript received March 11, 1954. This paper was prepared for delivery before the Montreal Meeting, October 26–30, 1952.

[2] Work partially supported by the Office of Naval Research.

[3] Present address: Experimental Station, E. I. du Pont de Nemours, Wilmington, Delaware.

[4] Present address: Research Institute, University of Arkansas, Fayetteville, Arkansas.

[5] For a review of the electrochemical applications of ultrasonic waves, see reference (9).

saturated with hydrogen gas when desired. The cathode surface was normally oriented at an angle of approximately 15° with respect to the wave front in order to avoid formation of standing waves. In addition, with the 15° angle, gas bubbles resulting from gas-type cavitation did not accumulate on the cathode surface but were swept away by unidirectional flow associated with ultrasonic waves of appreciable intensity.

Acoustical intensities have been calculated[6] from pressure amplitudes as determined with a barium titanate hydrophone (10).[7] Prior to electrochemical measurements, transmission characteristics of the glass bulb were checked by pressure amplitude measurements both inside and in front of the cell when it was filled with solutions similar to those used in actual electrodeposition. These data permitted calculation of acoustical amplitudes in the cell from acoustical measurements outside the cell. During electrochemical measurements, acoustical amplitudes were determined by moving the hydrophone momentarily to a point directly in front of the cell in the ultrasonic field. As a check, the hydrophone was placed in the cell in the position normally occupied by the cathode after electrochemical measurements had been completed. Response of the hydrophone was measured with a Ballantine vacuum tube voltmeter, Model 304. The hydrophone was calibrated by means of radiation pressure measurements over the range of acoustical parameters involved in the experimental work. This calibration was subsequently checked at intensities below cavitation levels against a similar hydrophone which had been previously calibrated by the U.S. Navy Underwater Sound Reference Laboratory at Orlando, Florida.

Absolute accuracy of the pressure amplitude measurements at or near the cathode surface for intensities of the order 1 watt/cm² or less was limited to a probable error of ± 15% because of nonhomogeniety of the acoustical field as a result of refraction and diffraction effects as well as the gas-type cavitation bubbles which formed in the cell. At higher intensities the absolute accuracy became progressively less because of acoustical complications associated with pressure amplitude measurements in the presence of gas-type cavitation bubbles.

Polarization measurements were made by the direct method. The Luggin capillary was introduced through a hole in the back of the cathode in such a fashion that the tip was flush with the cathode surface (Fig. 2). This avoided acoustical complications which would have arisen if the Luggin capil-

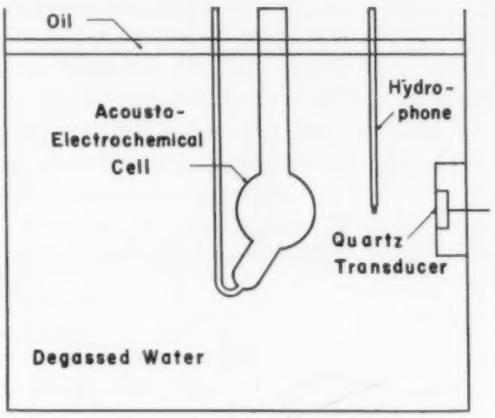

FIG. 1. Acoustical apparatus

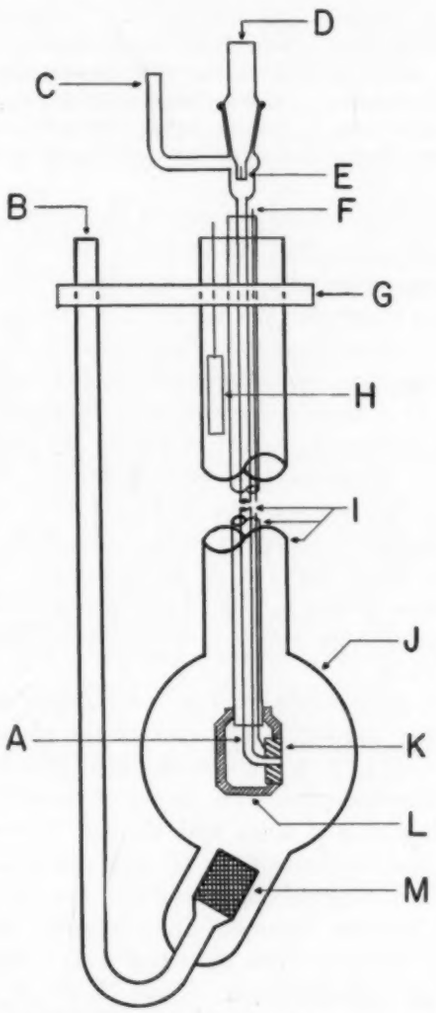

FIG. 2. Acousto-electrochemical cell. A—Luggin capillary; B—hydrogen gas; C—for filling capillary tube; D—solution bridge; E—asbestos; F—cathode lead; G—clamp; H—anode; I—glass; J—glass 0.001 in. wall; K—cathode; L—Lucite; M—glass frit.

[6] The acoustical intensity (I) is related to the rms pressure (p_o) by the equation $I = (p_o)^2/\rho c$ where ρ and c are the density and the velocity of sound in the solution.

[7] For details concerning construction and performance characteristics of this type of hydrophone, see reference (10).

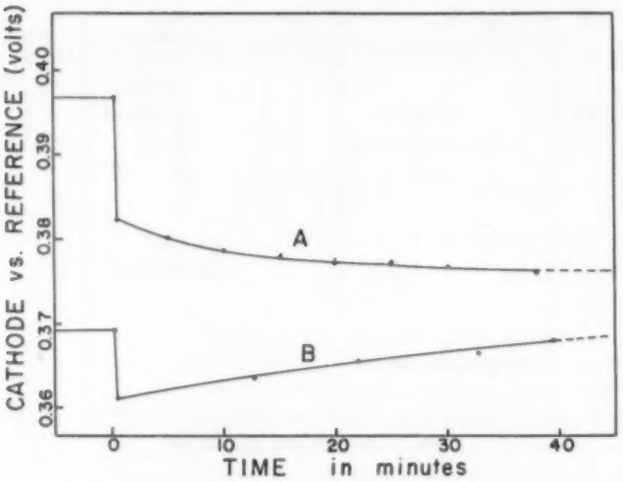

FIG. 3. Effect of ultrasonic waves on polarization as a function of time. Electrolyte: 0.17M $CuSO_4$ + 0.02M H_2SO_4; current density: 8 ma/cm²; temperature: 25° C; ultrasonic frequency: 1000 kc/sec; acoustical intensity: 0.8 watts/cm². Curve A: preplate below limiting current density; curve B: preplate above limiting current density.

lary had been placed in front of the cathode. From the Luggin capillary extended a solution bridge which connected with a saturated mercurous sulfate reference electrode. The part of the solution bridge adjacent to the Luggin capillary was filled with the plating solution, while the section of the bridge leading to the reference electrode was filled with a saturated potassium sulfate solution. A constricted capillary containing asbestos fiber was used to separate the two sections of the solution bridge as shown in Fig. 2. Apparent surface area of the copper cathode was 1 cm² for all measurements. The arrangement shown in Fig. 2 permitted removal of cathodes from the plastic holder for x-ray diffraction examination.

The copper anode used in polarization measurements was located in the neck of the glass cell as shown in Fig. 2. A voltage-regulated power supply (300 volts) was used as a source of current with a large resistance in series with the cell. Current was determined in terms of the *IR* drop across a standard 10-ohm resistance in series with the cell. Potential differences between the cathode and the reference electrode were measured with a Leeds and Northrup potentiometer, Type K-2. A Brown Electronik recording potentiometer with a response time of 2 sec for 90% deflection was used to follow small changes in voltage of the polarized cathode as a function of time.

Prior to each series of measurements, the copper cathode was polished with 2/0, 3/0, and finally 4/0 emery paper. In the polishing process the glass end of the Luggin capillary was also polished flush with the metal surface. The cathode was then placed in approximately 1*N* nitric acid for 60 sec. A preplate was deposited at a current density of 16 ma/cm² for 15 min in the solution subsequently used for polarization measurements. This current density was less than the limiting current density for all acid-sulfate plating baths used with the vertical cathode. Unless otherwise stated, polarization measurements were generally made with increasing current density by recording the potential approximately 30 sec after adjustment of the polarizing current to a specific value. This was immediately increased to a higher value and the procedure repeated.

One of the criteria for successful polarization measurements is reproducibility. Consistently lower and more reproducible polarization values were obtained with hydrogen-saturated solutions than with air-saturated solutions. Hence, subsequent measurements were made with hydrogen-saturated solutions. Hydrogen was purified by passing it through a conventional purification train.

Experimental Results

Data presented in Fig. 3 were obtained with ultrasonic waves at a frequency of 1000 kc/sec and an intensity of 0.8 watt/cm². The apparent current density was 8 ma/cm², while the solution was 0.17M $CuSO_4$ and 0.02M H_2SO_4. Curves A and B differ in that the former is for a cathode prepared in the manner described previously, while the latter is for a cathode prepared with part of the preplate at 30 ma/cm² for 10 min, then 16 ma/cm² for 15 min. The ratio of true to apparent surface area for the cathode represented by curve B was probably much greater than for that represented by curve A, since deposition above the limiting current density favors a porous, relatively high area deposit.

The immediate effect of ultrasonic waves in both cases was an almost instantaneous decrease in cathode potential. This initial change occurred so quickly that the recording potentiometer could not follow it. The rapid decrease in polarization results from disruption of concentration gradients by the ultrasonic waves.

Subsequent changes in cathode potential after the initial decrease are attributed to changes in the effective surface area of the cathode in both cases. Even in the absence of ultrasonic waves, the cathode polarization represented by curve A showed a slight tendency to decrease, while that represented by curve B tended to increase with time. These trends appear to be promoted by ultrasonic waves with both curves approaching some limiting value. Similar effects, although less marked, could be produced by ordinary agitation of the solution near the cathode.

In Fig. 4 data are presented for polarization immediately after introduction of the ultrasonic waves

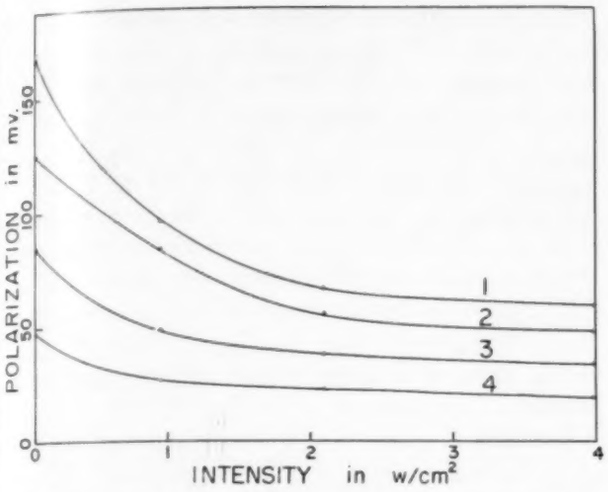

FIG. 4. Dependence of polarization on acoustical intensity and current density. Electrolyte: 0.17M $CuSO_4$ + 0.02M H_2SO_4; temperature: 25° C; ultrasonic frequency: 1000 kc/sec. Current densities: curve 1, 25 ma/cm²; curve 2, 20 ma/cm²; curve 3, 14 ma/cm²; curve 4, 8 ma/cm².

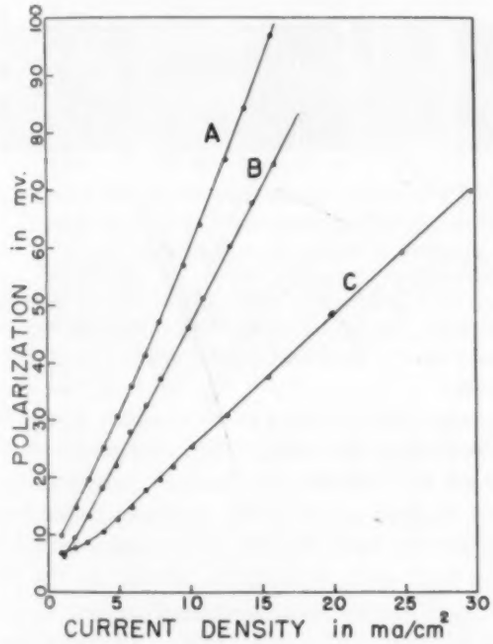

FIG. 5. Polarization at various current densities without ultrasonic waves (curve A), with ultrasonic waves at 1000 kc/sec and 4 watts/cm² (curve C), and with directional flow past the cathode surface (curve B). Electrolyte: 0.17M $CuSO_4$ + 0.02M H_2SO_4; temperature: 25° C.

(1000 kc/sec) as a function of acoustical intensity. Results in this graph as well as those in all subsequent graphs were obtained with a cathode preplated at current densities below the limiting value. The approach of the polarization to a limiting value with increasing acoustical intensity probably indicates that almost all of the concentration polarization has been removed. The evidence is not completely conclusive, however, inasmuch as intensity of the ultrasonic waves at the cathode surface could not be determined with sufficient certainty at higher intensities (e.g., 4 watts/cm²) because of gas-type cavitation bubbles. Similar results have been obtained with solutions of both higher copper sulfate concentration and lower *p*H. Polarization is most marked with solutions of lowest concentration, i.e., the solution represented in Fig. 4.

Fig. 5 represents polarization at various current densities in a 0.17M $CuSO_4$, 0.02M H_2SO_4 solution with ultrasonic waves (curve C), without ultrasonic waves (curve A), and with ordinary unidirectional flow of solution (curve B). The latter polarization measurements were made with a flow of approximately 1 m/sec parallel to the cathode surface in a specially constructed cell described elsewhere (11). While the effects of stirring and of ultrasonic waves are comparable, it is apparent that the ultrasonic waves are more effective in the present case.

The graph in Fig. 6 represents the effects of ultrasonic waves on polarization in a more concentrated solution: 0.86M $CuSO_4$ and 0.02M H_2SO_4. Polarizing as well as depolarizing effects of ultrasonic waves are less in the case of this solution than that represented in Fig. 5, as might be anticipated on the basis of concentration polarization. It is interesting to note that, in the case of curve C in Fig. 6, for the range 30–100 ma/cm² the polarization is a reasonably linear function of the logarithm of current density with a Tafel slope of approximately 0.08.

In Fig. 7 effects of ultrasonic waves (1000 kc/sec) on polarization are compared in hydrogen-saturated solution (B) and in degassed solution (A) in which there was insufficient dissolved gas to support gas-type cavitation. While there was appreciable depolarization in the degassed solution, the effect was greater in the hydrogen-saturated solution, particularly at high current densities. Thus, gas-type

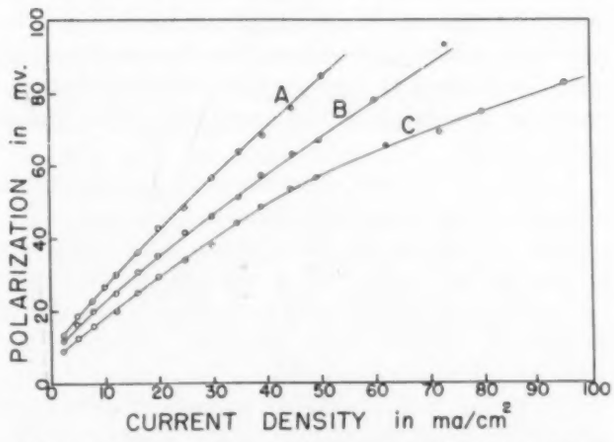

FIG. 6. Polarization at various current densities without ultrasonic waves (curve A) and with ultrasonic waves at a frequency of 1000 kc/sec and 0.9 watts/cm² (curve B) and 4 watts/cm² (curve C). Electrolyte: 0.86M $CuSO_4$ + 0.02M H_2SO_4; temperature: 25° C.

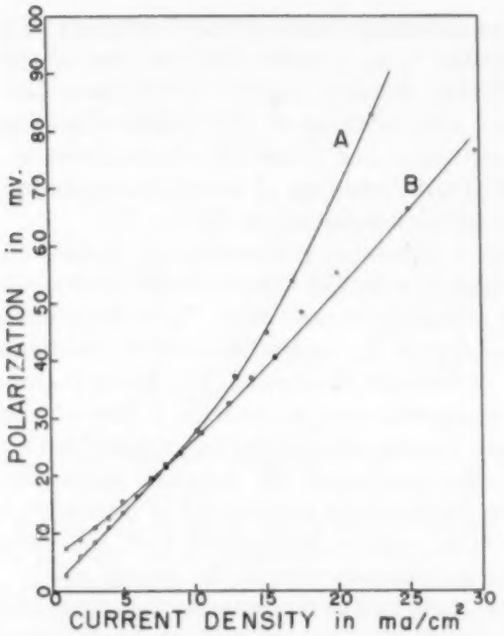

FIG. 7. Polarization at various current densities with ultrasonic waves in degassed solutions (curve A) and in hydrogen saturated solutions (curve B). Electrolyte: 0.17M $CuSO_4$ + 0.02M H_2SO_4; temperature: 25° C; ultrasonic frequency: 1000 kc/sec; acoustical intensity: 4 watts/cm².

FIG. 8. X-ray diffraction patterns of copper deposits. Electrolyte: 0.17M $CuSO_4$ + 0.02M H_2SO_4; current density: 20 ma/cm²; plating time: approx. 70 min. Pattern *a* (*left*), with quiescent solution; pattern *b* (*center*), with stirring; pattern *c* (*right*), with progressive ultrasonic waves (1000 kc/sec, 4 watts/cm²).

cavitation contributes appreciably to depolarization. The smaller, but nevertheless appreciable, depolarizing effect observed in the degassed solution can be explained at least partially in terms of unidirectional streaming effects associated with intense sound waves.

A sufficient number of polarization measurements also have been made with ultrasonic waves at a frequency of 200 kc/sec to establish that ultrasonic effects at this lower frequency are substantially the same as at 1000 kc/sec with respect to order of magnitude. At the lower frequency, however, the wave length was comparable to the cathode dimensions; hence, the associated acoustical diffraction effects rendered the quantitative aspects of the measurements somewhat questionable at 200 kc/sec.

Polarization measurements support the conclusion that the predominate effect of the ultrasonic waves is disruption of the concentration gradients. If this

TABLE I. *Crystallographic results*

Condition	Solution concentration: molarity		Current density ma/cm²	Time of deposition min	Relative orientation
	$CuSO_4$	H_2SO_4			
Static*	0.17	0.02	8	80	2
Stirred					4
Ultrasonics†					4
Static	0.17	0.02	20	75	1
Stirred					4
Ultrasonics					4
Static	0.86	0.02	20	72	5
Stirred					5
Ultrasonics					5
Static	0.86	0.2	20	72	2
Stirred					2
Ultrasonics					2

* No stirring or ultrasonic waves.

† Acoustical intensity: approximately 2.5 watts/cm²; frequency 1000 kc/sec.

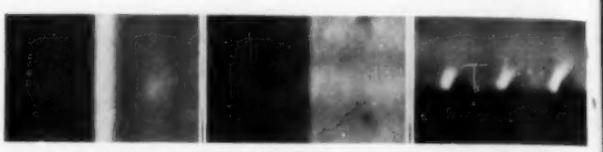

FIG. 9. Schlieren photographs of concentration gradients at copper cathode. Electrolyte: 0.86M $CuSO_4$ + 0.02M H_2SO_4; current density: 25 ma/cm². Fig. 9*a* (*left*): vertical cathode without ultrasonic waves. Fig. 9*b* (*center*): vertical cathode with progressive ultrasonic waves (1 watt/cm² at 1000 kc/sec). Fig. 9*c* (*right*): horizontal cathode with standing waves (= 0.1 watt/cm² at 1000 kc/sec).

is the case, changes in crystallographic properties of the electrodeposits should be comparable to those produced by ordinary mechanical agitation or stirring. A typical set of x-ray diffraction patterns of deposits with and without ultrasonic waves (1000 kc/sec) and with stirring are shown in Fig. 8*a*, *b*, and *c*. A glancing-beam technique similar to that of Hume-Rothery (12), and Wyllie (13) was used to obtain these diffraction patterns. In this part of the work, stirring was accomplished by passing a stream of hydrogen bubbles past the cathode in the cell shown in Fig. 2. It is apparent that both ultrasonic waves and stirring favored the preferred orientation of the 110 plane parallel to the electrode surface.[8] Grain-size changes were minor. In Table I, changes in the tendency for preferred orientation are compared on a relative basis in terms of an arbitrary scale extending from 1, for the least tendency for orientation, to 5 for the maximum tendency observed. From Table I it is evident that the ultrasonic waves produced an appreciable increase in the

[8] Other x-ray diffraction patterns, together with additional polarization data, are presented in reference (17).

tendency for preferred orientation only in the most dilute solutions in which concentration polarization was most marked. Furthermore, the effects of the ultrasonic waves and the unidirectional stirring on the preferred orientation are comparable.

Fig. 9 shows Schlieren photographs which indicate directly the effect of ultrasonic waves on the concentration gradient adjacent to the cathode surface. These photographs were obtained by optical techniques similar to those described by Bartlett (14). The darkest area in each photograph represents the cathode. The light region adjacent to the cathode surface in Fig. 9*a* is associated with the concentration gradient. The absence of this region in Fig. 9*b* demonstrates the effectiveness of ultrasonic waves at cavitation levels in disrupting concentration gradients. The Schlieren technique as used in this work was probably sufficient to reveal a diffusion layer of the order of 0.001 cm in thickness. Fig. 9 indicates the action of low intensity ultrasonic waves on the concentration gradients in a standing wave with the cathode surface perpendicular to the wave front. Experimental work in progress indicates that the regions of demarcation between the light and black areas in Fig. 9*c* probably correspond to the pressure loops or displacement nodes of the standing waves in the solution. This effect can be used to explain the half wave length ripples obtained by Young and Kersten (15) on the surfaces of metals electrodeposited in a standing wave.

The effects of ultrasonic waves on the electrodeposition of copper were examined at acoustical intensities as high as 100 watts/cm² in a converging sound field from a focusing type transducer. At these intensities, copper was not deposited in a coherent plate; rather a colloidal suspension of copper was produced. Even the base plate was appreciably eroded.

Significance of Results

On the basis of experimental results previously described, the following conclusions were reached concerning copper deposition in the presence of ultrasonic waves:

1. The depolarizing action of ultrasonic waves is primarily associated with the interaction of acoustical waves with concentration gradients at the cathode surface.

2. Ultrasonic waves at cavitation levels seem considerably more effective than conventional mechanical agitation in breaking up these gradients.

3. Structural changes at intensities of the order of a few watts/cm² or less generally reflect acoustically produced changes in concentration gradients at the electrode surface.

The effectiveness of ultrasonic waves in disrupting concentration gradients may be explained, at least in part, in terms of a microagitation effect. Conventional stirring can be used to reduce the effective thickness of the concentration gradient to 10^{-3} cm. Surface conditions at distances less than 10^{-3} cm are relatively unchanged even in the case of high speed unidirectional flow. Disturbances are produced at the electrode surface by ultrasonic waves, however, as the acoustical waves encounter a phase discontinuity and are largely reflected. Cavitation phenomena right at the electrode surface are particularly significant. As a result, the effective thickness of concentration gradients is reduced to a value considerably smaller than that obtained with stirring.

An accurate prediction of concentration polarization even in unstirred solutions is not readily made because of convection currents associated with the vertical cathode and because of edge effects. These convection currents were very evident in Schlieren photographs of the concentration gradients at the top and bottom of the cathode. On the basis of simple equations (16) for diffusion and electrolyte transport, the limiting current density in the unstirred solution represented in Fig. 5 should be approximately 15 ma/cm², whereas the actual value was approximately 30 ma/cm². Thus, it is not possible at this time to compare the depolarizing action of ultrasonic waves with the concentration polarization in a quantitative fashion.

While not likely, it is possible that the relatively large depolarizing effect of ultrasonic waves may not be entirely associated with concentration polarization; some decrease in activation polarization may occur. At higher current densities in more dilute solutions, there also may have been some *IR* drop included in polarization measurements even with this type of Luggin capillary. Preliminary measurements by the commutator technique with electrodes of similar construction and solutions of comparable concentrations lead to the conclusion that *IR* drop was not more than a few millivolts in dilute solutions.

Ultrasonic or sonic waves may have possible application in specialized plating processes where ordinary stirring is not sufficiently effective in breaking up concentration gradients. Such might be the case with small objects of irregular contour. The best way to introduce sound waves would probably be to drive the whole object being plated at a sonic or ultrasonic frequency. Ultrasonic waves should also prove significant in laboratory investigations of electrode processes where it is desirable to minimize the effects of concentration gradients.

Acknowledgments

The authors are pleased to acknowledge the assistance of Dr. John F. Yeager in obtaining polarization measurements with unidirectional flow, and Mr. Robert W. Penn in obtaining the Schlieren photographs.

Any discussion of this paper will appear in a Discussion Section to be published in the June 1955 Journal.

REFERENCES

1. T. Rummel and K. Schmitt, *Korrosion u. Metallschutz*, **19,** 101 (1943).
2. F. Levi, *Ricerca Sci.*, **19,** 887 (1949).
3. F. Muller and H. Kuss, *Helv. Chim. Acta*, **33,** 217 (1950).
4. F. Muller, *Angew. Chem.*, **62,** 25 (1950).
5. A. Roll, *Z. Metallkunde*, **41,** 339, 413 (1950); *ibid.*, **42,** 238, 271; *Metalloberflache*, **6B,** 49 (1952).
6. A. Roll and G. Schrag, *Z. Metallkunde*, **42,** 197 (1951).
7. B. Claus, *Z. tech. Phys.*, **16,** 80, 202 (1935).
8. B. Claus and E. Schmidt, *Kolloid-Beih.*, **45,** 1 (1936).
9. E. Yeager and F. Hovorka, *J. Acoust. Soc. Amer.*, **25,** 443 (1953).
10. E. Yeager, H. Dietrick, and F. Hovorka, *ibid.*, **25,** 456 (1953).
11. J. Yeager, Ph.D. Thesis, Western Reserve University, 1953.
12. W. Hume-Rothery and M. Wyllie, *Proc. Roy. Soc.*, **A181,** 331 (1943).
13. M. Wyllie, *Rev. Sci. Instr.*, **18,** 426 (1947).
14. J. H. Bartlett and L. Stephenson, *This Journal*, **101,** 571 (1954).
15. W. Young and H. Kersten, *J. Chem. Phys.*, **4,** 426 (1936).
16. *See*, for example, G. Kortum and J. Bockris, "Textbook of Electrochemistry," Vol. II, pp. 402-7, Elsevier Publishing Co., New York (1951).
17. W. Wolfe, E. Yeager, and F. Hovorka, Technical Report No. 10, Contract N7 onr 47002, Western Reserve University, December, 1952.

Kilogram Scale Reductions of Vanadium Pentoxide to Vanadium Metal[1]

ARTHUR P. BEARD AND DONALD D. CROOKS

Knolls Atomic Power Laboratory, General Electric Company, Schenectady, New York

ABSTRACT

The reduction of V_2O_5 with calcium to give 750–1000 gram buttons of massive ductile vanadium has been accomplished. Using an iodine igniter-booster and an optimum amount of excess calcium, the authors obtained 84% yields of metal. In this process oxygen impurity seems to be the main embrittling agent, while silicon impurity up to 0.2 wt % has no apparent effect on the vanadium.

INTRODUCTION

The production of vanadium metal by reduction of vanadium pentoxide with calcium, as reported by McKechnie and Seybolt in earlier work (1), was undertaken in order to provide material of sufficient purity and ductility for use in studies of its reactions with gases (2), methods of fabrication, and physical properties. In addition, it was desirable to determine if product purity could be retained in reactions yielding 750 to 1000 grams (instead of 125 g) and if yields could be increased substantially above the 74% value reported earlier.

EXPERIMENTAL PROCEDURE

Equipment.—In the small scale bomb reductions of vanadium pentoxide with calcium, using an iodine igniter-booster charge, McKechnie and Seybolt obtained small, ductile buttons of about 125 g (74% yield). The steel container, lined with a magnesia crucible, was 4 in. in diameter, 11 in. high, with ⅜ in. wall. This reaction vessel was made tight by compression of a steel cover on an annealed copper gasket. It was found that yields of about 270 g (about 78% of theoretical) of massive metal could be obtained by taking a reaction charge of 600 g V_2O_5, 1057 g calcium, and 300 g iodine, pressing the mixture into 3 in. diameter disks with 80 tons pressure, and performing the reduction in the described bomb. The amount of excess calcium needed to give ductile metal was also decreased from about 60% to about 53% excess. However, the frequency of explosive burnouts of the steel bombs increased when using this technique.

A new reduction vessel was designed and fabricated for producing vanadium. It was made from steel pipe, 6.6 in. O.D., with about 7/16 in. wall, and was about 20 in. tall. Six ½ in. diameter bolts were used to compress the steel cover on an annealed copper gasket to make the bomb tight. A flare fitting was brazed in the cover for flushing the bomb with dry inert gas.

A tapered magnesia liner, 5 in. at the top, 4½ in. at the bottom, 18 in. high, with ¼ in. wall was slipped into the steel container. Coarse grained magnesia was used between the liner and inside of the bomb for centering and support of the crucible. This type of liner proved to be quite successful since it could be removed easily from the steel bomb after a reduction was made. Liners formed directly in the bomb were unsatisfactory.

A 15-kw, 10,000 cycle, motor generator was used as the source of power for heating the bombs. An optimum heating rate of 50°–60°/min was used until the rapid temperature rise caused by reaction inside the bomb was detected by a thermocouple on the outside of the bomb. This temperature rise generally was noticed after about 12 min of heating. The maximum temperature reached on the outside of the bombs, in reductions using iodine boosters, was around 900°C about 19 min after the start of heating.

Chemicals.—The high purity vanadium pentoxide used in this work was obtained from the Electro Metallurgical Division of Union Carbide and Carbon. A typical analysis (figures are weight percentages) is given in Table I. Before being used in a reduction, the oxide was dried in air at 200°C.

Calcium, similar to that used by McKechnie and Seybolt (1), was used in this work. Iodine, used as an igniter-booster, was Eimer and Amends C. P. grade.

A series of reductions were made, varying the amounts of V_2O_5, excess calcium, and the iodine igniter-booster, in order to determine the optimum charge for the designed bomb. The V_2O_5, magnesia liner and cover, coarse magnesia grain and steel bomb were air-dried at ~200°C. After the liner had

[1] Manuscript received September 17, 1953. This paper was prepared for delivery before the New York Meeting, April 12 to 16, 1953.

TABLE I. *Analysis of high purity* V_2O_5

Element	Weight %	Remarks
C	0.003	Chemical analyses
H_2	0.047	
N_2	0.0114	
Si	0.30	
Be	<0.0005	Spectrographic analyses are approximate and may be in error by a factor of 3.
Mn	<0.005	
Al	<0.1	
Mg	0.003	
Pb	<0.05	
Cr	0.05	
Ca	<0.1	
Sm	<0.02	
Mo	<0.02	
Co	<0.04	
Fe	0.08	
Cu	0.0005	
Na	0.05	
Zn	<0.1	
Ni	<0.01	
Ti	0.02	

FIG. 1. Vandium button produced by bomb reduction of V_2O_5 with calcium.

cooled, it was filled with a well-mixed composition of calcium, iodine, and V_2O_5, and placed in the steel bomb. Coarse magnesia grain was jolted into the space between the bomb wall and liner. The space above the magnesia cover of the liner was also filled with magnesia grain. The steel lid was bolted down with six ½ in. diameter bolts by means of a torque wrench to insure uniform pressure on the copper gasket. After being evacuated and flushed several times with argon or helium, the reaction vessel was sealed under an atmosphere of inert gas. It was then heated by induction behind a concrete wall which was a safety shield for the experimenter.

RESULTS

In preliminary work on making large scale reductions, a number of attempts were made to form dense magnesia liners in the bomb. Reductions, using these liners, resulted in slag absorption from the reduction to such an extent that the molten vanadium button would wet and react with the liner. The dense, high-fired preformed magnesia crucibles absorbed some slag but a layer always separated the conglomerated metal from the liner proper. Also, as mentioned previously, this type of liner facilitated the removal of the reaction products after a reduction.

Pressed charges of 2180 g of V_2O_5, 3840 g of Ca, and 1090 g of I_2, and unpressed charges of 1635 g of V_2O_5, 2880 g of Ca, 818 g of I_2 were found to be optimum for the bomb size and heating cycle employed. An excess of calcium of 53–54% resulted in an optimum yield of metal of 84%. At 40% and 60% excesses the yields dropped 10% to 5%, respectively. Below about 40% excess calcium, the amount of oxygen in the vanadium button increases to more than 0.05 wt %, thus embrittling the metal beyond cold workability. The effect of changing the amount of iodine booster-igniter was not as apparent. Using half the amount considered optimum decreased the yield of about 4%. Using twice the amount influenced the yield very little.

The vanadium buttons obtained in this process are 770–1020 g, depending on size of charge used. The metal conglomerated quite nicely as shown in Fig. 1. Slag inclusions however were present and could not be completely leached out of the as-reduced button. The latter can be cold-rolled down to sheet without annealing. Comparison of typical analysis of vanadium produced in this work with other reported materials is given in Table II.

No direct correlation of oxygen content of the vanadium buttons with Vickers Hardness Number was found (2). This is understandable considering the variance in carbon, nitrogen, and silica contents of the buttons. All of these and other elements could influence the hardness. However, oxygen content above about 0.05% generally rendered the vanadium too brittle for cold working. This was first observed by McKechnie and Seybolt.

Some visual evidence of the constituent present at the grain boundaries of as-reduced vanadium is shown in Fig. 2, 3, and 4 as being carbide.

The silicon content of most of the metal produced in this work ran higher than in metal reported by McKechnie and Seybolt (1). It was thought that it could cause embrittlement, but up to concentrations

TABLE II. *Comparative analyses of vanadium*

Reported by	Oxygen	Nitrogen	Hydrogen	Carbon	Iron	Silicon	Calcium
	%	%	%	%	%	%	%
McKechnie and Seybolt (1)	0.031	0.016	0.005	0.21	<0.01	0.04	0.023
	0.017	0.013	0.002	0.20	<0.01	0.001	0.014
Kinzel (3)	0.05–0.12	0.02–0.04	0.001–0.004	0.03–0.07	—	—	—
Gregory, Lilliendahl, and Wroughton (4)	0.1–0.25	0.01–0.015	—	0.05	0.01	—	0.05
Beard and Crooks, this paper	0.028	0.005	0.001	0.126	—	0.065	<0.1*
	0.033	0.013	0.002	0.102	—	0.04	<0.1

* Spectrographic analyses of calcium are approximate and may be in error by a factor of 3.

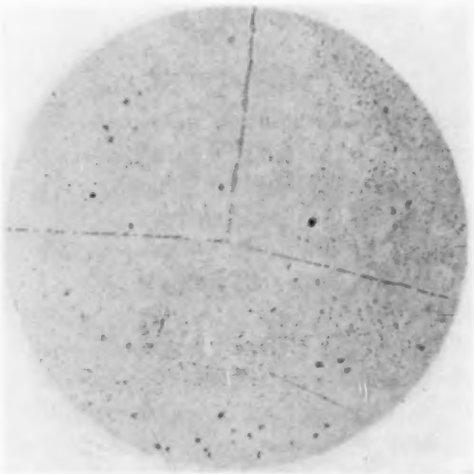

FIG. 2. As-reduced vanadium. % oxygen = 0.047, % nitrogen = 0.009, % carbon = 0.092, and VHN = 134. Etchant 10% hydrochloric acid. 250× B.F. before reduction for publication.

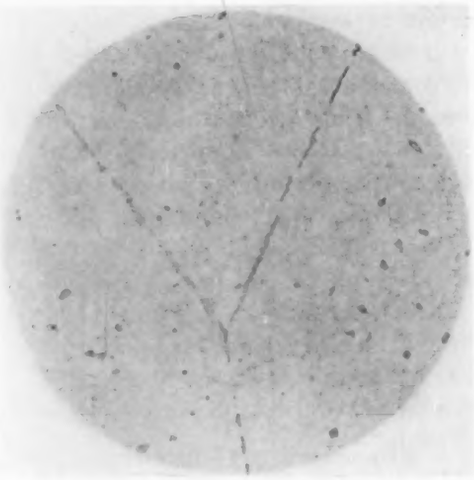

FIG. 3. As-reduced vanadium. % oxygen = 0.047, % nitrogen = 0.009, % carbon = 0.125, and VHN = 136. Etchant 10% hydrochloric acid. 250× B.F. before reduction for publication.

of 0.2 wt % no correlation between silicon concentration and increased hardness of the vanadium could be found. This silicon impurity was traced directly to the V_2O_5. The amounts of nitrogen in various

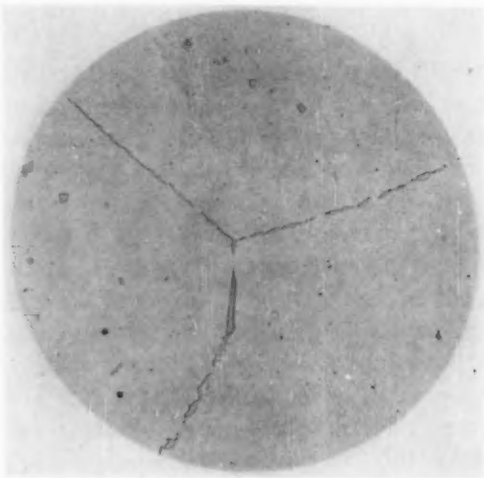

FIG. 4. As-reduced vanadium. % oxygen = 0.049, % nitrogen = 0.009, % carbon = 0.175, and VHN = 131. Etchant 10% hydrochloric acid. 250× B.F. before reduction for publication.

buttons were found generally to be less than one half that expected from analyses of the starting materials.

Conclusions

The feasibility of producing 750–1000 gram buttons of vanadium by reduction of V_2O_5 with calcium, using an iodine igniter-booster, and still retain the purity found in material produced on a 125 g scale by McKechnie and Seybolt has been shown. The percentage yield of massive metal has been increased from 74% to 84%. The amount of excess calcium necessary to give highest yield of ductile metal was reduced from about 60% to 54%.

Oxygen impurity in vanadium seems to be the main embrittling agent in this process. Silicon impurity up to 0.2 wt % does not seem to cause embrittlement of the vanadium.

Acknowledgments

The authors wish to express their appreciation for assistance in this work by coworkers and for dis-

cussions with A. U. Seybolt. Analyses in Tables I and II are by courtesy of L. P. Pepkowitz, W. S. Horton, and F. P. Landis of the General Electric Company.

Any discussion of this paper will appear in a Discussion Section to be published in the June 1955 JOURNAL.

REFERENCES

1. R. K. McKechnie and A. U. Seybolt, *This Journal*, **97**, 311 (1950).
2. A. U. Seybolt and H. T. Sumsion, *Trans. Am. Inst. Mining Met. Engrs.*, **197**, 292 (1953).
3. A. B. Kinzel, *Metal Prog.*, **58**, 315 (1950).
4. E. D. Gregory, W. C. Lilliendahl, and D. M. Wroughton, *This Journal*, **98**, 295 (1951).

Inert-Gas Forging[1]

CARL L. KOLBE

Research Laboratory, General Electric Company, Schenectady, New York

ABSTRACT

Apparatus has been designed and operated to enable a metal specimen to remain in argon gas during an entire heating and forging operation. A furnace capable of operating to 2500°C is coupled to a 250-lb pneumatic air hammer, so that materials may be forged at extremely high temperatures with a minimum of oxidation. Molybdenum and tungsten alloys have been forged between 1750° and 2200°C without visible surface oxidation. A titanium alloy was forged at 1500°C.

With this equipment there can be less diffusion of gases into the material, minor slippery oxide films, less surface cracking, easier deformation at higher forging temperatures than ever before possible.

INTRODUCTION

To obtain the best mechanical properties of a metal, deformation by forging, rolling, swaging, or extruding is usually required. These operations generally involve heating in air or in some protective atmosphere, followed by deforming in air. However, metals and alloys which have a great affinity for gases at high temperatures are now being fabricated and, as a result, new methods must be employed to reduce successfully the harmful effects obtained from heating or forging in air, hydrogen, or nitrogen. Pure beryllium, titanium, zirconium, and uranium may be deformed at moderately low temperatures and rolled in steel packs. These packs are excellent for keeping the material hot and reducing oxidation. However, this method has disadvantages. The working range is limited to a temperature below the melting point of the sheathing material; the material being worked is hidden from view; there is a probability of welding and sticking to the sheath material; and the cost of fabrication is high. Inert-gas forging helps eliminate these problems.

Refractory metals are being considered as base materials for high temperature applications, so it seems reasonable that higher forging temperatures will be needed if these materials are to be deformed successfully. Inert-gas forging can help protect metals from gross oxidation while at high temperatures, thereby reducing scaling and the loss of valuable material and ductility by oxidation.

EXPERIMENTAL PROCEDURE

Apparatus.—The apparatus included a forging hammer (250-lb Nazel pneumatic air hammer capable of 210 strokes/min), a furnace (with a graphite tube as the heating element and powdered graphite as insulation), and metal work chamber. A 3000 cycle, 100 kw induction coil was used to induce temperatures to 2500°C. The graphite tube had an inside diameter of 10.3 cm and was 91.5 cm long. The entire furnace was placed in a gas-tight aluminum box (Fig. 1). The work chamber connected the hammer to the furnace, so that the three pieces of equipment became an integral unit. In order that the hammer could be operated in its usual manner, the hammer die and anvil were connected to the chamber with rubber bellows (Fig. 2). The front of the work chamber had a partial glass top section so that the interior could be observed. The bottom of the front section consisted of a rubber apron and rubber bellows-type gloves for manipulation of the material from the furnace to the hammer. An additional chamber small enough to be flushed clear of air in a short time was used to introduce or remove specimens or equipment from the work chamber after the regular operation began. A molybdenum boat was placed in the furnace and could be shoved in and out with a molybdenum poker. The specimens could be placed on the boat for heating to temperature. In case of danger of reaction with the boat, a stabilized zirconia block or a pure magnesia block was used between the specimens and the boat. In all of the work described here, welding-grade argon was used. No further attempt to purify the gas was made. Argon was introduced through the rear of the furnace and out into the work chamber where it was intermittently removed through a valve whenever pressure on the rubber apron became too high.

Material.—Table I gives complete information on materials used and their conditions and temperatures of forging.

Procedure.—After the equipment was assembled, a Freon-gas detector was used to reveal leaks. The whole unit was partially evacuated and filled with

[1] Manuscript received September 14, 1953. This paper was prepared for delivery before the New York Meeting, April 12 to 16, 1953.

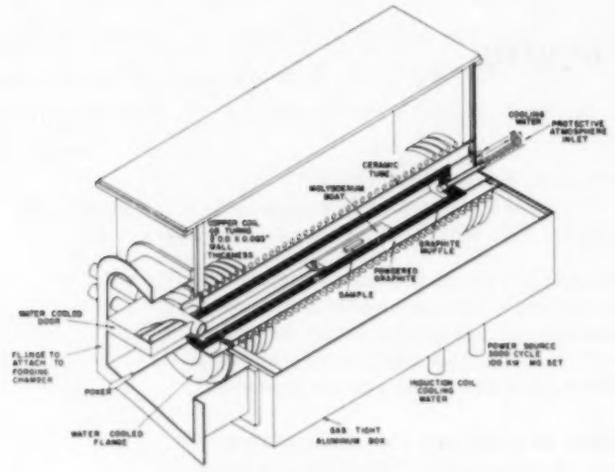

FIG. 1. Induction furnace details

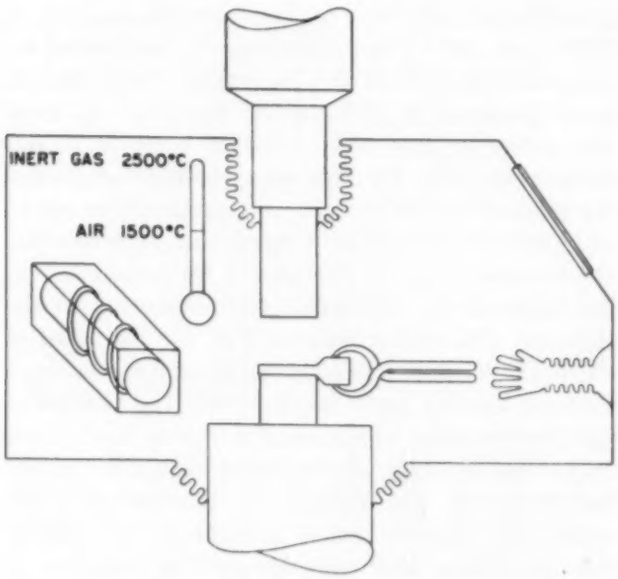

FIG. 2. Schematic drawing of the work chamber attached to the forging hammer and induction furnace.

TABLE I

Material	Condition	Forging temp (°C)
Mo	Arc-cast	1775
Mo-2.66Ti-0.084C	Arc-cast	1750, 1830, 1920
Mo-0.85V	Arc-cast	1800, 1920
W-30Mo-1.5Th	Sintered	2100, 2200
Ti alloy	Arc-cast	1500

argon. This operation was repeated three times. As the argon gas was being admitted for the final flushing treatment, the furnace was heated to temperature. Readings were taken from the furnace wall with an optical pyrometer. Specimens to be forged were placed directly on the molybdenum boat or on a ceramic slab and heated to temperature. The molybdenum boat was pulled forward in the furnace so that the specimen could be gripped with a pair of tongs and placed under the hammer. This final operation had to be performed quickly, since heat loss can be very great at such high temperatures.

EXPERIMENTAL RESULTS

A high degree of success was obtained in working all of the materials studied, but molybdenum-base alloys gave the best results. Pure molybdenum reduced to test-specimen size without any difficulty. Mo-Ti alloys could be reduced from 1.27 cm² to 6.4 mm² in one heat after some initial working. Weight losses on these small specimens were less than 0.5% when worked in argon atmosphere. Specimen surfaces were still bright, showing these losses were not caused by oxidation, but by small sections breaking off.

Mo-V alloys required temperatures above 1800°C for best results. Original work at 1800°C produced some edging cracks, but after these cracks were ground out and the temperature raised to 1920°C, no further edge cracks appeared. Some of this material was later reduced between 1200° and 800°C to 3.2 mm wire, which did not fracture after a 180-degree bend. This same alloy was later forged in air between 1800° and 2035°C with a 12% loss due to oxidation. Tensile tests showed no appreciable difference between the two materials. The W-Mo-Th alloy was forged from a 8.0 mm² sintered bar to a flat sheet 1.8 mm thick by 3.18 cm wide. This piece was later rolled in air to a sheet 0.36 mm thick by 3.8 cm wide with great difficulty and much edge cracking. Despite its reduction, the sheet was very brittle and could not be bent without heating.

An arc-cast button of Ti alloy was forged at 1500°C from 6.35 mm to 1.5 mm for tensile specimens and metallographic examination. Attempts to work this material in air previously had not been successful.

Temperatures reported throughout this paper must be considered as maximum temperatures, with the working range at the higher temperatures varying as much as 300°–400°C. For example, an alloy being reduced as much as 75% in one heat from a temperature of 1830°C may drop to a temperature as low as 1400°C before this operation is completed.

The atmosphere obtained during this work was inert enough to keep molybdenum alloys from oxidizing, but titanium alloys were slightly discolored.

Whenever possible, molybdenum alloys were forged as squares rather than the generally recommended octagons. The usual difficulty of developing a diamond shape during deformation was not encountered.

Conclusions

With the equipment described, materials can be worked at very high temperatures without the usual gross oxidation. For some alloys, this means less diffusion of gases into the material, minor slippery oxide films, less surface cracking, and easier deformation at higher temperature. Consequently, increased material recovery and improved forgeability are obtained.

Acknowledgments

Specimens for this work have come from various sources. Arc-melted molybdenum was from P. C. Rossin, General Electric Research Laboratory; the Mo-Ti-C was a salvage section of ingot No. 4–887 from Climax Molybdenum Company; the Mo-V alloy was purchased from the Climax Molybdenum Company; the W-Mo-Th alloy was from bar X51-3-11, Cleveland Wire Works, through J. Slivka; Ti alloy was furnished by J. McMullin, General Electric Research Laboratory. My gratitude to J. Nisbet, T. Doig, E. Jones, and other members of the Metal Processing Laboratory who have aided in this work.

Any discussion of this paper will appear in a Discussion Section, to be published in the June 1955 Journal.

Room-Temperature Ductile Chromium[1]

H. Johansen[2] and G. Asai

U. S. Bureau of Mines, Northwest Electrodevelopment Laboratory, Albany, Oregon

ABSTRACT

Development of the effort to find room-temperature ductile chromium is reviewed. Preparation and some mechanical properties of ductile chromium are described, as are techniques of making brittle chromium ductile by removal of surface layers. Reasons for the ductility, or lack of it, are advanced on the basis of experiments showing the effect of certain impurities, mechanical working, and heat treatment. No clear explanation for the surface phenomenon was obtained. Possible future uses of ductile chromium are discussed.

Introduction

The search for room-temperature ductile chromium has involved many investigators whose efforts have been summarized recently (1). Results of these investigations, until quite recently, were uniformly unsuccessful in obtaining room-temperature ductile metal.

Recently, room-temperature ductile sheet was produced from arc-melted electrolytic chromium (2) by a process described by Greenaway (3). Simultaneously, it was independently discovered at this laboratory that swaged chromium rod, pointed by an electrolytic etching process was ductile (4), and that ductility was dependent on removal of certain surface layers from the chromium.

Preparation and some mechanical properties of ductile chromium are the subject of the present paper. "Ductile" implies room-temperature ductility, unless otherwise specified.

Preparation of Ductile Metal

Preparation of ductile chromium has depended on at least two factors: production of metal of high purity, particularly with regard to oxygen, and discovery of certain techniques in hot and cold working of the metal.

Although first indications of ductility were observed in chromium produced by magnesium reduction of chromium chlorides, two other methods may be depended on for more certain results. One method is electrolysis of high purity chromic acid under special conditions of bath temperature and current density to produce electrolytic plate of very low impurity content—especially oxygen. This method has been described by Blum (5) and Greenaway (3, 6). Certain modifications in the method were developed at this laboratory (4) to enable greater production, since the electrolytic method suffers from a very low efficiency.

The second method is to reduce residual oxygen in commercial electrolytic chromium with hydrogen. A listing of the many earlier investigations of this method has been published (7).

The hydrogen reduction apparatus described in reference (8) has allowed production of chromium sufficiently pure to be made into ductile metal. In this process, powdered chromium metal is deoxidized with high purity hydrogen at 1200°C for 16 hr. Hydrogen is purified by a system using a cold trap, phosphorous pentoxide, and a zirconium getter.

Of the two methods, electrolysis gives the purer product; indeed, electrolytic plate made by this method, arc-melted and sheath-rolled at 850°C has given indication of ductility even without special surface preparation.

The hydrogen treatment method, however, lends itself to production of larger amounts, and, in addition to lowering the oxygen content, simultaneously lowers nitrogen, sulfur, and carbon contents.

One other method of production of chromium metal, the iodide dissociation method (9), should probably furnish ductile metal, although so far only individual grains have been reported as possessing ductility. The extreme difficulty of producing significant amounts of chromium metal by the iodide process seriously limits the usefulness of the technique.

Since the chief impurity remaining in electrolytic chromium is oxygen, purification attempts necessarily have revolved around removal of this element. In addition to the problem of removal, a reliable analysis for oxygen was sought. The method of Adcock (10), in which chromium is dissolved in hydrochloric acid and the residue considered to be the oxide, has been the standard method of oxygen analysis. For the lowest oxygen ranges, however, neither vacuum fusion nor the method of Adcock

[1] Manuscript received June 14, 1954. This paper was prepared for delivery before the Chicago Meeting, May 2 to 6, 1954.

[2] Present address: Department of Chemistry, University of Oregon, Eugene, Oregon.

give reliable results, and for the present work the appearance of the microstructure of a specimen of arc-melted chromium was used as the criterion of oxygen content.

Except where noted, all chromium tested in this work was purified by hydrogen treatment of commercial electrolytic chromium.[3] Purities have been better than 99.9% and usually better than 99.95%.

Mechanical Working

Techniques of working chromium from powder compacts have been described previously (7). The present investigation indicates that ductile sheet may be made by powder metallurgy, but with somewhat more difficulty than the arc-melting process (8). In general, hot work at a temperature of 1100°C is necessary while handling the arc-cast metal. After reductions of a minimum of 50%, cold work in the region of 800°C is required. As more cold work is done, the recrystallization temperature steadily declines so that final passes in swaging or rolling should be done from a furnace at less than 700°C.

Swaging

The following procedure has been used to produce 0.125 in. diameter rods from 2 in. diameter ingots by sheath swaging. Swaging unsheathed has been generally unsuccessful.

1. A 2 in. diameter arc-melted ingot was sheathed in stainless iron and swaged to 1 in. diameter at temperatures starting at 1100° and finishing at 900°C.

2. Recrystallization was accomplished by heating the swaging to 1200°C in hydrogen.

3. The swaging was resheathed in mild steel and swaged at 800°C to 0.5 in. diameter.

4. This was followed by recrystallization at 1200°C in hydrogen, resheathed, and swaged at 700°C to 0.125 in. diameter.

The as-swaged 0.125 in. diameter rods produced in this fashion are quite brittle to rapid bending at room temperature, although it was found that all would bend at very low strain rates. Typical examples of swaged rod are shown in Fig. 1.

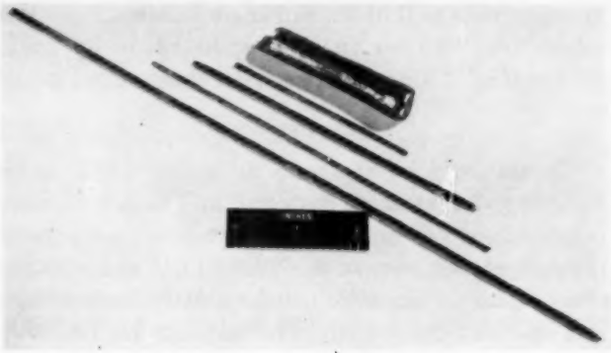

Fig. 1. Swaged rods

Rolling

Attempts have been made in the past to roll powder-compacted chromium in air directly. These attempts failed. All successful rolling was done with mild-steel sheathing which protected the chromium powder compacts from the chilling effect of the rolls and from air contamination. With the production of dense metal from the arc-melting process, protection from the atmosphere was not so crucial. In addition, with higher purity chromium, the brittle-to-ductile transition temperature was lowered so that rolling could safely proceed at lower temperatures; consequently the chilling effect was not so pronounced.

For preparation of thin, ductile sheet, rolling unsheathed with the resultant close control on dimension, surface finish, and extent of work, was a necessity.

Good quality sheet was prepared by the following procedures:

1. The arc-cast ingot, after a stress-relief anneal of 1200°C in hydrogen, was quartered longitudinally and hammer- or press-forged at 1100°C. Quartering of the ingot was found to eliminate a tendency of ingots to center burst on forging. Upset forging of arc-cast ingots has shown promise of being superior to the quartering method. Press forging was preferred for the smaller sizes.

2. The forging was recrystallized by heating to 1200°C in hydrogen. Again it was sheathed in mild steel and rolled at 700°–800°C to a reduction of about 50% in thickness. The chromium at this stage was very sensitive to surface chilling, hence the sheath was retained for the initial rolling step.

3. After desheathing, the sheet was rolled directly in air from an 800°C furnace to any thickness desired. The rolling temperature was gradually decreased so that final passes were made at an estimated sheet temperature of 400°C.

Reductions in rolling were moderate, of the order of 10%/pass initially, ending with 2%. Chromium

Fig. 2. Air-rolled sheet

[3] Purchased from Electro Metallurgical Company.

sheet as thin as 0.01 in. thickness was made by this procedure. Thinner sheet may be made by pack-rolling. Fig. 2 shows specimens of sheet rolled in air.

Wire Drawing

Chromium wire has been drawn at 600°C using swaged rod as starting material, and as low as room temperature on small wire diameters. Reductions in area per pass were of the order of 6 % at a starting size of 0.25 in. diameter using tungsten carbide dies in a lead-antimony bath. The smallest finished wire made by drawing had a 0.025 in. diameter. The following procedure has been found to produce consistent success in drawing wire: (*A*) the as-swaged rod at a starting size of about 0.25 in. is recrystallized by heating to 1200°C in hydrogen; (*B*) the rod is then drawn at 350°–400°C in a lead-antimony eutectic bath using Oildag[4] as a die lubricant.

Extrusion

Hot extrusion of 2 in. diameter ingots has proved successful. The ingots were sheathed in mild steel. Five ingots were extruded at 1100°C and all showed excellent results. Reductions in area were of the order of 80 %. The grain size of these extrusions after recrystallization was much smaller than that in swaged rods of equal reduction. Extruded material has been processed to ductile wire. Extrusion shows much promise in that extruded rods may be worked at lower temperatures on larger diameters; thus it offers hope for larger sections having ductility.

Surface Phenomenon

As noted above, removal of the surface layers of a swaged rod resulted in a remarkable increase in ductility of the specimen. It was soon established that the same technique applied to sheet and drawn wire as well.

The effect was first noticed while tipping rods for wire drawing in which a 250 g/l chromic acid-2.5 g/l sulfuric acid solution was used as an electrolyte. Chromium was made the anode and a strip of copper served as cathode. A current of 5–10 amp was passed through the cell for perhaps half a minute, or until a sufficient amount had been removed, sometimes as little as 0.002 in. in depth. Usually 0.005–0.01 in. on the diameter was removed.

The mode of removal of the surface layer does not appear to be significant. Mechanical, chemical, and electrolytic methods all confer the beneficial effect. However, electrolytic etching was found to give superior results, as well as the smoothest, brightest surface, so this method was usually employed.

Wain and Henderson (2) have reported ductility in chromium sheet as a result of chemical etching of the surface, and their results have been confirmed here using hydrochloric acid as the etchant. Mechanical removal of metal by use of polishing paper also serves to induce ductility, but it is somewhat less effective than chemical or electrolytic treatment. Fig. 3 shows typical specimens of room-temperature ductile chromium rod, wire, and sheet.

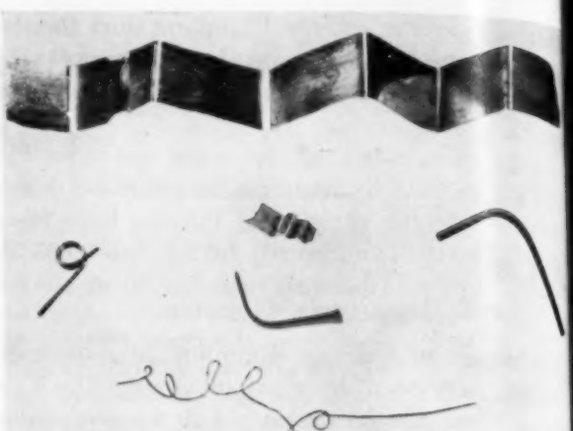

Fig. 3. Cold ductile wire, rod, and sheet

The phenomenon of dependency of ductility in chromium on the removal of certain surface layers has been anticipated in a British patent (11) obtained for a method of rendering brittle tungsten ductile by electrolytic removal of the surface layers. Shortly thereafter, this laboratory made tests on chromium sheet using conditions stated in the patent with entirely negative results.

Annealing appeared to improve bendability of unetched sheet slightly, but all test specimens annealed above 500°C broke at the slowest strain rate available. The etched specimens, however, continued to show excellent ductility in exploratory tests through 600°C when the number of reverse bends before failure began to fall off, until a specimen which had been heated to 900°C, then etched, could be bent only 10 times before failure. Since the recrystallization temperature was found by x-ray examination to be between 700° and 800°C, it was evident that chromium sheet may show some ductility in the recrystallized condition. Curiously, ductility in the recrystallized state could be produced in sheet, but not in wire.

Transition Temperature

The transition temperature of ductile wire was found to be in the range of 0° to −10°C as tested in bending with a ram speed of 60 in./min and as low as −66°C when tested with a ram speed of 0.079 in./min.

[4] Produced by Acheson Colloids, Port Huron, Michigan.

Tensile Tests

The tensile strength of electrolytic chromium at room temperature has been reported (15), as has that of sintered powder compacts (1), and of wrought and recrystallized chromium (16).

Room-temperature tensile tests were made on etched drawn wire in various conditions of heat treatment. A test of surface-treated wire was also carried out at 240°C. Specimens were prepared for testing by an initial etch of the entire wire, then the grip-ends were stopped off, and a center gauge section was reduced by further etching to insure fracture occurring in the gauge length. Specimens were held in Templin grips or modified Jacobs chucks. The loading rate was 0.02 in./min.

Mechanical Testing

The effect of temperature and purity on ductility and other properties of brittle chromium has been summarized for tests carried out exclusively on sintered powder compacts (1). High porosity of such test specimens leads to serious doubt of the validity of results recorded for mechanical properties as determined by bend, impact, and tensile tests. The present investigation gave quite different results, and the differences may be ascribed, in part at least, to the use of wrought chromium rather than sintered powder compacts, somewhat purer chromium, and surface preparation.

Bend Tests

Bend tests were made using equipment previously described (14) for testing brittle chromium to find the ductile-to-brittle transition temperature. One bender consisted of a simple two-point suspension so arranged that a manually depressed ram would strike the center of the test coupon or wire and rapidly bend or break it. The other bender operated in a similar fashion except that the rate of ram advance was adjustable by means of a variable speed drive mechanism.

A further test was frequently employed on thin specimens as a criterion of ductility: the number of times a specimen could be reverse bent rapidly by hand, before failure.

Results of bend testing air-rolled chromium sheet at room temperature (25°C) are shown in Table I. One sample as-rolled was shown to be bendable, but only at a slow strain rate. The same sheet after removal of 0.003 in. from each surface still had not broken after 50 reverse bends. After subsequent discovery of the present conditions for ductility, the treatment recommended in the patent was repeated and this time found to give full ductility. The explanation must be that the earlier chromium did not have proper characteristics for being made ductile, since careful etching to various depths did not produce ductile sheet. No specimen of the older chromium could be made ductile regardless of the extent of surface removal. This indicated that improved techniques for producing purer metal and for mechanical working to suitable structure were responsible for the improvement necessary to reach full ductility.

TABLE I. *Bend testing of* Cr *sheet S-1*

Condition of sheet	Max. strain rate* (in/in/sec) 10^{5}	Knoop hardness	Thickness after pickling	Reverse bends before failure
°C				
As-worked (0.013 in. thick)	12.8	255	0.007 in.	>50 times
200 Anneal	24	261	Not determined	
300 Anneal	24	255	Not determined	
400 Anneal	<7	255	Not determined	
500 Anneal	12.63	246	Not determined	
		271†		
600 Anneal	<2.9	252	0.0075	55
700 Anneal	<2.9	243	0.007	33
800 Anneal	<2.9	181	0.008	22
900 Anneal	<2.9	157	0.005	10

* Maximum strain rate for successful bending.
† On bend after bending.

Further indication of the surface removal effect has been noted for beryllium and vanadium. Kaufman, Gordon, and Lillie (12) reported that hot ductility in beryllium was improved by deep etching. Kinzel (13) noted the necessity for quite drastic surface removal to obtain vanadium sufficiently ductile for cold rolling.

The full explanation for the phenomenon of ductility obtained by surface removal techniques is lacking. Two possible causes are suggested immediately: contamination during the mechanical working steps, and/or a surface structure condition which may contain microcracks as a result of working. Fig. 4 shows on the left an as-drawn wire specimen which was deeply etched on one half and was

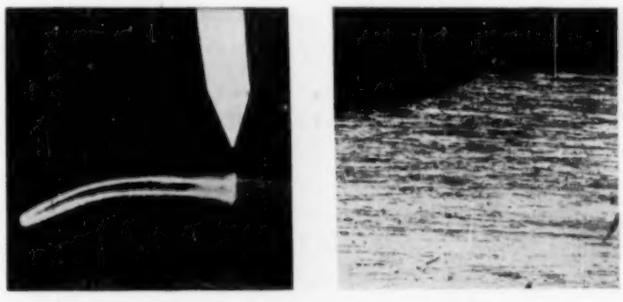

Fig. 4. Etched and bent wire on left (5×), arrow points to same zone in photomicrograph on right. 150× before reduced for publication.

bent cold. The arrow points to the boundary between the etched and unetched portions. The microstructure of the region indicated by the arrow is shown on the right. While the unetched zone indubitably shows a more strongly worked structure, the difference appears to be only a matter of degree. Hardness values taken across this specimen from outside edge to center showed that the average hardness (Knoop) in the edge region was 308 and the average for the interior was 246. No indication of a particular inclusion was visible.

As-worked.—The increased ductility of molybdenum and tungsten as a result of cold working is well known. Significant tensile test results are given in Table II and are plotted in Fig. 5 to show the effect of increasing cold work on the tensile properties of chromium wire. The results show that chromium work hardens to some extent, and that the rate of work hardening increases slightly with increased working beyond 80% reduction in area. However, wires drawn at 350°–400°C to result in a reduction in area of 95% without intermediate heat treatment, have very good bending properties in the as-worked conditions. The per cent elongation showed a variation which is to be expected considering the different diameters used and the short gauge lengths. However, a general lowering of per cent elongation with increase in work was indicated.

Two different types of fractures were exhibited by the as-worked specimens. There was the brittle, flat-granular failure which showed zero elongation, and there was a cup-cone fracture for the ductile failures. Test number 6 gave a 25% elongation and failed with a double cup-cone fracture as illustrated in Fig. 6.

Annealed.—The effect of heat treatment on the

TABLE II. *Tensile strength of cold* worked chromium*
Load rate = 0.02 in./min.

Test No.	Diameter at start (in.)	Diameter of test sample (in.)	%Red'n in area from drawing	Ult. str. 1000 psi	Elongation % in 1 in.
5	0.223	0.062	92.1	100.6	3†
26	0.216	0.062	91.8	100.6	2†
27	0.216	0.062	91.8	98.2	10
4	0.223	0.078	87.8	97.4	9
20	0.223	0.078	87.8	97.2	7
14	0.216	0.078	86.9	94.0	8
8	0.232	0.105	79.6	85.8	10
3	0.223	0.105	78.1	85.6	15
19	0.223	0.105	78.1	87.5	12
18	0.223	0.135	63.5	75.8	16
12	0.216	0.135	60.8	76.6	24
23	0.216	0.135	60.8	78.3	14
6	0.232	0.180	39.7	70.4	25

* Cold working was by drawing at 400°C.

† Broke outside gauge length; elongation due to "necking" not included in elongation values.

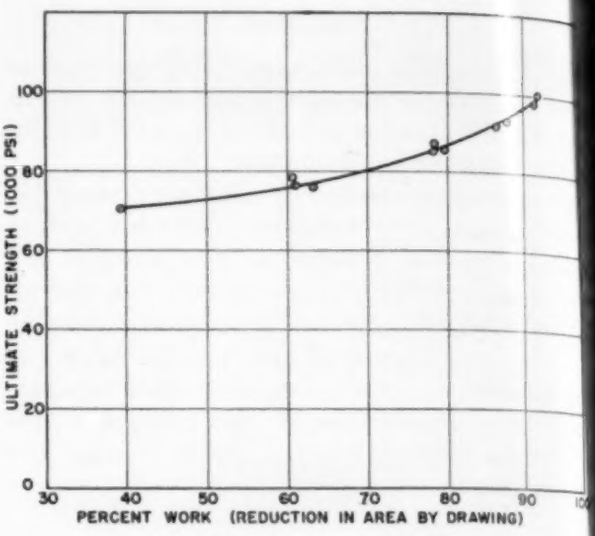

FIG. 5. Effect of cold work on ultimate strength

tensile strengths of 0.060 in. diameter wires was noted by comparing the as-worked wires with those annealed at 700°, 800°, and 900°C. The 700°C annealing was to represent stress relief, the 800°C anneal was to represent recrystallization, and the 900°C was to represent recrystallization and slight grain growth. All annealing was done in purified hydrogen or helium atmosphere. Since tensile strength of individual wires varied somewhat, annealed wires were compared with other portions of the same wire when possible. Results of these tests are given in Table III and show that: (*A*) annealing ¾ hr at 700° appears to reduce the ultimate strength by about 15% and correspondingly increases the elongation; (*B*) recrystallization by heating for ¾ hr at 800°C embrittled the specimens to the extent that they could not be held in the tensile grips to obtain a test.

Test at 240°C.—Three as-worked specimens were tested in tension at 240°C and the results compared with those tested at room temperature. Table IV

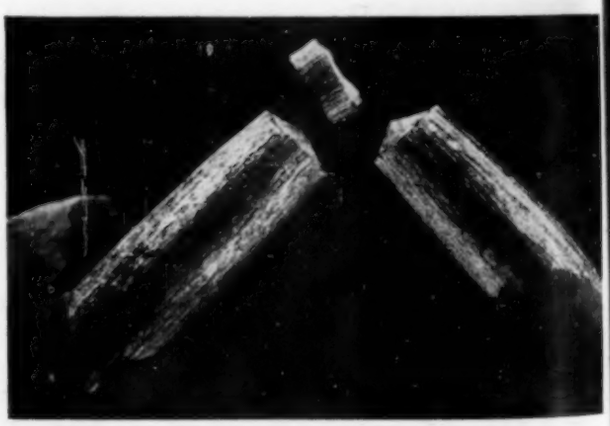

FIG. 6. Cup-cone tensile failure. 10× before reduced for publication.

TABLE III. *Tensile strength of as-worked and annealed wires*

Load rate 0.02 in./min.

Test No.	Material	Condition	Test diam. (in.)	Ult. str. 1000 psi	Elong. % in 1 in.	Remarks
32	W-28	As-worked	0.062	100.6	3*	
33	W-28	700°C–¾ hr	0.062	85.5	6*	
34	W-32	As-worked	0.062	100.6	2*	
35	W-32	As-worked	0.062	98.2	10	
36	W-32	700°C–¾ hr	0.062	85.5	7*	
37	W-38A	As-worked	0.062	112.1	7	
38	W-38A	As-worked	0.062	106.1	10	
39	W-38A	As-worked	0.062	106.9	9	
40	W-38A	700°C–¾ hr	0.062	91.7	12	
41	W-38A	700°C–¾ hr	0.062	90.0	12	
42	W-38A	800°C–¾ hr	0.062	Broke in grips		Recrystallized
43	W-38A	800°C–¾ hr	0.062	Broke in grips		Recrystallized
44	W-38A	900°C–5 hr	0.062	Broke in grips		Recrystallized with slight grain growth
45	W-38A	900°C–5 hr	0.062	Broke in grips		Recrystallized with slight grain growth
46	W-38B	As-worked	0.062	100.8	8	
47	W-38B	700°C–20 hr	0.062	95.3	0	
48	W-38B	700°C–20 hr	0.062	Broke in grips		

* Broke outside of gauge length; elongation due to "necking" not included in elongation value.

hows test results. Fracture of the 240°C tests were [redacted]ecking" and a definite silky ultimate strengths were n some reduction in cor[redacted]e-

act Tests

reported to have extremely This also is a matter of com- se who have attempted to t temperatures up to 325°C 0.5 ft lb, and at 700°C the 8 ft lb, so that chromium toughness even at tempera- transition temperature. ctile chromium, data on a few romium are included to show n temperature of about 350°C ellent impact strength.

nnotched Charpy specimens to compare better with other values (1). The 400°C test was made by removing the specimen from a furnace slightly above the test temperature and quickly placing it in the impact machine. Data are shown in Table V.

Room temperature impact values on as-cast material were so low as to be scarcely measureable. Results at a nominal 400°C, however, showed the large value of 118 ft lb. The specimens did not fracture, so a valid test was not obtained.

Lack of a suitable impact testing procedure for the smaller ductile rods and wires prevented inclusion of comparable data on ductile material.

TABLE IV. *Tensile strength of wire at 240°C*

Material	Test diameter	U. T. S. 1000 psi		Elongation % in 1 in.	
		25°C	240°C	25°C	240°C
W-29	0.135	79	71	16	16
W-29	0.104	86	78	10	7
W-29	0.078	93	88	8	5

TABLE V. *Impact test on as-cast chromium*

Specimen Number	Temp, °C (Nominal)	Impact ft lb	
1	Room	1.5	
2	400	119	Avg. 118
3	400	128	
4	400	106	

Torsion Test

No values for torsional strength of chromium have been noted in the literature. Excellent ductility in tension contrasts strongly with lower resistance to impact. Light peening with a hammer on ductile wire is sufficient to cause the wire to crumble. For that reason, behavior of ductile wire in torsion was of some interest.

A small torsion testing apparatus was constructed having a variable speed mechanism arranged to turn a chuck at a prearranged rate. Specimens were prepared by etching chromium wire which had been drawn as described, and all were in the as-worked condition. The specimen was placed between this chuck and another which was prevented from rotating by a lever arm with a weight attached. From the angle and weight needed to counterbalance the tor-

TABLE VI. *Torsion test*

Run No.	Mean diameter (in.)	Gauge length (in.)	Ult. strength psi	Ult. strain rev./in. (gauge)
T-2	0.055	2.75	92,200	9.35
T-3	0.051	2.50	93,000	10.4
T-4	0.051	2.88	95,100	20.5
T-6	0.051	1.75	94,800	19.0
T-10	0.051	3.00	92,400	23.4

sion the torsional strength was computed. All tests were at 25°C. Results of the tests are shown in Table VI. A typical torsion failure is shown in Fig. 7.

The results show an unexpected strength and ductility in torsion. A maximum ultimate strength of about 95,100 psi and a strain of 23.4 turns to the inch was obtained.

Creep Rupture

A creep rupture value for vacuum-cast electrolytic chromium has been recorded at 1 min for 20,000 psi and 871°C (17).

A single creep rupture test was carried out on a recrystalli[illegible] high purity chromium swaged [illegible] initially 10,000 psi at a temperatu[illegible]0 creep was noted over a period of one week, so the load was raised to 15,000 psi. The specimen had 0.01 in. elongation in 1.53 in. at the end of 1000 hr when the test was discontinued.

Effect on Ductility of Added Iron or Nickel

Regarding the effect of added elements on transition temperatures of chromium, it has been reported that iron and particularly nickel raise it (1).

To test the effect of added iron and nickel in making alloyed chromium wire using production techniques known to produce ductility in chromium alone, 1% alloys each of iron and nickel were made with high purity chromium. The powders were mixed, pressed into bars, sintered in hydrogen, and consumable arc-melted. The ingots were sheathed and swaged at 1000°C. The 1% nickel addition was found to be unusually hard in the as-cast condition (R_b88, while pure as-cast chromium is about R_b55) and shattered badly upon swaging at 1000°C. Remelting and reswaging of this ingot at 1250°C showed little improvement.

The case with the 1% iron alloy was different. Working to finished wire was accomplished with little difficulty, and the wire was ductile after surface removal. Hardness of the 1% iron alloy was about the same as that of pure chromium, i.e., about R_b55. One per cent iron increased the work hardening during wire drawing. Permissible reduction in area with the iron alloy during wire drawing at 400°C was about one-half that allowed with pure chromium, or about 45% and 95%, respectively, before annealing at 1200°C.

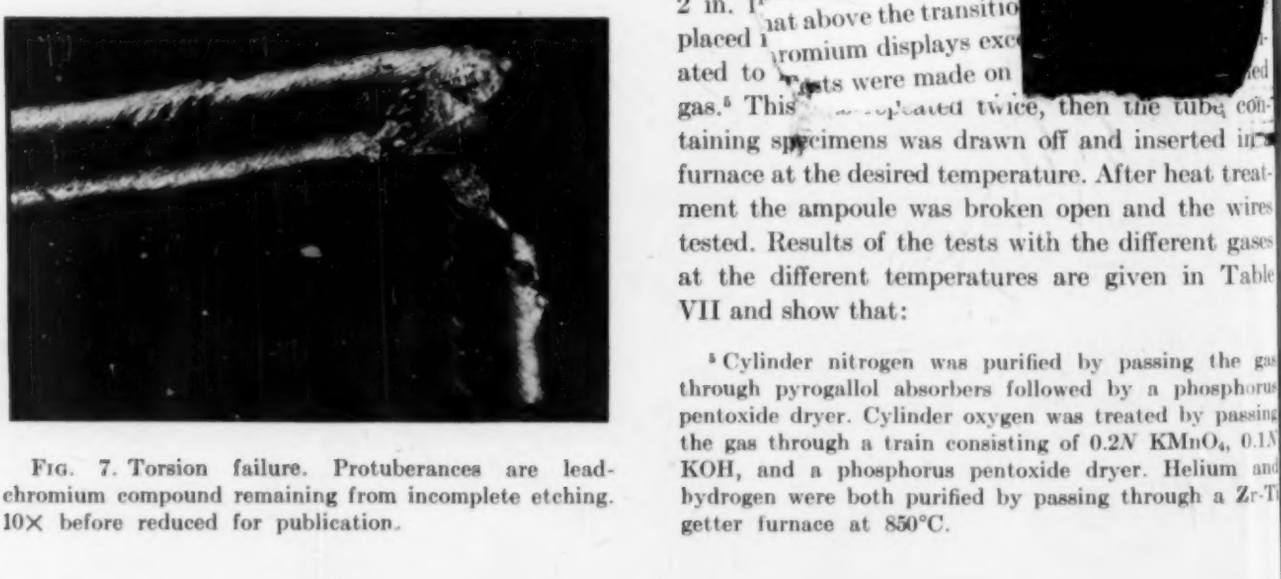

Fig. 7. Torsion failure. Protuberances are lead-chromium compound remaining from incomplete etching. 10× before reduced for publication.

Effect of Different Gases on Bending [illegible] of Wire

[illegible]y smoother "i[illegible] failure. The [illegible] lowered by 5–10% wit[illegible] sponding elongations.

Imp[illegible]

Chromium has been [illegible] low impact values (1). [illegible] mon experience to tho[illegible] work chromium cold. A[illegible] values did not exceed [illegible] values were only about [illegible] was considered to lack [illegible] tures well above the [illegible] While not a test of du[illegible] pecimens of as-cast ch[illegible] at above the transitio[illegible] romium displays exc[illegible] ated to [illegible]ts were made on [illegible] gas.[5] This [illegible] twice, then the tube containing specimens was drawn off and inserted in the furnace at the desired temperature. After heat treatment the ampoule was broken open and the wires tested. Results of the tests with the different gases at the different temperatures are given in Table VII and show that:

[5] Cylinder nitrogen was purified by passing the gas through pyrogallol absorbers followed by a phosphorus pentoxide dryer. Cylinder oxygen was treated by passing the gas through a train consisting of 0.2*N* $KMnO_4$, 0.1*N* KOH, and a phosphorus pentoxide dryer. Helium and hydrogen were both purified by passing through a Zr-Ti getter furnace at 850°C.

TABLE VII. *Effect of different gases on ductility*

Run	Ingot or wire	Diam	Gas	Temp, °C	Time (hr)	Color	Ductility as treated	Diameter as etched, in.	Ductility as etched	Remarks
O-1	SA4595	0.051	O_2	700	1	Scaly and green	Brittle	0.035	Bent	
O-4	SA5031	0.051	O_2	600	1	Scaly and green	Bent			
O-2	SA4595	0.051	O_2	500	1	Scaly and green	Bent			
O-3	SA5031	0.051	O_2	400	1	Slight green	Bent			
N-4	SA5031	0.054	N_2	600	1	Black and tan	Brittle	0.034	Bent	
N-5	W-23	0.052	N_2	500	1	Blue and tan	Brittle	0.045	Bent	
		0.036								
N-3	W-24	0.057	N_2	400	1	Slightly spotty	Bent and broke	0.040	Bent and broke	
		0.036								Bad sample
N-1	W-24	0.057	N_2	400	4¼	Spots of pale blue	Bent and broke	0.045	Bent and broke	Bad sample
N-6	W-29	0.052	Cyl. N_2	400	1	None	Bent			
N-7	W-29	0.052	Cyl. N_2	400	1	Slight tan	Bent			
N-8	W-36	0.052	Cyl. N_2	700	6	Gray and black	Brittle	0.048	Bent	
V-1	W-36	0.057	Vacuum	700	1	Metallic gray	Brittle	0.045	Bent	

1. Oxygen became harmful somewhere between 600° and 700°C.

2. Nitrogen became harmful somewhere between 400° and 500°C.

3. Hydrogen and helium gases gave inconclusive results since observations indicated that the embrittling effect may have been due to trace contamination.

4. Only one sample[6] was tested in vacuum. Annealing at 700°C for 1 hr resulted in a surface disturbance which rendered it unbendable in the as-annealed surface condition.

5. Oxidation at 700°C seemed to be more penetrating than nitriding at 700°C, due possibly to the nature of the surface layer, the oxide being rather scale like and nonadherent as compared to the nitrided layer.

6. Metallographic examination of four other samples[7] showed that there was no perceivable difference in nature or depth of the corrosion layer.

Gaseous exposure tests indicated that the influence of nitrogen might bear more attention, and attempts were made to compare nitrogen contents in the surface layer and the body of the material. In one case, the surface layer of a 0.250 in. diameter swaging was turned off and its nitrogen content compared with the interior of the swaging.

R-1040 body	0.002 % N
R-1042 outer layer	0.02 % N

In the other case, ductile 0.052 in. diameter wire was exposed to cylinder nitrogen at 700°C for 6 hr. The thickness of removal required to render it bendable again was estimated to be 0.00175–0.0015 in. Knowing this, the entire sample was sent for nitrogen analysis and compared with nitrogen content of another section of the same wire which was not exposed to nitrogen. The discolored layer (0.00075 in.) was removed before sa[illegible]

R-1086 nonexposed	[illegible] N
R-1087 entire exposed wire	0.0208 % N

By calculation, concentration of nitrogen in the brittle layer was found to be approximately 0.1 %.

Discussion

Previous attempts to explain the brittle-ductile phenomenon in chromium have relied to a large extent on the presence of certain impurities, principally oxygen since it is usually the impurity present in largest amount. Pursuit of the highest purity chromium possible was a logical approach to the question of ductility in chromium, but as purer metal was made, it became apparent that purity was not the whole story. Kind and extent of deformation were found to play a role. It has been asserted that oxygen has relatively little influence on the transition temperature (1), and the theory has been advanced that iron on the surface of chromium obtained from the steel sheath in rolling operations may be the cause of the brittleness (2). This is supported by investigators who found that iron raised the ductile-to-brittle transition temperature (1).

Results of the present investigation do not agree with these findings concerning oxygen and iron. It is agreed that oxygen may not be the sole cause of brittleness, but it is considered to be a contributing factor. The fact remains that to date the only room-temperature ductile chromium has also been low oxygen chromium. It is possible that iron in high

[6] (V-1), Vycor enclosed.

[7] O-1, O-5, N-5, and N-3, Table VIII.

concentration on the surface, as from sheath rolling, may contribute to the brittleness, but the present experiment with a 1% iron alloy appeared to give material as ductile at room temperature as pure chromium.

Experiments with various gaseous atmospheres and the influence on the ductility showed several unexplained features. Oxygen was not found to be injurious up to 600°C, while hydrogen, helium, and vacuum gave results similar to nitrogen. From appearances of the specimens it was suspected that traces of nitrogen present in the other gases may have been the embrittling agent. The concentration of nitrogen in the brittle layer was found to be about 0.1%, considerably higher than expected. At temperatures below 800°C (approximate recrystallization temperature) all specimens were ductile after etching, and oxygen specimens were ductile below 700°C without etching. Specimens heated in air to 600°C, however, were brittle before etching.

No explanation for the brittle behavior can be advanced on the basis of the present work. A cold-ductile wire can be made brittle by heating in gettered hydrogen to 600°C. By removing as little as 0.002 in. from the radius, the wire can be made completely cold-ductile again. These results suggest that brittleness in chromium may be due to any one or a combination of several factors. Impurities such as oxygen, nitrogen, and nickel are considered to have possible influence, and the extent of cold work may be a factor. Cold-ductile wire heated above the recrystallization temperature is completely and permanently embrittled. However, one sample[8] showed an elongation of 25% after only a 40% reduction in area, and a portion of the worked area was removed by etching. So it was apparent that a completely cold-worked structure was not absolutely necessary for maximum cold-ductility as was considered previously.

Possible uses for fully ductile chromium will certainly be in the field of heat engines, where as an alloying agent its properties of heat, corrosion, and wear resistance are already utilized. Full use of the pure metal will not be possible, however, until the impact strength at room temperature is increased. Nevertheless, in view of the present relative ease of hot-forgeability and the good hot impact strength, a possible use is for turbine-bucket material.

Potential electronic uses for ductile wire are anticipated where the high vapor pressure at temperatures above 800°C would not be a disadvantage. Use as a thermocouple element may be possible. The excellent oxygen gettering property would be of advantage for some uses.

The achievement of room-temperature ductile chromium leads to the confident expectation that further investigation may unlock all the secrets of ductility dependence, not only for chromium, but for other body-center cubic metals as well.

[8] Tensile test No. 6, Table II.

Acknowledgment

Acknowledgment is made to W. J. Knapp who designed and carried out the torsion tests, and to R. G. Nelson who reviewed the manuscript.

Acknowledgment is also made to A. U. Seybolt and C. E. Lacy of Knolls Laboratory who performed the hot-extrusion of chromium.

Any discussion of this paper will appear in a Discussion Section to be published in the June 1955 JOURNAL.

REFERENCES

1. A. H. SULLY, E. A. BRANDES, AND K. W. MITCHELL, *J. Inst. Metals*, **81**, 585 (1953).
2. H. L. WAIN AND F. HENDERSON, *Proc. Phys. Soc. (London)*, **66**, 515 (1953).
3. H. T. GREENAWAY, "Pure Chromium, Its Production and Freezing Point," Report SM 163, Department of Supply, Aeronautical Research Laboratories, Melbourne, Australia, January 1951.
4. G. ASAI AND H. JOHANSEN, "Massive Chromium," Final Report to Army Ordnance Corps, Watertown Arsenal Laboratory, Watertown, Mass., September 15, 1953.
5. W. BLUM, *Trans. Electrochem. Soc.*, **90**, 87 (1946).
6. H. T. GREENAWAY, S. T. JOHNSTONE, AND M. K. McQUILLAN, *J. Inst. Metals*, **80**, 109 (1951).
7. W. J. KROLL, W. F. HERGERT, AND L. A. YERKES, *This Journal*, **97**, 258 (1950).
8. H. L. GILBERT, H. A. JOHANSEN, AND R. G. NELSON, *J. Metals*, **5**, 63 (1953).
9. H. B. GOODWIN, R. A. GILBERT, C. M. SCHWARTZ, AND C. T. GREENIDGE, *This Journal*, **100**, 152 (1953).
10. F. ADCOCK, *J. Iron Steel Inst.*, **115**, 369 (1927).
11. F. G. VAN DEN BORSCH, D. J. C. PURSER, D. S. H. SHANNON, AND VACUUM SCIENCE LTD., British Pat. 554,829, November 1941.
12. A. R. KAUFMAN, P. GORDON, AND D. W. LILLIE, *Trans. Am. Soc. Metals*, **42**, 785 (1950).
13. A. B. KINZEL, *Metal Progr.*, **58**, 315 (1950).
14. H. L. GILBERT, H. A. JOHANSEN, AND R. G. NELSON, "Malleable Chromium and Its Alloys," U. S. Bur. Mines Rept. Invest. 4905, September 1952.
15. A. BRENNER, P. BURKHEAD, AND C. JENNINGS, *J. Res. Nat. Bur. Standards*, **40**, 31 (1948).
16. H. A. JOHANSEN, H. L. GILBERT, R. G. NELSON, AND R. L. CARPENTER, "Tensile Properties of Pure Chromium at Elevated Temperatures," U. S. Bur. Mines Rept. Invest. 5058, May 1954.
17. R. M. PARKE AND F. P. BENS, "Chromium Base Alloys," Symposium on Materials for Gas Turbines, *ASTM*, Nov., 80 (1946).

The Role of the Electric Arc Furnace in Utilizing Some Strategic Off-Grade Ores[1]

LLOYD H. BANNING

Ferrous Metals Branch, Region II, U. S. Bureau of Mines, Albany, Oregon

ABSTRACT

A dry-top, arc-resistance, electric smelting technique for recovering strategic metals from off-grade ores is described. Advantages of using a bulky form of reductant such as hogged wood waste in the furnace charge are pointed out. Smelting test data on nickel ores, a siliceous manganese ore, off-grade chromite concentrates, a fine grained chromite ore, and aluminum silicates are presented. The relationship between a theoretical smelting efficiency and slag-to-metal ratio is shown. The possibility of applying this dry-top, arc-resistance, electric smelting technique to other ores is indicated.

INTRODUCTION

It has been estimated that the United States consumed 2,300,000 short tons of manganese ore, 1,334,000 tons of chromite, 106,000 tons of nickel, and 6,000,000 tons of bauxite in 1953 (1). Unfortunately, our country is largely dependent on foreign sources for these vital ores. Approximately 7% of the manganese ore, 4% of the chromite, and 28% of the bauxite was produced from domestic deposits. About 1% of the nickel consumed in the country was produced as a by-product of the domestic copper refining industry. Stockpiling programs for manganese and chromite have materially increased the domestic production of these ores in the last two years. Domestic nickel production will also be increased when the Hanna Nickel Smelting Company starts operation of their new electric ferronickel smelter near Riddle, Oregon, late in 1954. Since 1947 the domestic production of bauxite decreased from 39% to its estimated present proportion of 28% of domestic consumption.

There are many known off-grade deposits of nickel, chromium, manganese, and aluminum ores in continental United States which are not amenable to conventional mineral dressing and chemical treatment processes. The Bureau of Mines began investigations several years ago to determine the feasibility of treating some of these off-grade ores by electric smelting processes. Ravitz and coworkers at the Intermountain Experiment Station, Salt Lake City, Utah, have published results of some of the Bureau's early smelting investigations on smelting off-grade nickel ores (2, 3). Torgeson and coworkers at the Boulder City, Nevada, station, have published results of matte smelting tests on Chamberlain, South Dakota, manganese nodules (4). Batch smelting tests on Mouat, Montana, and Coquille, Oregon, chromite concentrates have been described by Wessel and Rasmussen (5). The practicability of using hogged fuel in electric smelting charges when smelting Pacific Northwest ores was pointed out by Rasmussen (6). Cremer's report on nickel smelting investigations at the Northwest Electrodevelopment Laboratory was released in January 1954 (7).

Electric smelting research is being continued at the Northwest Electrodevelopment Laboratory, Albany, Oregon, on "selective reduction" operations where only part of the metal oxides are reduced to metal, on "nonselective reduction" operations where almost all of the metal oxides are reduced to metal, and on "complete reduction" operations where all of the oxides charged to the furnace are reduced and no slag is produced. This paper describes these various smelting techniques.

FUNDAMENTALS OF ARC FURNACE SMELTING

In arc furnace smelting operations carbon is added to the charge only to reduce the oxides to metal. The degree of reduction is dependent on the quantity of reductant in the charge. The heat for the reduction reaction is generated either by arcing on the molten bath, or by passage of the current through the molten slag, or by a combination of both. When an arc is maintained between the molten bath and the electrodes the operation is usually referred to as arc-resistance smelting; when the electrodes contact the slag the operation is referred to as slag-resistance smelting. Both roofed furnaces and open-top furnaces are used. Most of the smelting research at Albany has been carried out in open-top furnaces using a dry-top, arc-resistance, smelting technique.

In dry-top, arc-resistance smelting operations reductants and usually fluxes are mixed with the ore and charged to the furnace. The reductant may

[1] Manuscript received April 9, 1954. This paper was prepared for delivery before the Chicago Meeting, May 2 to 6, 1954.

be coke, charcoal, sawdust, hogged fuel, metallic reductants such as ferrosilicon, or mixtures of these materials. When fluxes are used, fluxing reagents such as limestone or quartz are mixed with the charge so that the resulting slag will be fluid enough to tap from the furnace. When the furnace is operating normally, the charge is kept at a uniform thickness; the electrodes extend through the charge, and the useful heat for conducting the smelting is generated by arcing from the electrode tips to the molten bath and by the current passing through the slag; gas produced by the reaction escapes through the porous charge as it feeds continually into the smelting zone. Metal and slag are tapped from the furnace at regular intervals.

The most noteworthy feature of the smelting method employed at Albany, Oregon, is the use of hogged fuel in the charge. Hogged fuel, a by-product of Oregon's extensive lumber industry, is a mixture of wood chips, splinters, and sawdust resulting from feeding slabs, edgings, and other saw mill wastes through a machine called a "hog." Some advantages of using hogged fuel in the furnace charge are: (*A*) it forms a porous charge through which gases can readily escape and prevents crusting of the charge; (*B*) a hogged fuel charge serves as a heat insulating roof over the smelting zone; (*C*) the electrical conductivity of the charge is low; (*D*) vaporization and dust losses are minimized; and (*E*) the temperature of the smelting zone may be varied by adjustment of the proportion of hogged fuel to other reductants in the charge.

When analyses of the charge materials are known, flux, carbon, and electric energy requirements for conducting any electric smelting operation can be calculated. Three reasons for using fluxes are: (*a*) to control slag melting temperature; (*b*) to prevent corrosion to furnace refractories; and (*c*) to improve recovery of the metallic constituents. The natural slag melting temperature can be determined with the aid of slag-phase diagrams (8). The amount of necessary fluxes to be added to the furnace charge for producing a fluid slag can be determined by the same means. Furnace charges that produce acid slags are usually smelted in carbon lined furnaces; however, such linings cannot be used when carbon is deficient in the charge as in the selective reduction of low-carbon ferronickel from siliceous nickel ores. Usually a high-iron slag is produced and, although the slag is acid, a basic magnesite lining is used because of its resistance to high iron slags. Enough limestone could be used to make the slag basic, but it is generally good practice to keep the slag volume to a minimum.

Carbon requirements may be calculated from molecular weights of the reactants and the equation for the reaction. An example of a carbon calculation is shown below:

$$NiO + C + \text{heat} = CO + Ni$$

Therefore, 12.01 (mole wt C) lb C are required per 58.69 (mole wt Ni) lb Ni reduced, or 0.204 lb C are required per lb Ni reduced.

In reducing a metal from its oxide it is assumed that the electrical energy required for the reaction is the same quantity as that liberated when the metal is oxidized. When calculating the efficiency of electrical energy utilization in the electric furnace the only energy considered useful is that required for this reaction. The change in heat content (electrical energy) of a given reaction, ΔH, is obtained by subtracting the heats of formation of all the reacting materials from the heats of formation of all the products (9). An example of a calculation for determining the theoretical electrical energy for reducing Ni from NiO is as follows:

$$NiO + C + \text{heat} = CO + Ni$$

-57.8 kcal (NiO heat of formation per mole) $+ 0 =$
-26.4 kcal (CO heat of formation per mole) $+ 0$

ΔH for producing one mole Ni from NiO $= (-26.4 + 0) - (-57.8 + 0) = 31.4$ kcal

ΔH for 58.69 g Ni (one mole) $= 31.4$ kcal

ΔH for 1 g Ni $= 31.4/58.69 = 0.535$ kcal

ΔH for 1 lb Ni $= 0.535 \times 453.59 = 242.7$ kcal

$$1 \text{ kcal} = 0.0011628 \text{ kwhr}$$

Therefore, $242.7 \times 0.0011628 = 0.282$ kwhr of electrical energy is the theoretical quantity required to reduce 1 lb of Ni from NiO.

The calculated carbon and energy requirements for producing metal from the ores discussed in this paper are:

	Ni	Fe	Mn	Cr	Ti	Al	Si
Lb of C/lb	0.204	0.215	0.218	0.346	0.501	0.668	0.856
Kwhr/lb	0.282	0.355	0.717	0.952	1.70	3.03	2.80

Slag-to-metal ratio, carbon specification for metal, slag conductivity, charge conductivity, and desired smelting temperature are most of the factors that determine the proper voltage-current relationship to use in a particular electric smelting operation. Although an exact formula for determining this relationship has not been developed, sufficient data are available to indicate certain operating principles. A comparatively high voltage-current relationship is employed where there is a high slag-to-metal ratio. This is especially true when it is desired to produce

a low-carbon metal such as ferronickel from siliceous nickel ores. Slags produced when smelting these ores have comparatively high resistances. Contamination of the metal with carbon and high electrode consumption is prevented by using a voltage-current relationship high enough to prevent the electrodes from contacting the slag. Low-carbon ferronickel can also be produced from ferruginous nickel ores. Slags produced from these ores have a lower electrical resistance, due to the presence of iron oxide in the slag; a lower voltage-current relationship is used.

In operations where no slag is produced, such as the production of aluminum-silicon alloys, a low voltage-current relationship is employed. In this case, it is also important to use a charge having a low electrical conductivity. If either the voltage-current relationship or the charge conductivity is too high, current flows through the charge causing the charge to heat above the smelting zone, the electrodes to rise, and the smelting zone to cool. A continuation of these conditions usually results in an inoperable furnace. Generally these conditions can be corrected by increasing the current to the furnace. However, the current at which the maximum heating occurs is not necessarily the maximum current at which the furnace will operate. The current at which the maximum heating occurs may be called the optimum current. Optimum current in an electric arc furnace can be determined by a method described by Cochran (10). Optimum current differs for each voltage tap in steel-making furnaces; in smelting furnaces, optimum current may differ for each ore being smelted as well as for each voltage tap.

Description of Smelting Furnaces

Two 3-phase, cylindrical, stationary, pit-type, electric arc furnaces are available for making continuous experimental smelting tests at the Northwest Electrodevelopment Laboratory. The large furnace, designated ESB, using 8-in. or 6-in. graphite electrodes has a shell 96 in. in diameter and 78 in. high. Diameter inside the refractory is 67 in.; the height is 58 in. The small furnace designated ESA, using either 3-in. or 4-in. graphite electrodes, has a shell 50 in. in diameter and 55 in. high. Diameter inside the refractory is 32 in., and the height is 39 in. Carbon brick or magnesite brick are used for furnace linings. Furnace hearths are usually rammed with carbon paste or periclase. Both furnaces are used as open-top furnaces; however, provisions have been made for using a roof on the smaller furnace.

The electrode clamp arm assemblies are cable-suspended with provisions for readily changing electrode spacing. Graphite electrodes are placed at the corners of an equilateral triangle. Electrode current is automatically controlled by a balanced-beam type regulator. Either furnace when in use is connected to a 1000-kva Westinghouse transformer which has six voltage taps. The secondary busses of the transformer may be connected in series or parallel; when connected in series the voltage is approximately twice the parallel connection voltage. The open circuit phase-to-phase voltage ranges from 38 to 106 volts on the parallel connection and from 80 to 220 volts on the series connection.

Selective Reduction Smelting Techniques

Selective reduction smelting techniques have been employed to recover low-carbon ferronickel from off-grade nickel ores, high-purity iron from high-phosphorous iron ore, and to remove iron from manganese slags. The selective reduction technique is best illustrated by the results of a few of the tests on nickel ores. Table I shows the results of two smelting tests on Riddle ore from Douglas County, Oregon, two smelting tests on Cle Elum ore from Kittitas County, Washington, and one on Red Flat ore from Curry County, Oregon. All ores were treated under dry-top smelting conditions. In addition, open-arc smelting was employed in one test on Riddle ore. In this test the molten pool between electrodes was never allowed to become covered with raw charge. Also, a roofed furnace was used in one test on Cle Elum ore. In this test coke was the only reductant.

A cooperative agreement for conducting smelting research on Riddle nickel ore was entered into by the M. A. Hanna Company and the Bureau of Mines in 1951. Smelting tests on Riddle ore, discussed in this paper, were made while the cooperative agreement was in effect. Although the results were promising, the Hanna Nickel Smelting Company chose another process for ferronickel production at their new plant.

Examination of Table I indicates that higher proportions of carbon are required in the charge when smelting an ore high in iron. Only 3.92 times the carbon required to reduce the nickel oxide in the ore was used in the test on Riddle ore. The alloy product contained about twice as much iron as nickel. In the test on Red Flat ore, 12.8 times the stoichiometric proportion of carbon was used to produce an alloy containing about 8.5 times as much iron as nickel and, in the test on Cle Elum ore to produce a similar alloy, 32.5 times as much carbon was added to the charge as was theoretically required to reduce the nickel in the ore. Part of the carbon was undoubtedly consumed in reducing the Fe_2O_3 to FeO. Analyses indicate that more nickel is lost in the slag when a higher grade nickel metal is produced. The calculated nickel recovery for the tests on Red Flat and Cle Elum ore were both higher than the recovery on

TABLE I. *Selective reduction tests on nickel ores*

Type of smelting	Riddle		Cle Elum		Red Flat
	Dry-top	Open-arc	Dry-top	Roofed	Dry-top
Ore analyses, %					
Ni	1.5	1.5	1.19	1.19	0.74
Fe	15.2	15.2	45.9	45.9	28.2
C,* ratio to stoich. prop.	3.92	3.92	46.7	32.5	12.8
Lb of limestone/100 lb of ore	None	None	12.0	12.0	None
Time of test, hr	88	20	27	53	72
Feed rate, lb ore/hr	471	343	460	266	409
Electrical conditions:					
Voltage, phase-to-phase	205	158	120	120	200
Current, amp	400	700	1600	1000	653
Kw input	206	197	300	200	225
Kilowatt-hours:					
Per ton dry ore	875	1145	1335	1580	1072
Per lb of Ni in metal	47.9	67.0	72.1	84.5	88.1
Per lb of metal,					
Theoretical	0.34	0.32	0.35	0.35	0.34
Actual	15.4	23.6	5.7	9.4	13.2
Efficiency, %	2.18	1.37	6.17	3.68	2.57
Electrode consumption, lb/ton dry ore	12.2	32.0	9.2	18.4	10.5
Slag-to-metal ratio	15.9	19.5	6.3	9.6	14.9
Typical metal analysis:					
Ni, %	32.2	35.2	7.85	11.12	10.8
Fe, %	69.2	63.1	—	—	86.8
C, %	0.05	0.05	0.05	0.10	0.36
Slag analysis, %					
Ni	0.22	0.21	0.04	0.05	0.08
Fe	15.0	15.7	39.8	42.5	33.0
Ni recovery in metal, %†	83.3	83.4	96.2	96.0	87.1

* Carbon required for NiO only.

† Recovery figures based on weights and analyses of slag and metal products.

Riddle ore mainly because lower grade ferronickel alloys were produced.

The highest voltage tap was used in the tests on Riddle and Red Flat ores. Lower voltage was employed in the tests on Cle Elum ore. The operation indicated that the high-iron slag from the Cle Elum ore was a better conductor of electricity than the slags produced from Riddle and Red Flat ore. Therefore, to maintain stable arcs in the furnace, a lower voltage was employed.

Calculations indicate that higher efficiencies were obtained at higher kilowatt inputs. Electrode consumption appeared to be inversely proportional to kilowatt input. Results also indicate that efficiency, which is the percentage relationship between the theoretical electrical energy requirement and the actual requirement, increased as the slag-to-metal ratio decreased. Perhaps, the most significant figure in Table I is the kilowatt hour consumption per pound of nickel recovered. This figure, inversely proportional to the nickel content of the ore, varied from 47.9 for 1.5% Ni Riddle ore to 88.1 for 0.74% Ni Red Flat ore.

Nonselective Reduction Smelting

Nonselective reduction smelting may be defined as smelting operations in which no attempt is made to prevent small amounts of carbon, silicon, and other impurities from reducing into the metal product. The quantity of carbon added to the charge is not as critical as in selective reduction smelting or in complete reduction smelting, and the slag-to-metal ratio is much lower than in selective reduction smelting. Typical examples of nonselective smelting operations are the production of pig iron, high-carbon ferrochrome, and silicomanganese.

Smelting Tests on a Siliceous Manganese Ore

Present General Service Administration stockpile specifications limit the SiO_2 plus Al_2O_3 content of manganese ores to 15%. Smelting tests at the Northwest Electrodevelopment Laboratory have shown that this limitation on SiO_2 and Al_2O_3 has little bearing on the usefulness of manganese ore for the manufacture of silicomanganese. Table II shows the results of four dry-top smelting tests on a siliceous manganese ore, rhodonite, from southern Oregon

TABLE II. *Smelting tests on a siliceous manganese ore*

	Test No.				
	71-1	68-1	68-3	5-3	85-2
Furnace used	Small	Small	Small	Large	Small
Ore analysis, %					
Mn	24.8	24.8	24.8	27.2	32.4
Fe	2.06	2.06	2.06	2.1	3.2
SiO_2	45.5	45.5	45.5	45.2	40.7
C,* ratio to stoich. prop.	1.43	1.38	1.20	1.34	1.20
Lb of limestone/100 lb ore	12	23	36	42	42
Time of test, hr	7.8	8.6	11	8.5	6.6
Feed rate, lb ore/hr	239	210	191	471	167
Electrical conditions:					
Voltage, phase-to-phase	124	110	110	124	120
Current, amp	870	1,000	1,000	2,300	960
Kw input	190	200	200	500	200
Kilowatt-hours:					
Per ton ore	1,610	2,000	2,040	2,080	2,460
Per lb metal					
Theoretical	1.04	1.05	1.03	1.07	0.96
Actual	5.43	5.11	4.13	2.94	3.53
Efficiency, %	19.1	20.5	24.9	36.4	27.2
Electrode consumption, lb					
Per ton ore	23.0	37.0	37.0	23.6	35.6
Per ton metal	148.4	134.0	134.0	80.8	110
Slag-to-metal ratio	3.80	3.31	2.96	2.01	2.14
Metal analysis, %					
Mn	64.7	65.9	63.8	66.3	73.7
Fe	8.6	8.5	7.7	6.9	6.0
Si	19.3	19.5	19.6	20.2	14.8
Slag analysis, %					
Mn	15.6	12.2	8.4	6.8	4.1
Fe	0.25	0.33	2.0	0.4	0.70
SiO_2	52.3	51.2	48.0	46.0	40.0
CaO	12.5	22.3	30.0	33.4	40.0
MgO	1.2	1.81	2.77	1.3	4.2
Basicity of slag**	0.29	0.52	0.76	0.82	1.24
Mn recovery in metal, %†	52.0	62.0	71.4	86.1	89.2

* Theoretical carbon required to produce silicomanganese.

** Basicity is the mole ratio of the basic constituents to the acid constituents.

† Manganese recovery based on weights and analyses of metal and slag products.

This ore contained more than 45% silica. The fifth test was made on a sink-float concentrate from this same ore. These particular smelting tests were selected to show the relationship between the basicity of the slag and the manganese recovery in the silicomanganese product. Limestone was used in all the tests for control of basicity. One of the tests, 5-3, was conducted in the large furnace, the remainder being conducted in the small furnace. Carbon varied between 1.30 and 1.43 times the stoichiometric proportion, the highest proportion being used in the test in which the smallest amount of limestone was added to the charge. The highest manganese recovery was made on the sink-float concentrate. The relationship between the basicity of the slag and the manganese recovery is plotted in Fig. 1.

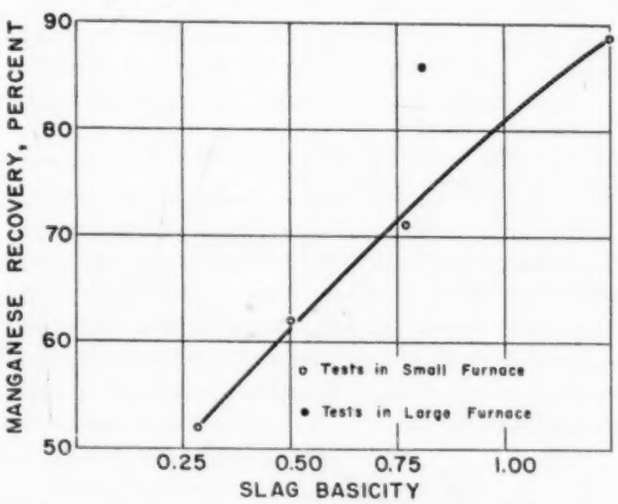

FIG. 1. Relationship between slag basicity and manganese recovery.

Results of smelting tests show a more efficient use of electrical energy and electrodes in the large furnace than in the small furnace. The calculated efficiency was up to 36.4% for the test in the large furnace and varied between 19 and 27% for tests in the small furnace.

Smelting Tests on Off-grade Chromites

Results of two smelting tests each on off-grade chromite concentrates from Mouat, Montana, and Coquille, Oregon, and one test on Iron King, Grant County, Oregon, chromite ore are shown in Table III. Quartz was the only flux used in the furnace charges. Hogged fuel and coke, correctly proportioned, were the reductants. The use of hogged fuel made it practical to smelt the chromite concentrates without previous agglomeration.

Four of the five smelting tests on chromite, shown in Table III, were made in the small furnace. One of the tests on Coquille concentrates was made at a phase-to-phase voltage of 158, the other three tests were made at a voltage of 200. The kilowatt input varied between 185 and 280, and was highest at the higher voltage. Electrode consumption was less and the reductant requirement was more when operating at the high voltage.

One smelting test on Mouat chromite concentrates was made in the large furnace. Results again indicated a more efficient use of electrical energy in the large furnace. Average calculated efficiency was higher for the chromite smelting tests than for the siliceous manganese smelting tests. The lower slag-to-metal ratio and the higher kilowatt input were factors contributing to the higher smelting efficiency.

The smelting test on Iron King chromite ore is noteworthy. The ore contained only 26.2% Cr_2O_3 and the slag-to-metal ratio was approximately twice as high as when smelting concentrates, but the kilo-

TABLE III. *Smelting tests on off-grade chromites*

Head sample	Mouat conc.		Coquille conc.		Iron King ore
Test No.	7	123	91	122	124
Furnace used	Large	Small	Small	Small	Small
Ore analysis, %					
Cr_2O_3	36.4	36.4	33.6	33.6	26.2
Fe	18.1	18.1	17.7	17.7	9.58
SiO_2	7.7	7.7	3.0	3.0	16.8
MgO	16.0	16.0	9.4	9.4	21.6
Al_2O_3	22.9	22.9	25.2	25.2	12.0
Lb of quartz/100 lb ore	20.8	22.0	20.0	20.0	17.0
C,* ratio to stoich. prop.	1.29	1.81	1.41	1.82	1.65
Time of test, hr	73	101.6	25	137	40.7
Feed rate, lb ore/hr	487.6	279.5	168	237	309
Electrical conditions					
Voltage, phase-to-phase	153	200	158	200	200
Current, amp	1800	900	700	900	900
Kw input, avg	450	280	185	255	248
Kilowatt-hours:					
Per ton ore	1848	2007	2200	2155	1610
Per lb Cr	4.33	4.53	4.81	4.53	4.50
Per lb metal					
Theoretical	0.766	0.698	0.726	0.718	0.758
Actual	2.15	2.24	2.40	2.19	2.65
Efficiency, %	35.6	31.2	30.2	32.8	28.6
Electrode consumption, lb					
Per ton ore	39.1	11.6	55.1	23.5	10.5
Per lb of Cr	0.092	0.026	0.120	0.049	0.029
Slag-to-metal ratio	1.41	1.34	1.38	1.08	2.55
Metal analysis, %					
Cr	49.8	49.4	49.9	48.3	54.8
Fe	36.0	37.4	34.6	34.9	32.5
Si	5.90	3.38	4.58	4.82	4.35
C	6.53	6.70	7.04	7.37	7.13
Slag analysis, %					
Cr	2.64	3.15	2.78	3.59	3.57
Fe	2.67	2.44	1.50	2.41	3.31
Cr recovery in metal, %†	93.0	92.1	92.9	92.5	87.2

* Percent of theoretical C required to reduce Cr and Fe in charge.

† Cr recovery based on weights and analyses of metal and slag products.

TABLE IV. *Complete reduction smelting*

Furnace used	Aluminum-silicon alloy		Chrome silicide	
	Small	Small	Large	Large
Materials charged, lb:				
Clay	100	74		
Quartz		26	100	100
Ferrochrome			55[a]	55[b]
C, ratio of stoich. prop	1.02[c]	0.95[c]	1.02[d]	0.97[d]
Time of test, hr	72	102	91.5	94.4
Feed rate, lb ore/hr	53	50	154	190
Electrical conditions:				
Voltage, phase-to-phase	52	38	42	54
Current, amp	1600	2100	5000	4500
Kw, input	135	140	350–400	420
Kilowatt-hours:				
Per ton ore	5080	5560	5000[e]	4321[e]
Per lb of alloy,				
Theoretical	2.67	2.62	2.80	2.80
Actual	7.1	6.7	7.34[f]	5.38[f]
Efficiency, %	37.6	39.1	38.1	52.0
Electrode consumption, lb				
Per ton ore	115	150	51.3[g]	55.14[g]
Per lb of alloy	0.16	0.18	0.067[h]	0.063[h]
Alloy analysis, %				
Al	46	33	—	—
Si	43	55	44.9	47.1
Cr	—	—	28.3	30.9
Fe	5.8	8	22.1	17.0
Ti	3.2	3	—	—
C	—	—	0.04	0.035

[a] Mouat ferrochrome.
[b] Iron King ferrochrome.
[c] Theoretical carbon required to reduce the SiO_2 and Al_2O_3 in the charge.
[d] Theoretical carbon required to reduce only the SiO_2 in the charge.
[e] Kilowatt-hour consumption per ton of quartz in the charge.
[f] Kilowatt-hour consumption per pound of silicon produced.
[g] Electrode consumption per ton of quartz in the charge.
[h] Electrode consumption per pound of silicon produced.

watt-hour consumption per pound of chromium recovered in the ferrochrome product was about the same as when smelting the higher Cr_2O_3 content concentrates. Eighty-seven per cent of the chromium was recovered in the metal product, which was only 5% lower than the recovery obtained when smelting concentrates.

Complete Reduction Smelting

Production of aluminum-silicon alloys, silicon, chrome silicide, and ferrosilicon are examples of complete reduction smelting processes. In these operations, all oxides charged to the furnace are reduced. No slag is tapped from the furnace unless there is a deficiency of reductant in the smelting charge. Electrodes are directly on the molten metal bath and a much lower voltage is used than when conducting a smelting operation in which slag is produced. Use of hogged fuel in the charge is especially beneficial in controlling the feed rate to the smelting zone and maintaining a continuous smelting operation.

Tests on the production of aluminum-silicon alloys containing from 33 to 46% aluminum, and on the production of chrome silicide are shown in Table IV. Tests on production of aluminum-silicon alloys were made in the small furnace; those on production of chrome silicide were made in the large furnace.

Tests on Aluminum-Silicon Alloy

The first research program on production of aluminum-silicon alloys was conducted in cooperation with the Apex Smelting Company of Chicago. It was during this smelting campaign that hogged fuel was first used in furnace charges. Promising test results obtained at that time have led to commercialization of the aluminum-silicon, 3-phase electric furnace, smelting process by the National Metallurgical Corporation at Springfield, Oregon.

Production of aluminum-silicon alloy in an electric arc furnace is probably the most difficult smelting operation conducted at the Northwest Electrodevelopment Laboratory. The correct quantity of

reductants properly proportioned is necessary to maintain a continuous smelting operation. A deficiency of carbon results in a selective reduction of silicon from the aluminum silicates and formation of a slag high in alumina. Unless tapping temperatures are extremely high, this slag cannot be drained from the furnace. An excess of carbon in the charge promotes formation of carbides which accumulate on the furnace hearth causing the electrodes to rise and eventually prevents tapping of the furnace. Data presented in Table IV indicate that an almost stoichiometric proportion of reductant was used.

In one test, only calcined clay and reductant were used in the furnace charge and a phase-to-phase voltage of 52 was employed; in the other test, quartz was mixed with the charge and the voltage was reduced to 38. The latter test was the easier operation. The difficulty of smelting aluminum silicates increases as the aluminum content of the charge increases. Efficiencies for these tests were considerably higher than for nonselective reduction smelting tests.

Tests on Production of Chrome Silicide

The silicon content of the chrome silicide product may be controlled by proportioning of quartz and ferrochrome in the charge. Standard grades of chrome silicide contain from 42 to 49% silicon, 34 to 41% chromium, and not over 0.05% carbon. Chrome silicide products containing less silicon usually exceed the maximum specifications for carbon.

Both chrome silicide smelting tests were conducted in the large furnace. The proportion of reductant used is comparable to that used in the production of aluminum-silicon alloys. Voltages used and electrical energy consumption per ton of oxides reduced were also comparable, although electrode consumption was considerably less. Results of these tests are shown in Table IV.

Effect of Slag-to-Metal Ratio on Smelting Efficiency

Efficiencies of all smelting tests presented in this paper are shown in the tables. These efficiencies have been calculated from theoretical electrical energy requirements and actual electrical energy requirements for production of the various alloys. For example, the theoretical electrical energy requirement for the production of ferrochrome from Iron King ore, shown in Table III, is calculated as follows:

54.8 (Cr content) × 0.952 (kwhr for production of 1 lb Cr)	= 0.521
32.5 (Fe content) × 0.355 (kwhr for production of 1 lb Fe)	= 0.115
4.35 (Si content) × 2.80 (kwhr for production of 1 lb Si)	= 0.122
Theoretical kwhr requirement per lb alloy produced	0.758

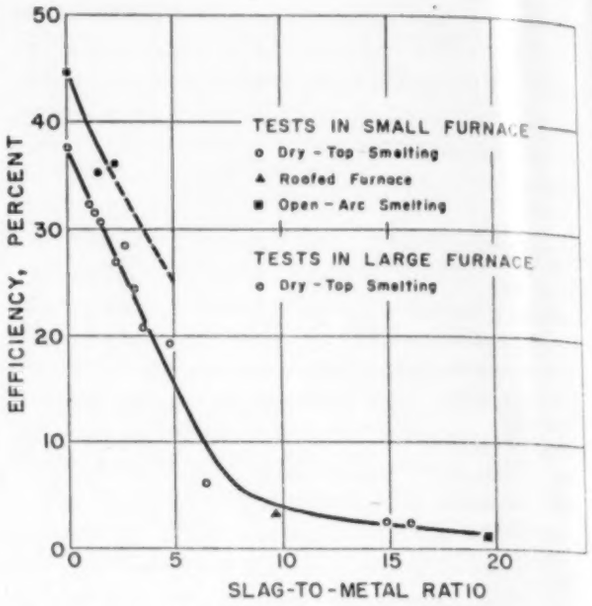

Fig. 2. Relationship between slag-to-metal ratio and smelting efficiency.

The actual electrical energy requirement for the production of 1 lb alloy was 2.65 kwhr. Using these data the efficiency of utilization of electrical energy is calculated to be 28.6%.

The relationship between the efficiency of electrical energy utilization and the slag-to-metal ratio for tests described in this paper is plotted in Fig. 2. The curves show how the efficiency of an electric smelting operation increases as the slag-to-metal ratio decreases, and indicate that this relationship is not materially affected by the type of material being smelted. Admittedly, other factors effect the efficiency of electrical energy utilization, for instance, the curves indicate that the efficiency is higher in a large furnace than in a small furnace. In one test on production of chrome silicide in the large furnace, the efficiency was calculated to be 52%. This efficiency is believed to be comparable to that attained in many commercial furnaces.

Conclusions

Smelting research in electric arc furnaces has indicated that some off-grade ores are amenable to treatment by smelting processes for the production of strategic metals. These investigations have led to some commercial developments. The National Metallurgical Corporation has begun production of aluminum-silicon alloys in an electric arc furnace at Springfield, Oregon. These alloys will be used to supply silicon for, and supplement aluminum in, commercial aluminum alloys. The Hanna Smelting Company plans to start production of ferronickel in electric arc furnaces near Riddle, Oregon, late this year. Previous to the initiation of these enterprises, the Bureau of Mines at Albany, Oregon, had

conducted smelting tests in cooperation with both companies.

Smelting tests have shown that a commercial grade silicomanganese can be produced from a siliceous manganese ore containing over three times the SiO_2 plus Al_2O_3 content acceptable under GSA stockpile specifications. Smelting tests on chromites have indicated that concentrates can be smelted without agglomeration and that a high recovery of chromium can be made by smelting a fine-grained chromite directly. These results indicate that production of silicomanganese from off-grade manganese ores, and ferrochrome and chrome silicide from off-grade chromites is commercially feasible.

Results of these tests indicate that the efficiency of electrical energy utilization is mainly dependent on the slag-to-metal ratio. A method has been described for determining this efficiency. Also, methods used in determining flux requirements, reductant requirements, and in selecting the proper electrical conditions for smelting operations have been described. These methods may be applied in selecting the proper conditions for carrying out electric smelting operations on ores other than those reported.

Any discussion of this paper will appear in a Discussion Section to be published in the June 1955 JOURNAL.

REFERENCES

1. *Eng. Mining J.*, **155,** No. 2, pp. 88–89, 99–100, 101, and 102 (1954).
2. S. F. RAVITZ, V. MILLER, AND F. B. PETERMANN, *Trans. Am. Inst. Mining Met. Engrs.*, **159,** 442 (1944).
3. S. F. RAVITZ, U. S. Bureau Mines Repts. Invest. 4122, September 1947.
4. D. R. TORGESON, T. E. EVANS, J. L. MORNING, F. W. WESSEL, AND R. G. KNICKERBOCKER, U. S. Bureau Mines Repts. Invest. 3917, September 1946.
5. F. W. WESSEL AND R. T. C. RASMUSSEN, *J. Metals*, **2,** 984 (1950).
6. R. T. C. RASMUSSEN, *J. Metals*, **4,** 1273 (1952).
7. H. CREMER, U. S. Bureau Mines Repts. Invest. 5021, January 1954.
8. E. F. OSBORN, R. C. DEVRIES, K. H. GEE, AND H. M. KRANER, *J. Metals*, **6,** 33 (1954).
9. F. H. GETMAN AND F. DANIELS, "Outlines of Physical Chemistry," 7th ed., p. 115, John Wiley & Sons, Inc., New York (1941).
10. D R. COCHRAN, *Blast Furnace Steel Plant*, **41,** 1031 (1953).

A New Furnace for Producton of Calcium Carbide and Other Products[1]

MARVIN J. UDY

546 Portage Road, Niagara Falls, New York

ABSTRACT

A new type of furnace has been developed for the manufacture of calcium carbide and high melting metals, alloys, and metallic carbides. The furnace is designed to move under the electrodes continuously, thus removing products as they are made. A large pilot plant furnace is needed to determine fully its advantages or disadvantages.

INTRODUCTION

The manufacture of CaC_2 had its beginning at the turn of the century, and many pertinent patents were issued between 1898 and 1908 (1–9).

Most early furnaces utilized single-phase power with top and bottom electrodes or with two suspended electrodes. Two of the most successful furnaces produced by these early workers were the continuous Horry furnace (1), and one presented by Leleux (6).

The Horry furnace, in operation at Niagara Falls during the period 1910–1915, was a rotary type, using single-phase power with two electrodes. The electrodes were suspended in a cast iron receptacle that moved away from the electrodes on the circumference of a vertical rotating wheel. To remove the carbide formed, segments on the circumference of the receptacle were removed when the carbide was cool enough. The segments were then used to extend the section of the receptacle around the electrodes, thereby forming a new section into which the charge was fed. Considerable early success was attained with this furnace as well as with the batch-type furnace.

The common drawback of all these early furnaces was the use of single-phase power, and this fact alone made it necessary to operate in small multiple units. Operating and maintenance costs were generally high. It was logical, therefore, that as the demand for calcium carbide grew, furnaces designed to use three-phase power were necessary. By 1915, or soon after, practically all CaC_2 was being produced in three-phase tapping furnaces.

In the operation of a three-phase tapping furnace for making CaC_2, there are difficulties in operation that have never been overcome, although calcium carbide furnaces have been increased in size to as much as 30,000 kva. A study of the melting point diagram of CaC_2 (10) will show clearly the reason for such difficulties in spite of furnace size, excellent electrical equipment and refractories, and greater technological skill.

Melting Point of Calcium Carbide and Its Effect on Furnace Operation

Pure CaC_2 melts at approximately 2300°C. Seventy per cent CaC_2 melts at approximately 1780°C, and 35% CaC_2 melts at approximately 1800°C.

The general practice today is to operate as close to 85% CaC_2 as possible, because this is the highest grade that can be successfully tapped from the furnace. Actually, commercial carbide averages about 80% CaC_2. Operating temperature of the present carbide furnace is, therefore, somewhat higher than 2100°C. The nominal 85% grade of CaC_2 yields 4.7 ft³ C_2H_2/lb CaC_2. U. S. specifications are as follows:

Size designation	Minimum average volume of acetylene gas evolved per lb at 60°F and 30 in. barometric pressure
Lump	4.5
Egg	4.5
Nut	4.5
½ by ¼	4.5
¼ by ⅛	4.5
Rice	4.3
14 ND	4.3

Rarely, however, does CaC_2 reach the customer with a yield as high as 4.7 ft³/lb CaC_2. Large producers are now making and selling acetylene directly to the user. However, carbide of less than 4.7 ft³/lb increases the ultimate cost.

Due to the high melting point of 85% CaC_2, operating problems are severe. Because there is 15% excess lime in 85% CaC_2, the problem of carbon balance is of prime importance. When the furnace is over-coked and purer carbide made, difficulty immediately results from higher conductivity of the

[1] Manuscript received March 19, 1954. This paper was prepared for delivery before the Chicago Meeting, May 2 to 6, 1954.

charge resulting in loss of control of electrode position. This difficulty usually shows itself in higher positions of electrode tips in the furnace and frozen CaC_2 on the bottom. Careful weighing of both carbon and lime is absolutely necessary. Segregation often takes place in getting the charge to the furnace, and unless the lime is really hard burned, lime air slakes, producing excessive dust. This inability to maintain proper carbon balance results in additional coke or lime being added from the working floor of the furnace. If the electrodes are high, lime is added, and if the electrodes are low, coke is added. In some cases, it has been the custom to add as much as 30% of the lime at the furnace working floor to keep the electrode tips in proper working position, in order to tap the carbide properly. This is quite a burden on the operators and demands considerable skill on their part. In some cases, 15% or more of the lime has been wasted as dust blown from the furnace. Electrode tip position in the charge is affected by the size of the lime and coke. Also, when a higher gas yield carbide is produced, tapping difficulties result.

Tapping of Calcium Carbide

Molten CaC_2 usually is tapped into cast metal molds or cars. While 85% CaC_2 chills rapidly on the surface, there is, nevertheless, considerable wear and tear on the molds. This comes chiefly from impurities like ferrosilicon which is reduced from silica in the lime and coke. The investment in molds for carbide is high. There has been some change in recent years, and some of the larger companies are now using casting wheels and casting into thinner ingots; however, casting wheels are expensive and require considerable maintenance. On larger furnaces when continuous tapping is approached, and on smaller furnaces where intermittent tapping is practiced, higher labor and maintenance costs are involved.

Development of New Process and New Type Furnace

Operational difficulties of a CaC_2 furnace and increasing labor costs led to re-examination of furnaces for the manufacture of calcium carbide. From a careful study of the CaC_2 production process and application of accumulated experience, an improved furnace, which seems feasible for commercial purposes, has been developed on a laboratory scale.

It appeared from a study of the melting point diagram for CaC_2 and lime that CaC_2 should be made readily at temperatures below the melting point of 85% CaC_2, or even down to 1800°C. It was reasoned, therefore, that high purity CaC_2 could be made directly in ingot form at a temperature below the melting point of 100% CaC_2. Also, if a furnace could be designed to use three-phase power, and at the same time operate with a carbon-to-lime ratio to produce high purity CaC_2 using 100% of the CaO present in the lime, the control of the carbon balance would be less critical. In addition, each unit of pure CaC_2 should be made with little or no increased power cost over the standard carbide made today. Dust losses could be reduced if the charge around the electrodes were reduced to a minimum.

In order to operate with the slight excess of coke required to make CaC_2 from 100% of the CaO, calcium carbide should be removed immediately from the vicinity of the electrode as fast as it is formed. This immediate removal of carbide would also remove excess coke, which in a normal furnace affects the position of the electrodes. In the proposed furnace, excess coke would have little effect on the electrode position. Also, less energy would be required since the CaC_2 would not need to be superheated for tapping. In addition, carbide is produced in ingot form continuously and is automatically removed from the furnace. This reduces labor costs in tapping. Furthermore, the furnace adapts itself to a low chargehead around the electrodes. Because of lower pressure in the low chargehead, dust losses are minimized. Under these conditions of lower pressure and lower temperature above the charge, a simple roof construction for recovery and control of fumes is possible. Early experimental work gave proof that these surmises were true and indicated that 100% CaC_2 can be made in place with little, if any, increased power cost per unit of pure CaC_2 over that required for the usual 85% max. CaC_2.

Experimental Furnaces

Two experimental furnaces using 150 kva were built,[2] one of the horizontal moving type and one of the vertical moving type in which the carbide was formed in place and removed as made. The horizontal type furnace differs radically from any previous furnace for CaC_2 production. Both furnaces show definitely that heat transfer from the arcs to the carbide and to the charge can be accomplished in very thin layers of charge (6–12 in.) above the tips of the electrodes. Reduced dust losses and cleaner carbon monoxide were observed. In the horizontal moving type, the electrode tips may be carried at the same level or at different levels. In the vertical type furnace, the electrode tips are at a constant level with the furnace moving down as the

[2] The work was carried out at Battelle Memorial Institute for the Research Development Corporation of Hamilton, Ontario, Canada.

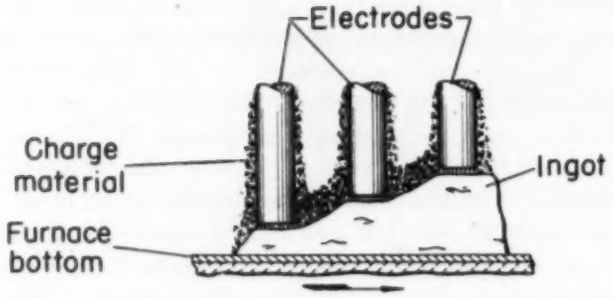

FIG. 1. Staggered electrode position of horizontal-type furnace.

CaC_2 is formed, thus removing the finished carbide out of the smelting zone.

The small horizontal laboratory furnace uses two ½-in. graphite electrodes placed at different levels and spaced so that the active areas around the electrodes do not quite touch. Under these conditions, the electrodes maintain their relative vertical position when on the automatic regulators. If spacing is too close, the electrodes take the same vertical position, the furnace is required to move faster, and the ingot of CaC_2 has less depth. Sufficient work has not been done to determine the relative values of these two types of operation.

Fig. 1 illustrates the electrode position and direction of movement of the car or furnace, also the different levels of the electrodes in the horizontal-type furnaces. This furnace body moved approximately ½ in./min. The voltage was 45–52 volts, electrode to ground.

In the vertical version, the furnace moves down away from the electrode. This furnace body moved at approximately ¾ in./min. In application, the furnace would be made of short vertical sections which would be removed from the ingot and returned to a position at top of the furnace around the electrodes.

Fig. 2 is an ingot of carbide produced in the horizontal furnace. It shows the beginning of the test run with the ingot coming up to approximately 1 ft in depth and then maintaining this depth until the test was stopped. The carbide averaged well above 5 ft^3 C_2H_2 per lb.

One example of the vertical-type furnace is shown in Fig. 3. In this version, the short section of the

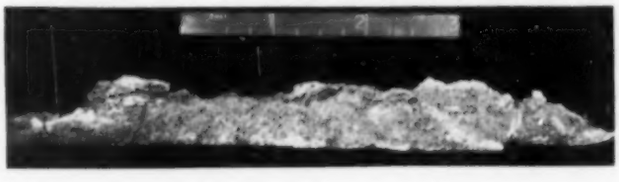

FIG. 2. Photograph of an ingot of calcium carbide produced in the horizontal continuous-ingot furnace. (Ingot was moved from right to left under the electrodes.)

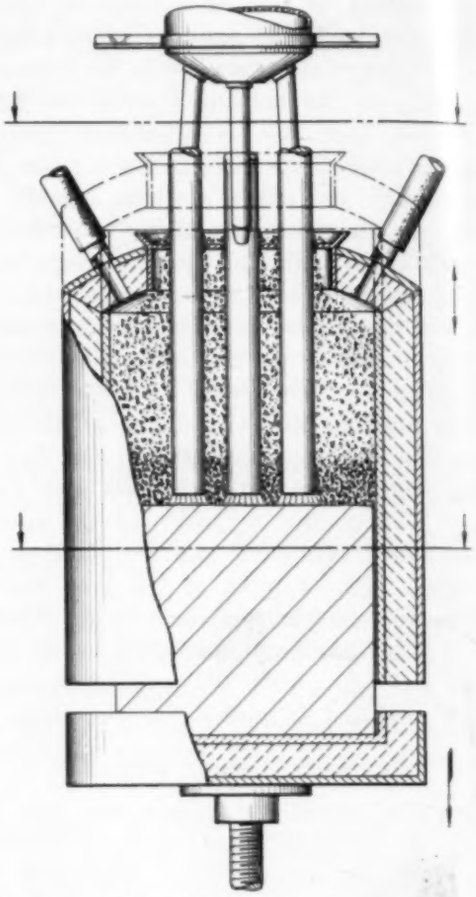

FIG. 3. Vertical furnace with reciprocating movement

furnace would be given a short reciprocating up and down movement to keep the ingot of CaC_2 free so that it can be lowered slowly.

Fig. 4 is an artist's drawing of a proposed 3000 kva horizontal furnace.

In general, it is believed at this time that for large furnaces of the order of 3000–30,000 kva, the horizontal version as shown in Fig. 4 will probably prove best from an engineering, cost, operating, and safety standpoint. The vertical furnace definitely has possibilities in smaller scale operations such as silicon carbide, aluminum carbide, ferrocarbo titanium, titanium carbonitride, calcium silicate, zir-

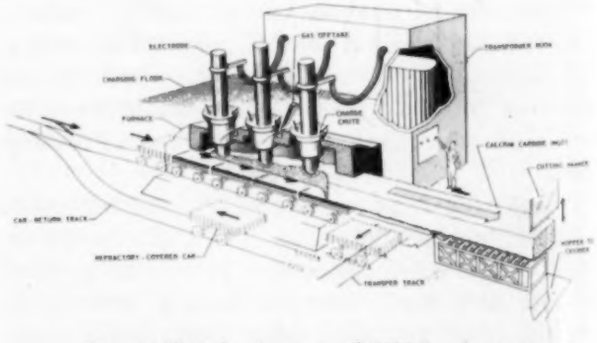

FIG. 4. Sketch of proposed 3000 kw furnace

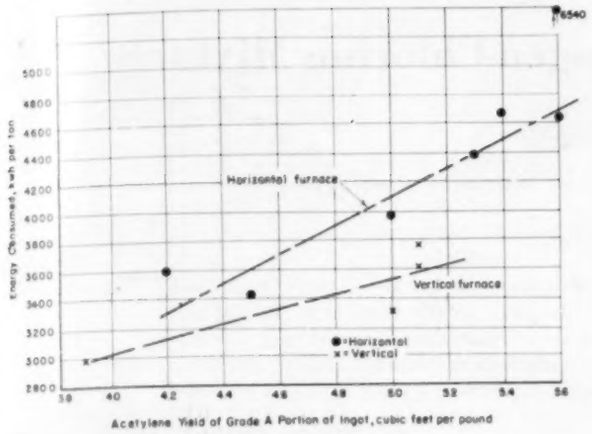

FIG. 5. Relationship of electrical energy consumed to acetylene yield of calcium carbide produced in laboratory furnace.

conium carbide, barium oxide, silicon metal, and other carbides, nitrides, and metals produced at high temperatures. Most of these products have already been made experimentally in the furnace.

Power Consumption Expected

The relationship of electrical energy consumed to acetylene yield of the carbide produced in the 150 kva furnaces is shown in Fig. 5. These data are based on short experimental runs. Conditions of starting and stopping undoubtedly influenced the results. Both furnaces would show greater efficiency when operated continuously, 24 hr/day.

With the 150 kva ingot furnace, the power consumption for CaC_2 yielding 4.7 ft^3/lb was indicated at about 3600 kwhr/ton, and for carbide yielding 5.6 ft^3/lb, the power consumption was indicated at about 4200 kwhr/ton. The high yield carbide was made from Mississippi lime and petroleum coke. It utilized 100% of the CaO present. A yield of 5.6 ft^3 acetylene/lb CaC_2 is approximately 19% more gas than obtained from the usual 85% CaC_2.

In any electric furnace scaled up from 150 kva to 3000–6000 kva or more, a decrease of 25% in power consumption can be expected. This would indicate about 3140 kwhr/ton CaC_2 having a 5.6 gas yield or a little more power than required in the present carbide furnace making CaC_2 with a gas yield of only 4.7 ft^3/lb.

Likewise, with 3600 kwhr for 80–85% CaC_2, one should expect a 25% decrease in power or approximately 2700 kwhr/ton of 80–85% CaC_2. However, these projected estimates of power consumption in large continuous ingot furnaces require substantiation in a pilot plant. It is felt that power consumption will be less per pound of acetylene than in present furnaces.

Dust losses are greatly reduced since the electrode tips are never submerged more than 6–12 in. in the charge. Under these conditions, carbon monoxide is freely evolved, eliminating formation of high pressure areas under the electrodes which causes blowing with resultant heavy dust losses.

In summation, the proposed furnaces appear to have a place in the manufacture of calcium carbide and allied products. Further development of the continuous-ingot type of furnace should result in a process with lower operating costs including less power consumption, lower labor costs, better operating conditions, easier material supply, minimized dust hazards, less air pollution, simpler roof construction, simplified gas collection, and possibly other advantages.

Any discussion of this paper will appear in a Discussion Section, to be published in the June 1955 JOURNAL.

REFERENCES

1. W. S. HORRY, U. S. Pat. 657,736, September 11, 1900.
2. J. ZIMMERMAN AND I. S. PRENNER, U. S. Pat. 671,008, April 2, 1901.
3. W. BORCHERS, U. S. Pat. 660,043, Oct. 16, 1900.
4. C. L. WILSON, C. MUMA, J. W. UNGER, *et al.*, U. S. Pat. 601,367, March 29, 1898.
5. J. M. MOORHEAD, U. S. Pat. 664,333, Dec. 18, 1900.
6. H. LELEUX, U. S. Pat. 654,463, July 24, 1900.
7. E. F. PRICE, U. S. Pat. 826,742, July 24, 1906.
8. J. C. KING, U. S. Pat. 872,352, Dec. 3, 1907.
9. C. E. WILSON, U. S. Pat. 943,290, Dec. 14, 1909.
10. C. H. AAL, *Chemistry and Industry*, **1950**, 830.

Explosive Limits of Hydrogen-Chlorine Mixtures[1]

A. W. Umland

The Dow Chemical Company, The Texas Division, Freeport, Texas

ABSTRACT

The lower explosive limit concentration of hydrogen (with upward flame propagation) in mixtures of chlorine containing oxygen, nitrogen, and carbon dioxide in proportions typical of electrolytic chlorine were determined at pressures from 0 to 135 psig. The explosive limit was found to be quite sensitive to variations of pressure and composition. It varied from about 3.1 to about 8.1% hydrogen depending on pressure and chlorine concentration.

Introduction

In the production of chlorine by the electrolysis of salt there are always a few per cent of other gases. These gases are made up of leakage air plus small amounts of hydrogen, oxygen, carbon dioxide, and carbon monoxide formed by secondary reactions occurring at the anodes and diaphragms. In a chlorine consuming process, as the chlorine is removed, these gases remain and increase in concentration. Ultimately the hydrogen concentration may increase until the mixture becomes potentially explosive. Therefore, in the interest of safety, it is desirable that explosive limits of hydrogen be accurately known in atmospheres of chlorine containing the usual impurities in the ratios present in cell gas at various pressures.

There have been few papers (1–5) published on the explosive limits of hydrogen and chlorine mixtures. Weisweiler (2) gives some explosive limits for pure hydrogen and chlorine. Lindeijer (3) gives the explosive limits with downward flame propagation at atmospheric pressure for three component systems of hydrogen and chlorine with nitrogen, carbon dioxide, oxygen, air, carbon monoxide, and nitric oxide. Since there has been no previous work published on the explosive limits of hydrogen in chlorine containing the usual impurities in cell gas at various pressures this work was undertaken.

The direction of flame propagation has a very marked effect upon explosive limits. Limits obtained when the column of gas is ignited at the bottom of the column allowing the flame to travel up (upward flame propagation) are less than those obtained with downward propagation. In fact, a downward limit mixture of some gases will give a severe explosion with upward flame propagation. Consequently, limits determined in this work are for upward flame propagation.

[1] Manuscript received May 5, 1954. This paper was prepared for delivery before the Chicago Meeting, May 2 to 6, 1954.

The definitions in the literature of explosive limits have been quite varied. A number of criteria have been proposed, among these are per cent combustion of gases, presence of flame, pressure rise, and velocity of flame propagation. The most acceptable definition is the lowest concentration of the gas in which a flame will continuously propagate through the entire volume of gas. The definition used for this work is the lowest concentration of hydrogen that will give an appreciable pressure rise. This was adopted because a flame can seldom be seen in a near limit explosion of a hydrogen-chlorine mixture even in a darkened room.

To obtain satisfactory explosive limits the experimental apparatus must meet certain requirements. The bomb should have an inside diameter of at least 5 cm (6, 7) to minimize wall effects. The source of ignition must have sufficient energy for positive ignition of the gases yet not high enough to cause disruptive effects in the bomb or give a partial ignition in the immediate vicinity of the ignitor (8).

Experimental

Explosive limits were determined in a stainless steel bomb having an inside diameter of 5 cm and a length of 20 cm. The volume of the bomb was 432 ml. A cross section of the bomb is shown in Fig. 1. The bomb was closed at one end with a high-pressure sight glass to permit visual observation of the determination. The opposite end was closed with a piece of 0.003 in. thick brass shim stock to serve as a safety rupture disk. A magnetically driven stirrer was provided for mixing the gases in the bomb. The stirrer was essentially a small centrifugal blower drawing the gases downward through the bomb and discharging into a 1 cm x 2 cm duct extending along one side of the bomb to the top of the bomb, thus providing positive circulation of the gases in the bomb.

A modified "spark plug" with a variable spark gap was provided for igniting the gases. The high voltage

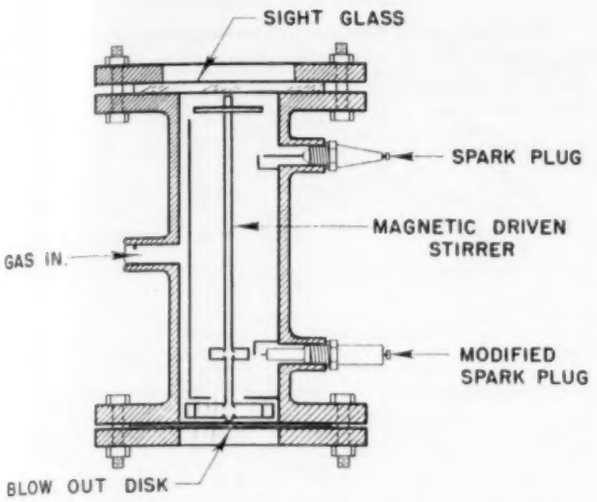

FIG. 1. Cross section of the bomb used for the determination of explosive limits.

electrode was fixed and used Teflon insulation. The other electrode was an eccentric metal plate on the shaft of the stirrer. The spark gap was varied by turning the stirrer shaft.

The assembled bomb was mounted vertically behind a heavy wood shield. A mirror was provided for viewing the bomb through a safety glass window in the shield.

A Foxboro recording pressure gauge with a range of 0–150 psi and having a 24-min clock was provided for recording the pressure wave of an explosion.

A high-pressure measuring buret was provided for measuring the volume of hydrogen added. This consisted of two graduated tubes, connected at the bottom, containing a confining liquid (hexachlorobutadiene). By proper setting of the valves at the top of the buret, hydrogen can be added to one tube to force the hydrogen in the other tube into the bomb as shown in Fig. 2. The connecting tubing between the bomb, gauges, etc., was made of ⅛ in. O.D. copper capillary tubing.

The electric spark for ignition was supplied by a high voltage power supply consisting of two model "T" Ford coils having their secondary windings in series feeding a rectifier doubler. The output of the power supply was 35,000 v D.C. A battery of 12 500 mmfd 25,000 v condensers were connected in series—parallel with the output of the power supply by a switch giving five steps of capacitance varying from 250 to 1500 mmfd. This provided a means of varying the intensity or energy of the spark.

The gas mixtures tested were mixed from commercially available gases. First, a stock gas containing the desired proportion of oxygen, nitrogen, and carbon dioxide was prepared. From this stock gas, mixtures containing approximately 5, 10, 20, 30, 40, and 50% chlorine were prepared. The lower explosive

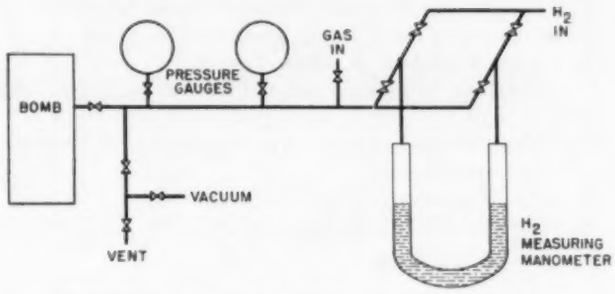

FIG. 2. Schematic diagram of the apparatus

limits of these mixtures with hydrogen were determined at pressure increments of 20 psi.

A gas mixture to be tested was placed in the bomb at the desired pressure (the bomb was first thoroughly evacuated). The valve at the bomb was closed, and the connecting tubing was evacuated and then filled with hydrogen to the same pressure. A measured volume of hydrogen at this same pressure was added to the bomb and mixed for ten minutes. The mixture was sparked, and any pressure rise from an explosion was recorded on the pressure recorder.

The per cent hydrogen added was calculated from the volume added using the ideal gas equation by the following equations:

$$\% \text{ Hydrogen} = \frac{H_1}{B + H_1} \times 100$$

$$H_1 = V_1 - V - (L + M + G - V_1)\left(\frac{B + L + M + G - V}{B + L + M + G - V_1} - 1\right)$$

If more than 28 ml of hydrogen was required, then:

$$\% \text{ Hydrogen} = \frac{\left(\frac{H_1 B}{B + H_1} + H_2\right) 100}{B + H_2}$$

$$H_2 = V_1 - V_2 - [L + M + G + V_2 - T]\left[\frac{B + L + M + G - T + V_1}{B + L + M + G - T + V_2} - \frac{(M + G - T + V_1)(T - 2V_1)K}{(B + L + M + G - T + V_2)P_1} - 1\right] - [M + G - T + V_1][T - 2V_1]\frac{K}{P_1}$$

B = Volume of bomb = 432 ml.
L = Volume of connecting tubing and gauges = 42 ml.
M = Volume of dead space above graduation of buret = 6 ml.
P = Initial pressure of charged gas in bomb psia.
P_1 = Pressure of gas after addition of hydrogen from side 1 of buret, psia.
P_2 = Pressure of gas after addition of hydrogen from side 2 of buret, psia.

h = Height of calibrated portion of buret = 6.75 in.
G = Volume of buret at top graduation = 28 ml.
V = Initial reading of buret 1.
V_1 = Reading of buret after addition of hydrogen from side 1.
V_2 = Final reading of buret 1 after addition of hydrogen from side 2.
T = Total volume of liquid in buret.
S = Specific gravity of seal liquid = 1.664.
$K = \frac{Sh}{27.7\,G} = 0.01448$.
H_1 = Volume of hydrogen added to bomb from side 1 of buret.
H_2 = Volume of hydrogen added to bomb from side 2 of buret.

Results

Approximately 1800 individual runs were made to determine the lower explosive limits with upward flame propagation of hydrogen with 30 mixtures of chlorine, oxygen, nitrogen, and carbon dioxide at pressure increments of 20 psi up to about 135 psig. These results are tabulated in Table I and are shown plotted vs. the pressure in Fig. 3, 4, 5, and 6. Each point shown is the result of from four to ten or more individual runs. The standard deviation of a single run is about 0.1%; consequently, the probability of the error of a single point being not greater than ±0.2% is about 90–95%.

The effect of pressure on explosive limits varies with each gas mixture and is unpredictable. Comparatively small changes in pressure or composition of the gas may make marked changes in the explosive limits; consequently, extrapolation or interpolation from the observed data can lead to large errors.

The effect of variation of chlorine concentration on the explosive limit of a typical cell gas mixture is shown in Fig. 7. The explosive limit reaches a maximum between 10 and 30% chlorine. This indicates that explosions with low chlorine concentrations are primarily hydrogen-oxygen explosions. The high heat capacity of the chlorine tends to increase the limit until the chlorine concentration is high enough for the "mass action" to shift to a hydrogen-chlorine explosion.

Increasing the temperature of the gas in general lowers the explosive limit, while decreasing the temperature raises the limit (Fig. 8). The explosive limit decreases with increasing oxygen concentration (Fig. 9). Replacing part of the nitrogen of air with carbon dioxide raises the explosive limit.

Fig. 10, 11, 12, and 13 give calculated curves for obtaining the safe operating limits of a chlorine consuming process. Final chlorine concentration is plotted vs. initial hydrogen concentration for various initial chlorine concentrations. For a given initial chlorine and hydrogen concentration the curve gives the final chlorine concentration at the explosion limit. All points to the left of the initial chlorine concentration line are safe mixtures while points to the right of the line are explosive.

TABLE I. *Typical results*[2]

Composition of the gas mixtures before addition of H_2 and the % H_2 at the lower explosive limit with upward flame propagation:

Gas No.	% Cl_2	Balance
1	0	A mixture of:
10	11.1	46.5% N_2
12	29.8	32.5% CO_2
13	5.7	21.1% O_2
14	19.1	
15	40.4	
17	52.5	

Pure Chlorine		Gas No. 1		Gas No. 10	
psig	% H_2	psig	% H_2	psig	% H_2
103	3.2	127	6.0	135	5.6
81	3.2	106	5.9	127	5.8
61	3.7	85	5.9	107	6.7
41	3.6	64	5.8	86	6.7
21	4.0	43	5.4	64	6.9
1	4.1	21	5.3	43	6.6
		11	5.3	22	6.4
		1	5.4	1	5.8

Gas No. 12		Gas No. 13		Gas No. 14	
psig	% H_2	psig	% H_2	psig	% H_2
138	6.4	138	6.6	139	7.3
128	6.5	128	6.4	130	8.1
106	6.4	107	6.9	108	7.8
85	6.0	86	6.2	87	7.3
64	6.0	64	5.8	65	7.8
43	5.8	44	6.2	44	7.9
21	5.4	21	5.8	22	7.2
1	6.0	1	5.2	1	6.8

Gas No. 15		Gas No. 17	
psig	% H_2	psig	% H_2
135	5.0	134	4.4
126	4.8	124	4.6
104	4.8	103	4.2
84	4.8	82	4.2
63	4.8	62	4.4
43	5.0	42	4.2
22	5.2	21	4.6
1	5.6	1	5.0

Discussion

Typical data for determinations of explosive limits are given in Table II. An indication of the pre-

[2] An extended version of this table has been deposited as Document 4400 with the ADI Auxiliary Publications Project, Photoduplication Service, Library of Congress, Washington 5, D. C. A copy may be secured by citing the Document number and by remitting $1.25 for a photoprint or for a 35-mm microfilm. Advance payment is required. Make check payable to: Chief, Photoduplication Service, Library of Congress.

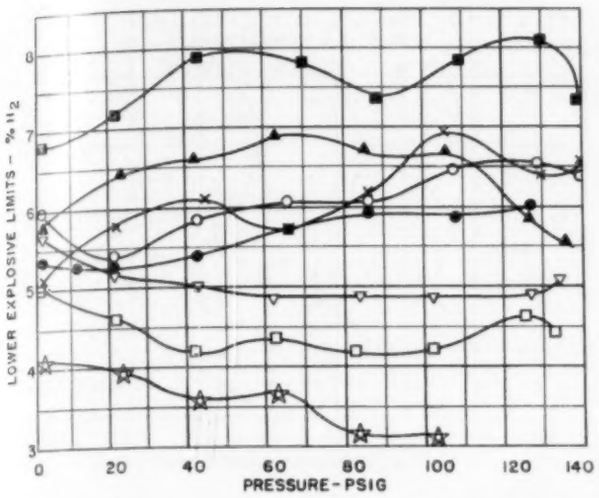

FIG. 3. Effect of pressure on the lower explosive limit of H_2-Cl_2 mixtures. Analysis of the gases before the addition of H_2 was: —●— 0.0% Cl_2; —×— 5.7% Cl_2; —▲— 11.1% Cl_2; —■— 19.1% Cl_2; —○— 29.8% Cl_2; —▽— 40.4% Cl_2; —□— 52.5% Cl_2; —☆— 100% Cl_2; balance a mixture of 46.5% N_2, 32.5% CO_2, and 21.1% O_2.

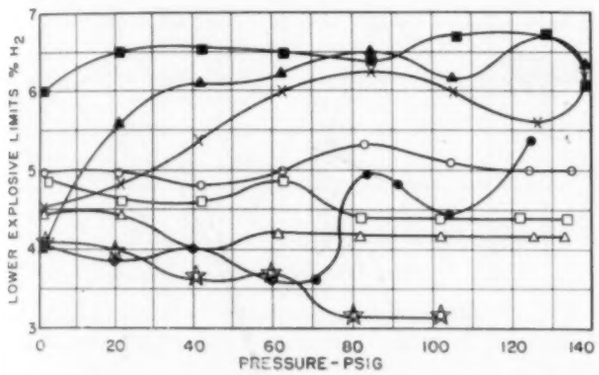

FIG. 4. Effect of pressure on the lower explosive limit of H_2-Cl_2 mixtures. Analysis of the gases before the addition of H_2 was: —●— 0.0% Cl_2; —×— 5.2% Cl_2; —▲— 11.1% Cl_2; —■— 17.3% Cl_2; —○— 29.8% Cl_2; —□— 41.2% Cl_2; —△— 53.9% Cl_2; —☆— 100% O_2; balance a mixture of 79.1 N_2 and 20.9% O_2.

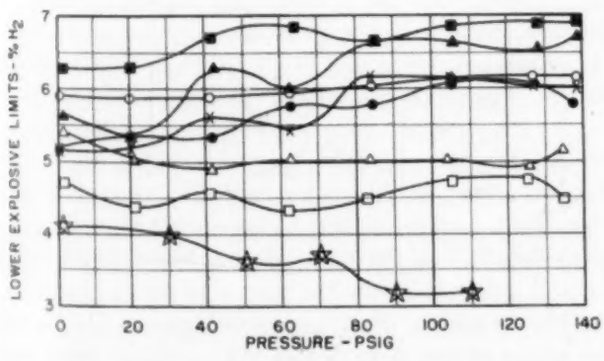

FIG. 5. Effect of pressure on the lower explosive limit of H_2-Cl_2 mixtures. Analysis of the gases before the addition of H_2 was: —●— 0.0% Cl_2; —×— 4.8% Cl_2; —▲— 8.9% Cl_2; —■— 21.8% Cl_2; —○— 29.3% Cl_2; —△— 40.4% Cl_2; —□— 54.0% Cl_2; —☆— 100% Cl_2; balance a mixture of 34.7% CO_2, 30.6% O_2, and 34.7% N_2.

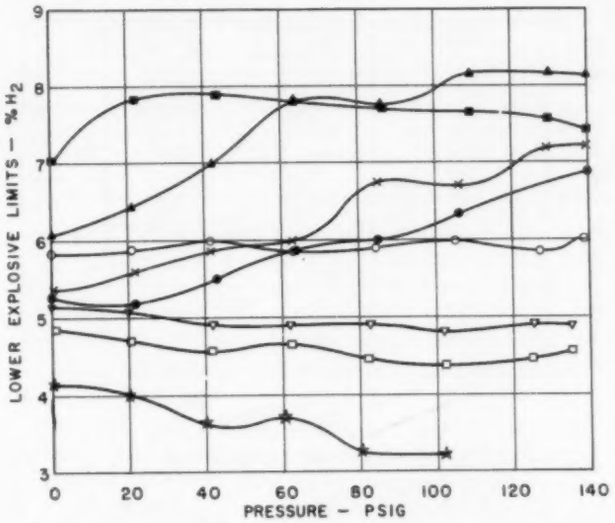

FIG. 6. Effect of pressure on the lower explosive limit of H_2-Cl_2 mixtures. Analysis of the gases before the addition of H_2 was: —●— 0.0% Cl_2; —×— 3.9% Cl_2; —▲— 9.4% Cl_2; —■— 19.5% Cl_2; —○— 29.1% Cl_2; —▽— 40.1% Cl_2; —□— 49.0% Cl_2; —☆— 100% Cl_2; balance of 38.3% CO_2, 14.3% O_2, and 48.4% N_2.

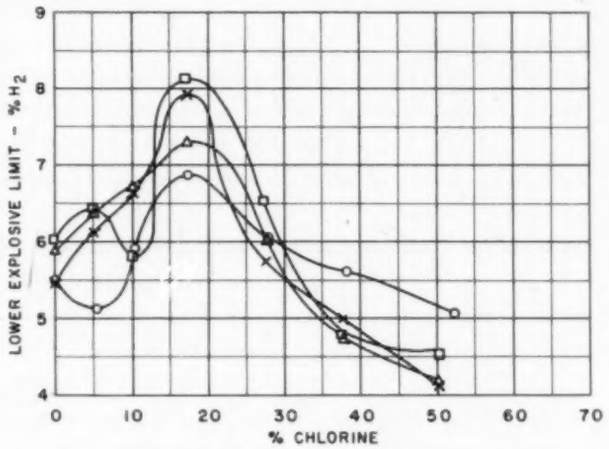

FIG. 7. Effect of chlorine concentration on the lower explosive limit: —□— 130 psig; —△— 90 psig; —×— 40 psig; —○— 0 psig. The inert gas contained 46.5% N_2, 32.5% CO_2, and 21.1% O_2.

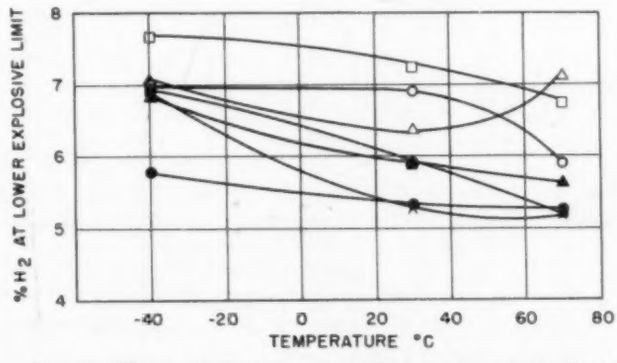

FIG. 8. Effect of temperature on the lower explosive limit at various pressures. Analysis of the gases before the addition of H_2 was: —×— 0.0 psig, 0.0% Cl_2; —●— 40 psig, 0.0% Cl_2; —▲— 90 psig, 0.0% Cl_2; —■— 130 psig, 0.0% Cl_2; —△— 0 psig, 10.4% Cl_2; —○— 40 psig, 10.4% Cl_2; —□— 90 psig, 10.4% Cl_2; balance a mixture of 46.5% N_2, 32.5% CO_2, and 21.1% O_2.

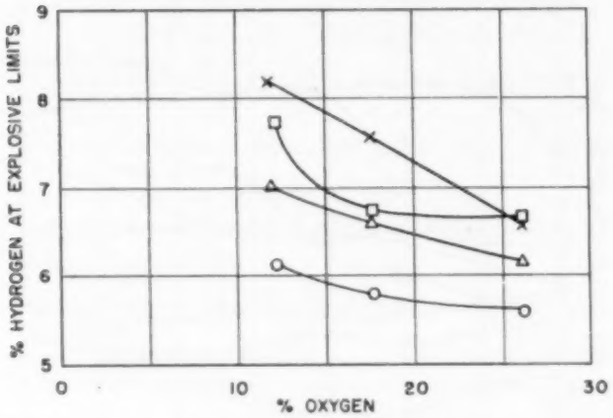

FIG. 9. Effect of oxygen concentration on the lower explosive limit of a mixture of 10% Cl_2, 30% CO_2, balance N_2 with upward flame propagation: —○— 0 psig; —△— 40 psig; —□— 90 psig; —×— 130 psig.

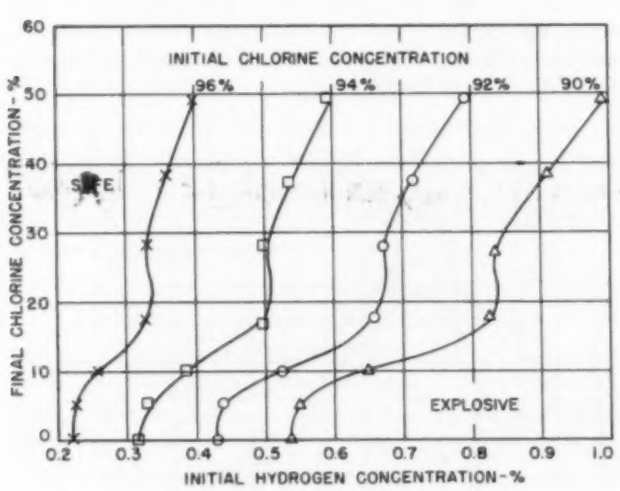

FIG. 10. Safe operating range for a chlorine consuming process at 0 psig. Analysis of the inert gas was 46.5% nitrogen, 32.5% carbon dioxide, and 21.1% oxygen.

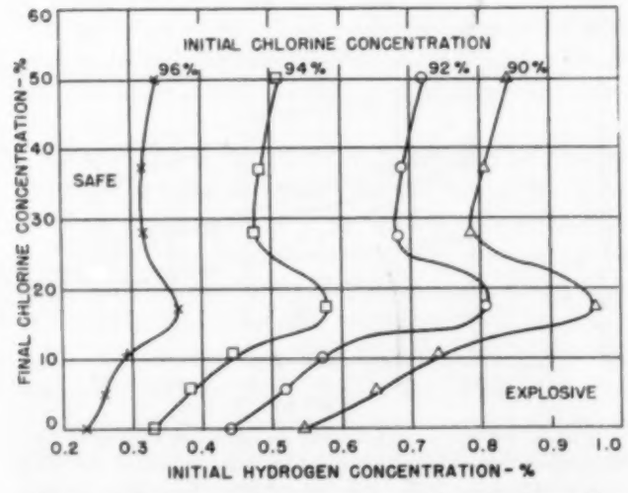

FIG. 11. Safe operating range for a chlorine consuming process at 40 psig. Analysis of the inert gas was 46.5% nitrogen, 32.5% carbon dioxide, and 21.1% oxygen.

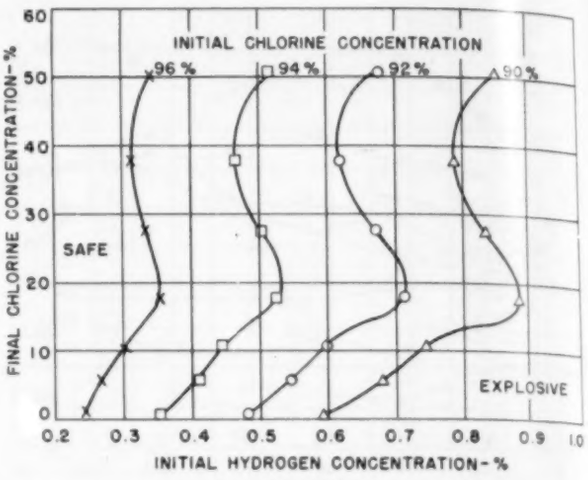

FIG. 12. Safe operating range for a chlorine consuming process at 90 psig. Analysis of the inert gas was 46.5% nitrogen, 32.5% carbon dioxide, and 21.1% oxygen.

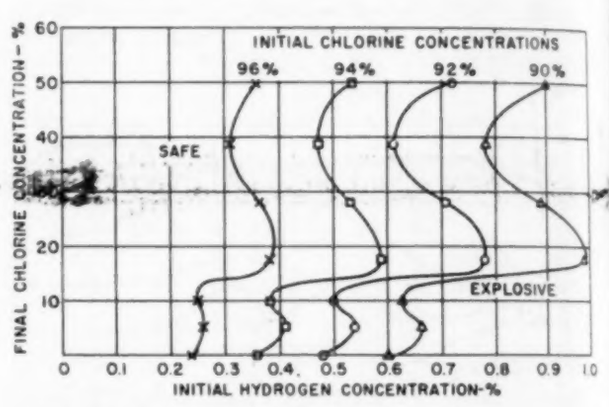

FIG. 13. Safe operating range for a chlorine consuming process at 130 psig. Analysis of the inert gas was 46.5% nitrogen, 32.5% carbon dioxide, and 21.9% oxygen.

cision of the determinations was obtained by plotting the hydrogen concentration vs. the pressure rise for individual runs. A statistical analysis of this plot was made by calculating the "least squares" regression line of the data (ignoring those points that had no pressure rise) and determining the standard error of the intercept on the hydrogen concentration axis. The standard error was found to range from 0.05 to 0.1%. Therefore reasonable confidence limits (90–95%) of a determination would be ±0.2% hydrogen. Since the values reported in this paper were the lowest values at which an explosion occurred, the distribution of errors will be somewhat skewed. The probability that the true value is less than the observed value is somewhat less than the probability of it being greater than the observed value. The larger standard errors were found with the gas mixtures which gave the smaller change in pressure rise with change in hydrogen concentration. This was caused by errors in the observed pressure rise from damping, friction, hysteresis, inertia, etc., in the pressure

TABLE II. *Typical data*

Run No.	Initial pres. psig	Final pressure after adding H_2 psig	Vol. H_2 added ml	% H_2	Pressure rise psi
Gas No. 2:					
558	80	84	20.0	4.0	0
559	80	84	24.0	4.8	0
560	80	84	25.0	4.9	6
561	80	85	28.0	5.5	24
562	80	85	26.0	5.1	9
563	80	84	25.0	4.9	4
564	80	84	24.0	4.8	0
565	80	84	24.5*	4.9*	5
Gas No. 4:					
1395	130	138	30.0	5.9	0
1396	130	139	34.0	6.7	0
1397	130	140	38.0	7.4	>20
1398	130	139	35.0	6.9	0
1399	130	139	36.0	7.0	>20
1400	130	139	35.5	7.0	>20
1401	130	139	35.0	6.9	>20
1402	130	138	33.0	6.5	0
1403	130	139	34.0	6.7	0
1404	130	139	34.5*	6.8*	15
1405	130	139	34.0	6.7	0
Gas No. 31:					
1469	20	23	36.0	7.1	9
1470	20	22	35.0	6.9	[illegible]
1471	20	22	34.0	6.7	6
1472	20	22	33.0	6.5	6
1473	20	22	31.0	6.1	0
1474	20	22	31.5	6.2	0
1475	20	22	32.0	6.3	0
1476	20	22	32.5*	6.4*	5

* Explosive limit.

recorder. These errors probably could have been minimized by using a strain gauge on the bomb with a suitable high speed recorder for the pressure recorder.

Extremely erratic results were obtained on the first determinations on this project. These were found to be caused by poor gas mixing and improper ignition. The ignition problem was solved by increasing the voltage of the power supply. The first bomb used was provided with a swinging metal vane inside the bomb for mixing the gases. The vane was moved by rocking the bomb. This would not give satisfactory mixing of the gases in any reasonable time. A new bomb was made of stainless steel and had a magnetically coupled stirrer. This stirrer had three propeller blades on a single shaft and could be operated at 3000 rpm for 30 min without having satisfactory mixing. For example, analyses of successive samples taken from a mixture theoretically containing 10% hydrogen varied from 7 to 12%. The final design of the stirrer gave satisfactory gas mixing after 10 min at 3000 rpm. Table III gives some check analyses on hydrogen addition and mixing. Hydrogen was added to nitrogen in the bomb and mixed for 10 min. Analyses were made using a mass spectrometer. The analyses check the calculated concentration of hydrogen with the experimental error of the analyses (±0.1% hydrogen).

TABLE III. *Check analyses on hydrogen addition and mixing*

Initial pres. N_2, psig	Final pres. after addition of H_2, psig	Vol. H_2 added, ml	Calc. % H_2	% H_2 analyzed
100	107	35	6.9	7.0
100	104	22	4.4	4.5
130	143	50	9.6	9.6
60	68	50	9.6	9.5
10	13	50	9.7	9.6

Hydrogen was added to nitrogen in the bomb and mixed for 10 min. Analyses were made using a mass spectrometer.

Some of the points on the calculated curves on Fig. 7, 8, and 9 appear inconsistent. These errors were caused by the necessity of interpolating between some of the observed data in order to have them at the same pressure. The data in Fig. 8 showing the effect of temperature on the explosive limits do not have the precision of the other data in this paper. They were obtained as an afterthought, and there was not enough gas for the desired degree of replication of the determinations. Also, the temperatures varied ±10°C from the desired value.

Since there have been no published data comparable to most of the data presented in this paper, there can be no comparison of results with those obtained by others. However, the explosive limit of hydrogen with air (4.1% H_2) determined in this paper checks with the value obtained by others (7).

Any discussion of this paper will appear in a Discussion Section to be published in the June 1955 JOURNAL.

REFERENCES

1. P. MATHIEU, *J. phys.*, **7,** 166 (1917).
2. A. WEISWEILER, *Z. Elektrochem.*, **42,** 499 (1936).
3. E. W. LINDEIJER, *Rec. trav. chim.*, **56,** 105 (1937).
4. T. I. KUNIN AND V. I. SERDYUKOV, *J. Gen. Chem. (U.S.S.R.)*, **16,** 1421 (1946).
5. E. A. MASON, W. C. BAUER, AND R. R. QUINCY, "Explosions in Chlorine Absorption Systems," Item No. 53-23, Industrial Liaison Office, Massachusetts Institute of Technology, Cambridge (1953).
6. G. W. JONES, *Chem. Rev.*, **22,** 1 (1938).
7. H. F. COWARD AND G. W. JONES, "Limits of Flammability of Gases and Vapors," Bull. 503, U.S. Bureau of Mines (1952).
8. E. W. LINDEIJER, *Rec. trav. chim.*, **56,** 97 (1937).

Discussion Section

THE REACTION OF SILVER ALLOYS WITH SULFUR IN MINERAL OIL

II. Examination of Reaction Films and Mechanism of Reaction

H. O. Spauschus, R. W. Hardt, and R. T. Foley (pp. 6–9)

J. T. WABER[1]: The authors have presented a very interesting paper. There is, I believe, an alternate mechanism which might be proposed which will lead to a linear growth law. When the surface reaction is slow in comparison with diffusion, a constant reaction rate will obtain. Recent detailed theoretical calculations briefly reported by Williams and Wallace[2] showed that at temperatures below 135°F the rate of formation of chloride ions at the silver chloride-solution interphase was slow in comparison with the rate of arrival of Ag ions.

In the case of the alloys at hand, there can be changes in the concentration and mobility of free electrons due to the presence of alloy atoms dissolved in the sulfide film. Such a change in the availability of electrons would affect the rate of sulfide ion formation and, hence, an effect on the linear rate would be expected. If such a mechanism does operate, the rate law will change to a parabolic one at moderately higher temperatures.

A strained sulfide layer of constant thickness next to the metal was proposed to account for the linear law. Presumably this layer restricted diffusion so as to be rate-controlling: it was not clear from the presentation whether x-ray changes attributed to strain were not due to shifts in the lattice parameter which, in turn, were due to alloy atoms dissolved in the Ag_2S.

R. T. FOLEY: If a boundary reaction as described by Williams and Wallace[2] were the rate-determining step, the linear rate behavior would be accounted for. The case discussed involves silver chloride which is almost a pure ionic conductor. Thus, electronic conductivity would control the reaction rate.

On the other hand, silver sulfide is an N-type semiconductor. We may assume that lattice defects consist of metal ions and quasi-free electrons. [There are reports indicating a sulfur excess (silver deficit), but in view of several recent studies,[3] this does not appear reasonable.] Solution of a divalent or trivalent cation sulfide in the silver sulfide would tend to increase the number of free electrons and decrease the number of silver ions. The concentration gradient and, thus, the reaction rate would be decreased. This has been shown, in an earlier paper,[4] to be the case qualitatively. The authors contend that the alloying sulfide in solution is concentrated in the first formed film. Thus, the observed rate is linear because the controlling step is diffusion through a layer of constant thickness rather than an increasing thickness of reaction product.

We do not believe that the strains arise from coherency stresses. One would expect the same stresses in silver, silver-thallium alloys, and silver-cadmium alloys. Only the latter gave appreciable distortions and lowered reaction rates.

The explanation for the lower rate must be based on a difference on valency.

The authors thank Dr. Waber for his stimulating suggestions.

This Discussion Section includes discussion of papers appearing in the JOURNAL OF THE ELECTROCHEMICAL SOCIETY, **101**, No. 7–12 (January–June 1954).

[1] Los Alamos Scientific Laboratory, Los Alamos, N. Mex.

[2] WILLIAMS AND WALLACE, *J. Chem. Phys.*, **21**, 1294 (1953).

[3] M. H. HEBB, *J. Chem. Phys.*, **20**, 185 (1952).

[4] *See* Fig. 3, R. T. FOLEY, M. J. BOLTON, AND W. MORRILL, *This Journal*, **100**, 538 (1953).

THE ELECTROLYTIC PREPARATION OF MOLYBDENUM FROM FUSED SALTS

II. Preparation of Reduced Molybdenum Halides

Seymour Senderoff and Abner Brenner (pp. 28–30)

A. C. LOONAM[5]: How much of the molybdenum gets through the diaphragm and is oxidized at the anode?

S. SENDEROFF: In preparing K_2MoCl_6 by electrolysis of a solution of K_2MoO_4 in strong hydrochloric acid, followed by precipitation of the salt with HCl gas, an over-all yield of 70% was obtained. While some of the loss was due to solubility of the K_2MoCl_6, most of it was probably the result of loss of molybdenum through the diaphragm. However, no attempt was made in this work to minimize this loss by improvement of the diaphragm. Undoubtedly, a thicker diaphragm with finer pores would reduce the loss of molybdenum to the anolyte. Further, it should be noted that the anolyte remaining at the end of a run can be added to the catholyte of succeeding runs to recover the molybdenum which passes through the diaphragm.

M. A. STEINBERG[6]: Can you describe the type of Mo crystals produced?

S. SENDEROFF: The type of crystals produced varies with current density, temperature, and other operating conditions, as described in the first paper in this series.[7]

THE ELECTROLYTIC PREPARATION OF MOLYBDENUM FROM FUSED SALTS

III. Studies of Electrode Potentials

Seymour Senderoff and Abner Brenner (pp. 31–38)

M. A. STEINBERG[8]: 1. What is the cathode material for coherent Mo deposits at 600°C?

2. How do you visualize the transport of oxygen ions to the cathode in oxygenated salt baths?

S. SENDEROFF: 1. For the deposit shown in Fig. 9 of an

[5] 70 East 45th Street, New York 17, N. Y.

[6] Horizons, Inc., Cleveland, Ohio.

[7] S. SENDEROFF AND A. BRENNER, *This Journal*, **101**, 16 (1954).

[8] Horizons, Inc., Cleveland, Ohio.

earlier paper,[7] the cathode was a silver-plated steel tube. A tungsten cathode was used for the deposit shown in Fig. 7 and 8.[7]

2. One need not consider the oxygen or oxygen-containing ions as involved in electrical transport at all. Most of the current through the bath is probably carried by the potassium and chloride ions. Since both the oxygen and molybdenum in the bath probably are contained in complex ions of low mobility and low concentration, the transfer of both the oxygen and the molybdenum to the cathode is probably governed by diffusion and not greatly dependent upon the charge of the ions in which they appear.[9]

L. M. Litz[10]: It is of interest to note in connection with your emf measurements in molten salts certain measurements reported by Rempel and Ozeryanya.[11] These authors used the reversible chlorine electrode and obtained the following potentials in equimolar NaCl-KCl baths containing 0.1M concentration of the metal chloride at 690°C: Zn, 1.883; Fe, 1.582; Co, 1.514; Cu, 1.414; Pb, 1.390; Ag, 1.287; Bi, 1.181; Ni, 1.179. The position of Ni in this series is particularly interesting.

S. Senderoff: We have not measured the potential of nickel under the conditions described in Table I, but preliminary experiments on electrochemical replacement indicate that nickel has a potential in this system close to that of silver. Verdieck and Yntema[12] also found that nickel is more noble than copper in molten $AlCl_3$-KCl-NaCl.

Morris Eisenberg[13]: Dr. Senderoff's choice of Ag/AgCl as a reference electrode is certainly a wise one. However, this raises a few questions.

1. What is the potential of this reference electrode relative to the normal hydrogen electrode?

2. What is the temperature coefficient of the Ag/AgCl reference electrode in this temperature range?

3. How significant are the liquid junction potentials in your baths?

S. Senderoff: 1. I don't know. An approximate value of this potential may be obtained by measuring the potential of a chain of cells with progressively lower-melting electrolytes with molten AgCl at one end and aqueous HCl at the other, but such a value would have little or no thermodynamic significance.

2. Again, I don't know. If the reference electrode is kept at the same temperature as the electrode under study during potential measurements, the temperature coefficient of the potential of the reference electrode is not needed for thermodynamic calculations. Furthermore, the temperature coefficient of a half-cell is not determinable by strictly thermodynamic measurements.

3. In the systems under study, the current across the boundary of the liquid junction is probably carried largely by potassium and chloride ions. This situation is analogous to the use of a KCl bridge when measuring potentials in aqueous systems. We believe, therefore, that the liquid junction potentials are small enough to be ignored in the experiments we have described.

F. Trumbore[14] and G. C. Fryburg[15]: The statement of Senderoff and Brenner that nickel may be more noble than copper in the KCl-LiCl system was of especial interest to us. A few years ago at the Lewis Flight Propulsion Laboratory we were engaged in an attempt to determine the thermodynamic properties of the copper-nickel alloy system by the emf method and found that cells of the type

$$Ni/Ni^{++} \text{ (in fused KCl-LiCl)/Cu-Ni alloy}$$

gave voltages opposite in sign to that expected and showed very erratic behavior. It was noticed that the alloy electrode lost copper during the course of an experiment and became coated with small crystals of nickel. Moreover, cells of the type

$$Cu/Cu^{+} \text{ (in fused KCl-LiCl)/Cu-Ni alloy}$$

gave reasonable voltages of the expected sign. These facts indicated a reversal or near reversal of nobility of the two metals in going from the aqueous to the fused salt system. In connection with these and other studies conducted by one of us at the Bell Telephone Laboratories a number of crude experiments were performed to get some idea of the relative nobilities of various elements in the KCl-LiCl system. These experiments consisted simply of adding a given metal to a solution of the chloride of a second metal in KCl-LiCl and observing the presence or absence of displacement of the second metal from the solution. These experiments indicated the following "nobility" series (elements to the left of > will displace those to the right):

$$(Li, K) > (Mg, Al) > Zn > (Ge, Cd, Fe, Si) > Cu > (Pb, Sn) > (Co, Ni) > (Sb, Ag)$$

This series is, of course, qualitative and may not represent the true order of the standard electrode potentials because of the various ion species, activities of the ions in the melts, etc. However, the relative positions of Zn, Fe, Cu, and Ag agree with those of Senderoff and Brenner.

Quantitative data on standard electrode potentials of other metals in the KCl-LiCl and other fused salt systems should be of considerable value to workers in the emf field. The stability of emf cells of the type mentioned above depends to a large degree on the difference in nobility of the two metals because the magnitude of this difference determines the equilibrium constant of the exchange reaction

$$Ni + 2Cu^{+} \rightleftarrows 2Cu + Ni^{++}$$

(in the copper-nickel case), and may control the rate of transfer of the metals between the electrodes. Statements have appeared in the literature that in order for the emf method to be applicable to a given alloy system the nobility differences based on the emf series in aqueous solutions should be on the order of 0.2 volt[16] to 0.7 volt.[17] Such

[9] C. Wagner, *This Journal*, **101**, 181 (1954).

[10] National Carbon Company, Cleveland, Ohio.

[11] Rempel and Ozeryanya, *Z. Fiz. Khim.*, **25**, 1181 (1951).

[12] Verdieck and Yntema, *J. Phys. Chem.*, **48**, 268 (1944).

[13] Stanford Research Institute, Menlo Park, Calif.

[14] Bell Telephone Laboratories, Inc., Murray Hill, N. J.

[15] National Advisory Committee for Aeronautics, Lewis Flight Propulsion Laboratory, Cleveland, Ohio.

[16] N. W. Taylor, *J. Am. Chem. Soc.*, **45**, 2865 (1923).

[17] O. Kubaschewski and O. von Goldbeck, *Trans. Faraday Soc.*, **45**, 948 (1949).

statements neglect the possibility that considerable changes may occur in the relative values of electrode potentials in going to fused salt electrolytes, as indicated above in the qualitative series. Furthermore, simple consideration of the equilibrium constant for the exchange reaction shows that, in certain cases, even if the two metals have the same standard electrode potential in the fused salt system it should be possible, by proper choice of the concentration of the ion of the less noble metal and of other conditions, to minimize metal transfer to the extent that reliable data could be obtained. Thus, data on electrode potentials in fused salt systems might show that certain alloy systems could be studied for which the emf method was formerly thought to be unsuitable.

S. SENDEROFF: Since making the measurements described in the paper, we have done some calculations which indicate that the inversion of the positions of copper and nickel in the emf series should not have been so surprising to us and to others who have observed it. We calculated the equilibrium constants, K, at 730°C for the reaction, $MCl_n + n/2H_2(g) \rightarrow M + nHCl(g)$ from Brewer's thermodynamic data for the metal halides at elevated temperatures. When log K thus calculated was tabulated for about a dozen metals, a list was obtained which is equivalent to the idealized emf series to be expected at that temperature, since log K for the reaction is proportioned to E^0 against a hypothetical hydrogen electrode at that temperature. Negative values of log K would correspond to the "active" metals above hydrogen, and positive values to the "noble" metals below hydrogen. It turns out that on the basis of this strictly thermodynamic calculation, Cu^+ and nickel are both below hydrogen, and nickel is below copper. Some other metals whose potentials have been measured fall in the correct order.

While we have not carried this further as yet, it seems that as more thermodynamic data at high temperatures become available, it will be interesting to compare such calculations with potential measurements to throw light on the state of the electrolyte in molten salts, and to judge the reversibility of electrode systems.

ANODIC BEHAVIOR OF ALUMINUM AND ITS ALLOYS IN SULFURIC ACID ELECTROLYTES

Ralph B. Mason and Phyllis E. Fowle (pp. 53–59)

R. C. SPOONER[18]: The authors are to be congratulated on a clear and interesting presentation of their investigation of conditions governing the anodizing of aluminum and its alloys. It is regretted that the paper does not discuss in detail the voltages required under the various conditions employed, since this information is essential for consideration of the coating formation mechanism.

The coating ratio-metal loss curves in Fig. 2 and 3 at 72 amp/ft² which tilt upward are of special interest. Their shape is attributed to a decreased rate of solution of the coating at the bottom of the pores because of a build-up of solution products within the pore channels. Later in the paper, the possibility is mentioned that the "pores are fewer in number because of a higher voltage across the primary or barrier layer." In view of the noted abnormal increase in voltage accompanying rises in coating ratio, this suggests that the larger ratios may be due, in part at least, to a reduction in the number of pores so lowering the surface area exposed to electrolyte attack and thus decreasing the amount of coating dissolved.

The authors' comments would be appreciated on the following two queries: 1. Did the proportionately large edge effect with the small panels employed at the higher current densities (e.g., 2 in.² at 72 amp/ft²) cause "burning"? 2. What was the effect on the voltage required for a fixed current density of the addition of 2% oxalic acid to the 12% sulfuric acid solution?

RALPH B. MASON AND PHYLLIS E. FOWLE: 1. No trouble with "burning" was encountered with the small aluminum samples at the high current densities except in the case of 24S-T at a temperature of 34°F. In this case it was not possible to use a current density higher than 24 amp/ft². In the oral presentation of the paper it was pointed out that it is usually impractical to use current densities as high as 48 or 72 amp/ft². In the laboratory, small samples can be readily coated provided there is adequate cooling and agitation of the electrolyte.

2. There was no significant change in voltage when 2% oxalic acid was added to the 12% sulfuric acid solution. It is to be regretted that certain papers discussing the mechanism of coating formation have overstressed the importance of voltage. In the case of the sulfuric acid electrolytes, the voltage data and theory will not stand up under a rigid analysis.

EXTRACTIVE METALLURGY OF ZIRCONIUM BY THE ELECTROLYSIS OF FUSED SALTS

II. Process Development of the Electrolytic Production of Zirconium from K_2ZrF_6

M. A. Steinberg, M. E. Sibert, and E. Wainer (pp. 63–78)

N. F. MURPHY[19]: Did the graphite electrode give off powdered graphite to the melt which would codeposit with the zirconium? Did the graphite porosity decrease on prebaking?

M. E. SIBERT: There was no evidence of any loss of graphite from the graphite anode. The only carbon contamination encountered has resulted from accidental breakage of the protecting graphite sleeve on the cathode support rod.

There is no notable change in porosity of the graphite regardless of treatment. Leakage develops after a number of runs when the crucible becomes saturated with salts.

MORRIS EISENBERG[20]: Do you need a protective atmosphere for the storage of the zirconium powders?

M. E. SIBERT: A protective atmosphere is not required for storage of this electrolytic zirconium powder. We have had no instances of spontaneous ignition of this powder when stored in air. Apparently either a protective oxide film is formed in the aqueous recovery procedure, or the

[18] Chemical Division, Aluminium Laboratories Ltd., Kingston, Ontario, Canada.

[19] Virginia Polytechnic Institute, Blacksburg, Va.

[20] Stanford Research Institute, Menlo Park, Calif.

hydrogen content is appreciably less than those powders which are subject to this hazard.

CORROSION INHIBITION IN ACID SOLUTION

Cecil V. King and Edward Hillner (pp. 79–83)

A. C. MAKRIDES[21]: The experiments reported by the authors are interesting in more than one connection. It appears from their results that complexing or chelating agents are excellent inhibitors of the dissolution of iron under strongly oxidizing conditions. This suggests that the mechanism by which organic inhibitors function is not "poisoning" of hydrogen evolution as proposed by Elze and Fischer[22] and by Bockris and Conway.[23] These same compounds have no effect or actually accelerate dissolution of zinc (with the exception of sodium gluconate which shows about 50% inhibition). This further suggests that inhibition by organic compounds is directly related to the stability of the adsorption complex formed between the metal and the inhibitor, and the consequent decrease in dissolution rate of the surface layers of the metal, rather than to any mechanical blockage of hydrogen ion discharge. As pointed out elsewhere[24] recent theories of chemisorption on metals lead to the prediction that chemisorption of such compounds would be stronger on iron, which has *d*-bond character, than on zinc.

Inhibition by $K_2Cr_2O_7$ is known to be dependent on the *p*H of the solution.[25] The *p*H of the reference corroding solution was about 1.7; addition of the complexing agent generally raised this by 0.4, or more, *p*H units. The observed increase in effectiveness of inhibition by $K_2Cr_2O_7$ in these solutions could, therefore, be caused by the higher *p*H. In two cases out of three where the *p*H of the solution was adjusted to 1.7, or close to this, after addition of the complexing agent, the complexing agent appears to have decreased rather than increased the inhibition effectiveness of $K_2Cr_2O_7$.[26] It would be helpful in the interpretation of results to know if this point has been checked by the authors.

C. V. KING AND E. HILLNER: Essentially Dr. Makrides raises three pertinent questions. They are:

1. Do complexing agents in general inhibit iron dissolution (in the reference solution with no dichromate), and is the inhibition due to adsorption?

2. Do most complexing agents accelerate the dissolution of zinc in the same solution?

3. Is the main effect of the complexing agents on dichromate inhibition due to raising the *p*H?

These questions can be answered as follows:

1. The inhibition by gluconic and citric acids and by EDTA may be due to adsorption on iron; no experimental evidence is available. It is certainly not due to blocking or "poisoning" hydrogen evolution, but may be due to blocking the formation of atomic hydrogen, or some step in the reduction of nitrate. We now have evidence that other chelating agents are poor inhibitors without dichromate, and that neocupferron, which forms insoluble chelates with ferrous and ferric ions, inhibits, but not by adsorption.

2. The dissolution of zinc appears to be diffusion controlled in all the solutions without dichromate. Gluconate lowered the rate because the molecular acid diffuses more slowly than hydrogen ion. EDTA increased the rate because of the extra acid present (molecular acid as well as hydrogen ion). Citric acid, as reported, seemed to have little effect because less HCl was present; the diffusion coefficient of citric acid is smaller but it dissolves more equivalents per molecule. These effects are independent of *p*H within wide limits.

3. The *p*H of the reference solution is 1.8 rather than 1.7; the activity coefficient of HCl at these ionic strengths is very close to 0.80. Actually only one case is shown[27] where corrosion is smaller (at the same or a lower *p*H) than in the reference solution. The effect of dichromate should have been shown at several HCl concentrations to cover the *p*H range, or it should have been stated that dichromate enhances inhibition by the complexing agent, at the same *p*H. Actually, later experiments show more conclusively that these and other complexing agents do enhance dichromate inhibition at the reference *p*H.

THE PROTECTIVE ACTION OF PIGMENTS ON STEEL

M. J. Pryor (pp. 141–148)

U. R. EVANS[28]: Dr. Pryor's study of aqueous extracts of lead and zinc pigments is most welcome, and adds greatly to our knowledge. Where it overlaps with earlier work, the facts are in general accord. It must, however, be remembered that the poor showing of red lead in aqueous extract is no argument against red lead paints, where inhibition is largely due to the degradation products of lead soaps—many of which have been identified and estimated in this laboratory by van Rooyen and Mayne;[29] they are mostly salts of dibasic organic acids. However, even in red lead oil paints, the addition of litharge consistently improves performance, as shown in the seven-year outdoor tests organized from Cambridge.[30]

Earlier laboratory tests[31] showed clearly that, in the absence of oil, litharge is highly superior to red lead. The following are the losses of weight (in units of 10^{-4} gram)

[21] Department of Chemistry, University of Texas, Austin, Texas.

[22] J. ELZE AND F. FISCHER, *This Journal*, **99**, 259 (1952).

[23] J. O'M. BOCKRIS AND B. E. CONWAY, *J. Phys. & Colloid Chem.*, **53**, 527 (1949).

[24] N. HACKERMAN AND A. C. MAKRIDES, *Ind. Eng. Chem.*, In press.

[25] *See*, for example, G. G. BERWICK, *Chemistry & Industry*, **1953**, 408.

[26] *See* Table III, Zinc and EDTA, and Table IV, Iron and citric acid, C. V. KING AND E. HILLNER, *This Journal*, 101, 79 (1954).

[27] *See* Table III, Iron, C. V. KING AND E. HILLNER, *This Journal*, **101**, 79 (1954).

[28] Department of Metallurgy, University of Cambridge, Cambridge, England.

[29] D. VAN ROOYEN AND J. E. O. MAYNE, *J. Appl. Chem., London*, **4**, 384 (1954).

[30] S. C. BRITTON AND U. R. EVANS, *J. Soc. Chem. Ind., London*, **58**, 90 (1939).

[31] K. G. LEWIS AND U. R. EVANS, *J. Soc. Chem. Ind., London*, **53**, 25T (1934).

obtained when steel (or iron) specimens are rotated for 20 hr at 25°C in tubes partly filled with liquid, with or without pigment, but also containing air or oxygen.

In the oxygen experiments, pure litharge was used; in the air experiments, pigment-type litharge or red lead was used. The numbers for percentage areas visibly corroded are also shown. Each experiment with pigment is the mean of two measurements; those for experiments without pigment are mostly the mean of 3 or 4 measurements. The specimens were rectangles of sheet measuring 3 x 1 cm.

Material	Gas	Liquid	Weight loss			Percentage of area visibly corroded		
			No pigment	Litharge	Red Lead	No pigment	Litharge	Red Lead
Steel MS2	Air	Distilled water	44	1	9	17	0	3
Steel MS2	Air	0.001M NaCl	45	1	21	10	0	5
Steel MS2	Air	0.001M Na_2SO_4	122	4	52	29	1	6
Steel MS2	Air	Sea water	124	16	38	80	2	35
Electrolytic Iron	Oxygen	0.001M Na_2SO_4	78	0	—	17	0	—
Steel H33	Oxygen	0.001M Na_2SO_4	206	4	—	65	0	—
Steel P1	Oxygen	0.001M Na_2SO_4	117	10	—	20	3	—

The tentative explanation offered in 1935, emphasizing *p*H values and the basic character of inhibitive pigments, was not very unlike Dr. Pryor's theory which emphasizes reserve alkalinity. Neither seems entirely satisfactory today; one would like to know whether a buffer system of the same reserve alkalinity, based on soluble salts, would inhibit corrosion to the same extent in presence of chlorides.

Without finally rejecting reserve alkalinity as an explanation, it is well to explore alternatives. The rise of potential with time, which is attributed by Dr. Pryor to litharge acting as an anodic inhibitor, could also be attributed to an increase in rate of supply of oxygen per unit area of bare metal (an increase which is to be expected if a film is gradually spreading over the surface). It is well known that increased oxygen supply, whether obtained by increased pressure or by movement of the liquid, will render the cathodic polarization curve less steep, and thus raise the value of the potential at which it intersects the anodic curve. Furthermore, the increased oxygen supply improves the chance of obtaining passivity instead of corrosion.

If, in completely stagnant liquid, a metal surface is completely covered with a film except for small gaps of radius r and area a, separated by distances large compared to r, the rate of arrival of oxygen is approximately proportional to $a^{1/2}$ so that the rate per unit area of bare metal is proportional to $a^{-1/2}$. As the area of the gaps becomes small the supply per unit area of gap becomes better, although (for a fixed number of gaps per unit area) the supply per unit area of specimen becomes worse.[32]

If we postulate that litharge is adsorbed on metal, but not on iron oxide, the facts are easily explained. Adsorbed molecules are continually attaching and detaching themselves, and it is unlikely that protection can be explained by assuming that the whole metallic surface becomes covered with attached litharge molecules; there will always be some gaps. Oxygen at high pressure will arrive quickly enough to build a passivating film; but at low pressure it will not arrive quickly enough to prevent iron entering the liquid at sensitive spots as cations, electrical neutrality being maintained by the cathodic reduction of oxygen on the area between the sensitive spots. If, however there is adsorption of litharge molecules (however partial and transitory), the increased rate of arrival of oxygen at points where it is required may suffice to cause film building to predominate over film breakdown, and since lead oxide is postulated to be not adsorbed on iron oxide, the final film will be iron oxide free from lead.

M. J. Pryor: Dr. Evans' comments and his experimental data are greatly appreciated. It is agreed that the relatively poor showing of a red lead in these experiments does not necessarily imply that it is a poor paint pigment since, if vehicles of the linseed oil type are used, inhibiting lead soaps can be formed. This probably applies also to basic lead carbonate which had no detectable inhibitive action in the form of an aqueous extract. The usefulness of these pigments in paint systems is affected by such factors as the nature of the vehicle and the geometry of the pigment particles which were not considered in this investigation.

Dr. Evans raises the question of whether a buffer system of similar reserve alkalinity based on soluble salts inhibits corrosion to the same extent in the presence of chlorides as the aqueous pigment extracts under similar conditions. Chlorides break down the protection afforded by aqueous pigment extracts relatively easily, and similar buffer systems based on soluble salts are generally more effective inhibitors in chloride containing solutions. Since buffering action is presumably required mainly at the small anodic areas rather than in the bulk of the solution, the rate of transport of the ions responsible for buffering to the anodic areas is clearly important. It is reasonable to suppose that soluble anions would migrate to the anodic areas more rapidly than colloidal or massive lead hydroxide or a positively charged $Pb(OH)^+$ ion of presumably low transport number and thus provide better buffering at the points where this property is most urgently required.

The alternative explanation of the mechanism of inhibition by litharge extracts advanced by Dr. Evans is a reasonable one but falls somewhat outside the scope of present experimental work. For instance, the writer's investigation was mainly an attempt to clarify some of the macro-

[32] It is assumed that the oxygen is used up on arrival, so that the rate of arrival is $CD/\int_r^\infty dr/2\pi r^2 = 2\pi CDr = 2\pi^{1/2}CDa^{1/2}$ where C is the oxygen concentration in the body of the liquid and D the diffusivity.

chemical reactions occurring during interaction of aqueous pigment extracts and steel. However, such detailed consideration of inhibitor mechanisms is clearly in order and the theory of reserve alkalinity can be extended as follows to provide such a picture. The potential of steel in a litharge extract is a mixed polarized potential and it can be determined from the Nernst equilibrium potentials of the individual anodic and cathodic reactions that very high polarization of both reactions occurs. High polarization of the cathodic reaction is normally observed on steel in somewhat alkaline solutions, but a high degree of anodic polarization is dependent on the presence of an inhibitor. The structure of many passivity films formed in anodic inhibitors has been shown to be duplex[33, 34] and to consist of small inclusions of corrosion product in a matrix of γ-Fe_2O_3. According to the concepts of Müller,[35] anodic polarization is dependent on the resistance and, hence, on the size of these pores in the oxide film. If the pores (which are filled with corrosion product) are very small, the anodic polarization and thus the potential will be very high and the rate of corrosion very low whereas, if the pores are larger, the anodic polarization and the potential will be lower. In inhibitor solutions a localized production of hydrogen ions at the anodic areas occurs due to the formation of hydrated oxide. If the solution in the region of the anodic areas is unbuffered, the *p*H will fall and low *p*H values are detrimental to the formation of protective films of oxide and corrosion product; consequently, the size of the anodic areas will tend to increase. If, however, the solution at the anodic areas is buffered, protective films of oxide and corrosion product may form at these points and the size of the anodic areas will tend to remain small. This also implies that buffering action at the small anodic areas is more important than buffering action in the bulk of the solution.

At the present time, there appears to be insufficient direct experimental evidence to distinguish between these views. Thus Dr. Evans' comments emphasize the need for further experimental study of these points.

DIAPHRAGM TYPE AMALGAM CAUSTIC-CHLORINE CELL

Chas. Potter and A. L. Bisio (pp. 158–161)

RALPH M. HUNTER[36]: A study of the construction of this cell would lead one to suspect that the lower voltage could have been caused by a current leak between the cathode lead and the amalgam. Such leak could give the authors the benefit of the amalgam decomposition potential. Are they sure that this did not happen?

A. L. BISIO AND C. POTTER: The lower voltage is caused by operation of the cell as a Sorensen cell, amalgam decomposition occurring as a result of a local cell set up between the amalgam and the graphite. We doubt whether any leakage of current occurred.

[33] J. E. O. MAYNE, J. W. MENTER, AND M. J. PRYOR, *J. Chem. Soc.*, **1950**, 3229.

[34] M. J. PRYOR, M. COHEN, AND F. BROWN, *This Journal*, **99**, 263 (1951).

[35] W. J. MÜLLER, *Trans. Electrochem. Soc.*, **76**, 167 (1939).

[36] Dow Chemical Company, Midland, Mich.

EFFECT OF CHAIN BRANCHING ON ELECTROCHEMICAL CARBON-HALOGEN BOND FISSION. POSSIBLE MECHANISM FOR THE PROCESS

Philip J. Elving, Joseph M. Markowitz, and Isadore Rosenthal (pp. 195–202)

GARRETT W. THIESSEN[37]: In the macroelectrolysis[38] of α-bromopropionic acid, (watery solution, K-salt) the main yield appears to be ethylidene bromide, i. e., 1,2-dibromoethane. This is (R + Br) if the acid is R·COOH, and an unusual result. Identification has been handicapped by (*a*) decomposition with evolution of HBr on distilling; (*b*) lack of existence of a suitable derivative in literature. The constants agree approximately, most significant being density greater than that of concentrated H_2SO_4. Br analysis close, but not quite high enough.

No unsaturation was found in the escaping electrolysis gases.

PHILIP J. ELVING, JOSEPH M. MARKOWITZ, AND ISADORE ROSENTHAL: The result described by Dr. Thiessen is most interesting, and, as he implies, quite unexpected. It would seem that any mechanism which could be contrived to account for his result would necessarily involve decomposition of the carboxylate group.

Of course, there is no necessary relation between this result and the result of the polarographic reduction of 2-bromopropanoic acid. Dr. Thiessen describes his experimental conditions as "macro-electrolysis" (with platinum electrodes). One assumes that he did not control the cathode potential, but used constant current. Consequently, a variety of products might be formed at potentials much greater than those encountered in polarographic work.

It is virtually certain that no ethylidene bromide is produced in the polarographic reduction of 2-bromopropionic acid. The former substance has a half-wave potential of -1.31 v vs. S.C.E. at 25° in 0.5*M* NH_3-NH_4Cl buffer at *p*H 8.3. Under the same conditions, 2-bromopropanoic acid exhibits only one wave with a half-wave potential of -1.14 v. If ethylidene bromide were a product, a second wave would appear when 2-bromopropanoic acid is electrolyzed under these experimental conditions; such a wave is not observed.

PREPARATION AND EXAMINATION OF BERYLLIUM CARBIDE

M. W. Mallett, E. A. Durbin, M. C. Udy, D. A. Vaughan, and E. J. Center (pp. 298–305)

J. A. UPPER[39]: In this paper under Hardness Measurements, it was stated that "Readings of 2678, 2520, and 2613 were obtained with a 50-gram load and 2740 with a 25-gram load. It appears that the hardness of Be_2C is greater than that of silicon carbide and approaches the hardness of boron carbide." These statements were made regarding Knoop hardness measurements made on a Tukon hardness tester.

[37] Monmouth College, Monmouth, Ill.

[38] Unpublished research at Monmouth College; Pt electrodes.

[39] Norton Company, Niagara Falls, Canada.

Regarding the above statements, we would like to submit the following information.

From observations made in the Norton Research Laboratory in Worcester, Massachusetts, it does not appear that Be_2C is as hard as silicon carbide. Typical Knoop hardness data for the very hardest materials are:

Material	*Knoop hardness (100-gram load)*
B_4C	2800
B	2500
SiC	2500
TiC	2500
Be_2C	2300
ZrC	2100
Al_2O_3	2050
WC	1900

The Knoop hardness determinations set forth above (excepting Be_2C) were obtained from a paper by Thibault and Nyquist.[40] Values for Be_2C were more recently obtained.

The paper under discussion also quotes Knoop hardness readings obtained at both 50- and 25-gram loads on the Tukon tester. In the paper by Thibault and Nyquist[40] it is pointed out that the Knoop numbers obtained at different loadings are not directly comparable. In order to obtain comparable data, all tests must be conducted at a common load. The cause of the variation of the measured Knoop hardness with indenting load is discussed in a paper by Tarasov and Thibault.[41]

MANLEY W. MALLETT: We wish to thank Mr. Upper for drawing our attention to the fact that Knoop hardness numbers based on indentations made by a 25- or 50-gram load are not directly comparable with numbers determined from indentations made at higher loads. Accordingly, we should revise our statement on the hardness of Be_2C to read that it lies between those of zirconium carbide and silicon carbide.

THE NATURE OF THE ZINC-CONTAINING ION IN STRONGLY ALKALINE SOLUTIONS

Thedford P. Dirkse (pp. 328-331)

J. J. LANDER[42]: The author is probably aware that, because x and y are known with certainty, perhaps z might be determined by a plot similar to that with which the value of y was determined, i.e., by graphing $E_{Zn} - 0.0295\ y \log a_{OH^-}$ vs. $\log a_{H_2O}$ and determining the slopes of the resultant curves at several values of M_{Zn}. The results should be interesting, because if the experimental data are of sufficient precision, they should show whether z has an integral value or whether it varies over a rather wide range of a_{OH^-}. Thus his data itself might possibly determine whether or not degree of hydration can be expressed exactly. Evidently, determination of z has been ruled out on the basis of *a priori* considerations, which, even if based on previous experimental evidence, do not necessarily apply to this work which seems to be of high quality.

T. P. DIRKSE: A plot such as that suggested by Dr. Lander can be prepared from the data used in the paper referred to. Using two different concentrations of zinc such a plot gives reasonably straight lines (*see* accompanying graph). The two lines are parallel and the slope of each is 0.114. This is reasonably close to 0.118 which corresponds to a value of four for z. It is striking that there is a regularity of behavior and that the plot gives an integral value for z. It is possible that this indicates that four water molecules are specially bound in each zinc complex although there is a tendency at present to discount the significance of such hydration numbers.

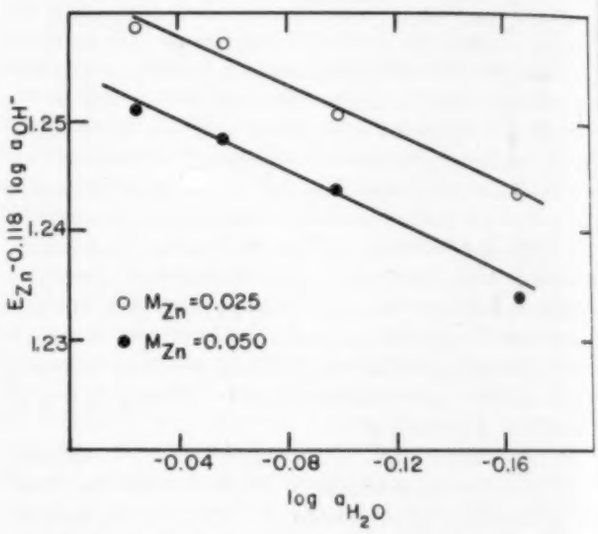

Variation of $[E_{Zn} - 0.118 \log a_{OH^-}]$ with $\log a_{H_2O}$

[40] N. W. THIBAULT AND H. L. NYQUIST, "The Measured Knoop Hardness of Hard Substances and Factors Affecting Its Determination," 28th annual convention, American Society for Metals, Atlantic City, November 1946.

[41] L. P. TARASOV AND N. W. THIBAULT, paper delivered at 28th annual convention, American Society for Metals, Atlantic City, November 1946.

[42] Naval Research Laboratory, Washington, D. C.